Universidade Federal do Rio Grande do Norte

Programa de Pós-Graduação em Ecologia

Tese de Doutorado

TEMPERATURA E RECURSOS DETERMINAM INTERAÇÕES COMPETITIVAS, TRÓFICAS E TAMANHO CORPORAL EM PEIXES RECIFAIS DO ATLÂNTICO OCIDENTAL

Por: Leonardo Capitani

Orientador: Prof. Dr. Ronaldo Angelini

Coorientador: Prof Dr. Guilherme O. Longo

Natal, RN, Brasil, Abril, 2021

TEMPERATURA E RECURSOS DETERMINAM INTERAÇÕES COMPETITIVAS, TRÓFICAS E TAMANHO CORPORAL EM PEIXES RECIFAIS DO ATLÂNTICO OCIDENTAL

Trabalho apresentado ao Programa de Pós-Graduação em Ecologia da Universidade Federal do Rio Grande do Norte, como parte do requerimento para a obtenção do título de Doutor em Ecologia.

Orientador: Prof. Dr. Ronaldo Angelini

Co-orientador: Prof. Dr. Guilherme Ortigara Longo

Natal, RN, Brasil, Abril, 2021

Universidade Federal do Rio Grande do Norte - UFRN
Sistema de Bibliotecas - SISBI
Catalogação de Publicação na Fonte. UFRN - Biblioteca Setorial Prof. Leopoldo Nelson - -Centro de Biociências - CB

Capitani, Leonardo.
Temperatura e recursos determinam interações competitivas, tróficas e tamanho corporal em peixes recifais do Atlântico Ocidental / Leonardo Capitani. - Natal, 2021.
143 f.: il.

Tese (Doutorado) - Universidade Federal do Rio Grande do Norte. Centro de Biociências. Programa de Pós-graduação em Ecologia.
Orientador: Prof. Dr. Ronaldo Angelini.
Coorientador: Prof. Dr. Guilherme Ortigara Longo.

1. Relações tróficas - Tese. 2. Temperatura - Tese. 3. Produtividade primária - Tese. 4. Recifes - Tese. 5. Modelagem - Tese. 6. Atlântico Ocidental - Tese. I. Angelini, Ronaldo. II. Longo, Guilherme Ortigara. III. Universidade Federal do Rio Grande do Norte. IV. Título.

RN/UF/BSCB CDU 574

Elaborado por KATIA REJANE DA SILVA - CRB-15/351

O que aprendi fazendo ciência?

Primeiro, não existe evidência cientifica definitiva e inquestionável. Segundo, somos limitados na capacidade de entender a realidade e por isso, viva a honestidade cientifica de afirmar que não sabemos com certeza absoluta. Terceiro, a união dos seres humanos é a única força global que pode e deve atuar constantemente para avançar na construção de um conhecimento científico que gere paz e justiça social. Esses três pontos me deixam com esperança e uma impressionante curiosidade de ver o quanto ainda será descoberto no futuro. Aceitar isso, conviver com a incerteza e ter fé na capacidade humana de vencer novos desafios me faz ser otimista para o futuro da humanidade e desse mundo maravilhoso e complexo no qual vivemos.

Leonardo Capitani

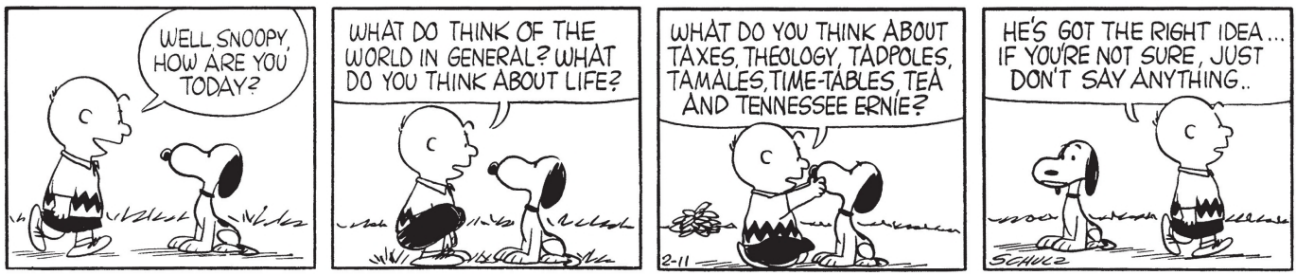

Charles M. Schulz, *The complete Peanuts: 1959-1960*.

Agradecimentos

Em primeiro lugar, obrigado, mãe. *Grazie mamma per avermi avviato sulla strada dell'ecologia e per essere sempre un' esempio di onestá, e lotta contro le ingiustizie e le diseguaglianze di questo mondo*.

Agradeço ao meu orientador, Prof. Ronado Angelini, que me deu a oportunidade de iniciar meu doutorado no PPG Ecologia de Natal. Ele sempre me apoiou e me ajudou não só no campo científico, mas também na esfera humana. Quase como um pai, foi sempre presente e teve palavras de carinho nos momentos de grande esforço e dificuldade. Sempre citarei o Ronaldo como exemplo para quem é pesquisador e faz um trabalho maravilhoso em um ambiente competitivo com muita pressão. Agradeço também ao meu co-orientador, Prof. Guilherme Longo, por acreditar no meu projeto de pesquisa, e por dar o exemplo de como fazer ciência inclusiva e incisiva sem ficar com raiva ou se impor de forma autoritária. Todo o Laboratório de Ecologia Marinha (LECOM) é uma grande família unida que me acolheu de braços abertos. Estou convencido que é e será um laboratório de referência nacional e internacional para o avanço da ciência brasileira no presente e no futuro.

Agradeço aos amigos e amigas / colaboradores com quem realizamos as pesquisas nos três capítulos desta tese, entre eles Dr. Júlio Neves de Araujo, Dr. Edson Vieira, Dr. Natalia Roos e Dr. Asta Audzijonyte. Em particular, quero agradecer a Luca Schenone, na Argentina, porque passamos horas e horas conversando sobre estatísticas e viramos amigos íntimos sem nem perceber. Muito obrigado Luca! Agradeço ao Prof. Paulo Inácio de Knegt López de Prado por manter momentos de encontro como a Southern-Summer School on Mathematical Biology em São Paulo. Destes eventos nascem as colaborações humanas fundamentais com as quais a ciência pode refletir o provérbio "a unidade faz a força".

Entre os amigos que conheci nestes quatro anos de doutorado, gostaria de citar entre todos, Emmanuel, Diego, Divna, Marco, Pedro e Lidiane. Considero a amizade uma das mais belas relações “ecológicas intra-específicas” que existem no planeta Terra e agradeço sinceramente a todos aqueles que me dirigiram uma palavra de carinho nos momentos difíceis. Porque é justo nos momentos difíceis que aparecem os amigos e as amigas. Também quero mencionar minha namorada Erika Talita, lindíssima, gentil e sensível como uma flor. Graças ao seu exemplo, Talita, descobri o quanto o ser humano pode mudar e melhorar.

Por fim, gostaria de agradecer ao sistema público nacional de educação brasileiro. Mas quero que o agradecimento seja uma homenagem a uma nação que sempre me acolheu com bondade e alegria, dando-me os meios materiais e espirituais para viver uma vida plena. Tenho e sempre terei palavras de grande admiração pelo Brasil e espero de todo o coração poder retribuir tudo o que tive tornando-me professor da rede pública. Em particular agradeço ao Programa de Pós-Graduação em Ecologia da UFRN que tem excelentes profissionais em seus diferentes níveis (professores, alunos e técnicos) e também sou grato a à Coordenação de Aperfeiçoamento de Pessoal de Nível Superior - Brasil (CAPES) - Código de Financiamento 001 pela bolsa de doutorado.

Espero agradecer a este país e seu sistema educacional que me acolheu desde o mestrado, despertando com esta tese, a curiosidade de quem é jovem e se pergunta por que o mar é azul ou como os peixes vivem debaixo d'água. Acredito firmemente que a educação é um dos meios mais poderosos para melhorar as injustiças e sofrimentos dos mais desfavorecidos e espero poder retribuir e contribuir com a educação brasileira nas próximas décadas sendo professor na rede publica.

Abstract

Reef ecosystems are the most complex, biodiverse and productive marine systems. Despite representing less than 0.09% of the surface of the oceans, these ecosystems sustain fundamental ecological processes, such as nutrient recycling, feeding, reproduction and evolution of many species. In these ecosystems there are non-linear relationships between physical variables (temperature, acidity, salinity, dissolved oxygen) and biotic components (primary production and species abundance). On the physical side, water temperature is a crucial factor that can affect the phenology, growth and trophic interactions of many reef species. On the side of biological interactions, it is known that the colonization of shallow waters by herbivorous fish may have facilitated the formation of reefs as we know them today, leading to specific changes in the trophic relationships within these environments. Surprisingly, there is a lack of general understanding on how temperature, resource availability and trophic interactions jointly shape reef environments in the western Atlantic Ocean. The study uses mathematical approaches to unravel reef trophic interactions and their dependence on temperature and resource availability, with enormous potential for the consolidation of ecological theories or the discovery of new ecological patterns. This thesis is organized in three chapters, in which we explore the relationship of temperature and available resources on reef species standing biomass in three different ways. **In the first chapter**, using a controlled field experiment on the reef of Rocas Atoll, we tested mechanistic models of the functional response of the fish *Acanthurus chirurgus* with its resource algae *Digenea simplex*. The results indicate that the herbivory process by *A. chirurgus* is best described by a model where the amount of algae and the density of *A. chirurgus* are equally important to define the per capita resource consumption. These results shed new light on the dynamics of herbivorous fish-algae interactions in the western Atlantic Ocean, highlighting the fundamental importance of considering the effect of consumer density on herbivore-plant models for reef ecosystems. **In the second chapter**, we modeled the food web of Rocas Atoll reef ecosystem and analyzed the changes in standing biomass and energy flow through all trophic levels in response to future warming over the 21st century. By the end of the century, total standing biomass will decrease by 1%, 8 % and 44% under low, medium and high ocean warming scenarios. As total biomass decreases, the ecosystem structure shifts and favor invertivorous fishes, suspension feeding zooplankton, and algal turfs while corals collapse. Moreover, we projected that the mean ecosystem trophic transfer efficiency will decrease by ~2% between 2012 and 2100, leading to less efficient and slower biomass transfers in the future reef state. Such food web degradation can alter the dominant biomass flow jeopardizing biomass replenishment, resulting in a less productive ecosystem with increasing dependency on pelagic energy subsidies. **In the third chapter**, we used data on reef fish body size over 61° degrees of latitude in the Western Atlantic (from North Carolina, USA to Santa Catarina, Brazil). We tested for the existence of a non-linear relationship between the mean fish body size and sea water temperature (SST). We found no clear indication that seawater temperature is affecting the mean body length of reef fish across species. We provide comprehensive evidence that 31% of species (n= 6) were smaller in warmer waters, while 15% (n = 3) were bigger in warmer waters throughout the species' natural distribution. We also found no relationship between the species' maximum observed length and the sensitivity to increasing sea water temperature in the spatial distribution range observed for each species. With this thesis, we hope to contribute to the construction of a more solid and general basis on the factors (physical and biological) that influence one of the most important biological processes in reef ecosystems: resource intake (predation) and the consequent conversion of resources into new living biomass.

Keywords: reef ecosystems, prey-predator interactions, temperature, primary productivity, functional response, Western Atlantic Ocean

Resumo

Os recifes são os ecossistemas marinhos mais complexos, biodiversos e produtivos. Embora representem menos de 0.09% da superfície dos oceanos, esses ambientes sustentam processos ecológicos fundamentais, como a reciclagem de nutrientes, alimentação, reprodução e evolução de muitas espécies. Nestes ecossistemas se dão relações não lineares entre variáveis físicas (temperatura, acidez, salinidade, oxigênio dissolvido) e componentes bióticos (produção primária e abundância das espécies). Entre as interações físicas, a temperatura da água é um fator crucial que pode afetar a fenologia, o crescimento e as relações tróficas de muitas espécies recifais. Entre as interações biológicas, é sabido que a colonização de águas rasas por peixes herbívoros pode ter facilitado a formação dos recifes como os conhecemos hoje em dia, levando a mudanças nas relações tróficas destes ambientes. Apesar de avanços recentes, ainda falta uma compreensão geral das relações de temperatura e interações tróficas em ambientes recifais do Atlântico Ocidental. Este estudo, com enfoque matemático das relações tróficas recifais e da dependência delas com a temperatura, foi feito em escalas local e regional, e com enfoques ecossistêmico, de comunidade e específico. Tentamos preencher uma lacuna de conhecimento e oferece uma oportunidade para o teste de teorias ecológicas, incluindo a descoberta de novos padrões macroecológicos. Esta tese está organizada em três capítulos, nos quais exploramos a relação da temperatura e de recursos disponíveis com as espécies de peixes recifais de três maneiras distintas. **No primeiro capítulo**, através de experimento de campo controlado no ecossistema recifal do Atol das Rocas, testamos modelos mecanicistas da resposta funcional do peixe herbívoro *Acanthurus chirurgus* com seu recurso alimentar a alga *Digenea simplex*. Os resultados indicam que o processo de herbívoria por *A. chirurgus* é melhor descrito por um modelo onde a quantidade de alga e a densidade de *A. chirurgus* são igualmente importantes para definir o consumo per capita de recurso. Estes resultados aportam nova luz sobre a dinâmica das interações peixes herbívoros - algas no Atlântico Ocidental, evidenciando a fundamental importância de considerar o efeito da densidade do consumidor em modelos peixe herbívoro-alga para ecossistemas recifais. **No segundo capítulo**, modelamos a teia trófica do Atol das Rocas e analisamos as mudanças na biomassa disponível e fluxos de energia em todos os níveis tróficos como uma resposta ao aquecimento do oceano ao longo do século 21. Os resultados suportam a hipótese que num Oceano Atlântico mais quente, as interações tróficas dos organismos recifais devem se modificar e diminuir, provocando uma diminuição na eficiência de transferência de biomassa para os consumidores primários e secundários. No caso do Atol das Rocas, até 2100, a biomassa total do ecossistema diminuirá em 1%, 8% e 44% nos cenários de baixas, médias e altas emissões de CO_2. Isto alterará a estrutura trófica do ecossistema recifal, deixando-o dominado por produtores primários (turfs de algas) e peixes invertívoros, enquanto predadores de topo, consumidores primários e corais escleractínios diminuirão severamente. Tal modificação da teia trófica diminuirá o fluxo de energia, o que resultará num ecossistema menos produtivo e com maior dependência de subsídios pelágicos. **No terceiro capítulo**, utilizamos dados de tamanho medio individual de peixes recifais ao longo de 61° graus de latitude no Atlântico Ocidental (desde a Carolina do Norte, EUA até Santa Catarina, Brasil), para testar a existência de um padrão não linear na relação entre o tamanho médio individual e a temperatura da água do mar. Os resultados obtidos indicam que não existe uma relação global não linear entre o comprimento médio de peixes e a temperatura da água do Oceano Atlântico. Ao, contrario, esta relação é especie-specifica: negativa para seis espécies e positiva para três espécies. Com esta tese, espero contribuir com a construção de uma base mais sólida e geral sobre os fatores (físicos e biológicos) que influenciam um dos processos mais importantes nos ecossistemas recifais: o consumo alimentar (predação) e a consequente conversão de recursos em nova biomassa disponível.

Palavras chaves: relações tróficas, resposta funcional, presa, predador, temperatura, produtividade primaria, recifes, modelagem, Atlantico Ocidental

Summary

General Introduction

How species interact?

How species interact to each other has always been an important area of research in Ecology (Berryman 1992, Abrams 2000). From the times of Lotka and Volterra in the 1920s, passing through the fundamental theoretical studies of Rosenzweig-MacArthur and Sir. Robert May of the 1960s and 1970s, a great deal of theory has accumulated on the use of mathematical models capable of faithfully representing the consumer-resource interactions (Lotka 1925, Volterra 1926, Rosenzweig and MacArthur 1963, May 1973). Ecologists have long wondered about the factors that regulate species' population fluctuations, and early research suggested that resource availability plays an important role (Kendall et al. 1999, Turchin 2003). Researchers found that when resources (food, nesting sites, or refuges) were limited, populations would decline as individuals competed for access to the limiting resources (Ivlev 1961, DeAngelis et al. 1975, Arditi and Ginzburg 1989). Such bottom-up control helped to regulate the population around carrying capacity (Arditi et al. 2004). More recently, scientists have discovered that predation can also influence the size of the prey population by acting as a top-down control (Scharf et al. 2000, Baum and Worm 2009, Detmer et al. 2017). In reality, the interaction between these two forms of population control work together to drive changes in populations over time (Carr et al. 2002, Sinclair et al. 2003, Hawlena et al. 2012).

In this sense, the consumer's functional response (e.g., the rate at which an individual consumer kills prey) turns out to be a very useful conceptualization for connecting population dynamics to individual-based explanations (Turchin 2003). While the standard assumption states that consumer's consumption rate is better described by a function of prey density only, the generality of this view remains debated on a theoretical basis and in the light of some empirical observations (e.g. consumer abundance often affects the consumption rate of individual consumers) (Arditi and Ginzburg 2012). Moreover,

consumer's functional response is an important element that link the behavior of individuals of the same species and the dynamics of populations of different trophic levels with consequences for the organization of biological communities and ecosystems process such as primary production and nutrient cycling (Jennings and Warr 2003, Schmitz et al. 2010, Hernández-León et al. 2020). At present, the most pressing task is to use both empirical measurements and theory to learn more about functional responses in complex systems, such as reef ecosystems.

Reef ecosystems: complex and unique environments in the marine realm

Reef ecosystems are one of the most important and unique ecosystems on our planet (Reaka-Kudla 1997, Knowlton et al. 2010, Heron et al. 2018), with two main features: high complexity of species interactions and high biological productivity (Odum and Odum 1955, Hatcher 1988, Fox et al. 2018). This last characteristic derives mainly from two factors: high structural complexity, and the connection with the oceanic pelagic system. Structural complexity and habitat diversity are positively related to fish abundance, species richness and trophic structure (Darling et al. 2017). Still, 41% of the reef fish's productivity derives from pelagic subsidies, and are essential to sustain the biodiversity and biomass of reef organisms (Morais and Bellwood 2019). On the contrary, but complementary, reefs are sources of energy and enrich ocean waters with organic matter dissolved through microbial production (Sorokin 1993). Therefore, reef environments offer enormous possibilities for studying ecological dynamics and the fundamental processes that regulate them.

Brazilian reef ecosystems: particularities

Brazilian reefs are distributed over about 3000 km, from 5º 50′N to 18º 00′S in the Western Atlantic Ocean (Aued et al. 2018). Sea surface temperature (SST) is the most conservative parameter along the Brazilian coast, varying in the north and northeast from 30°C during summer and fall (February to May) to 28°C from the end of winter to the beginning of summer (August to December), and in the east

coast from 30°C (February to May) to 27°C (July and August) (Banzon et al. 2016, Leão et al. 2019). The minimum temperature, however, shows a marked decrease from north to south. On the northeast coast, it decreases from 25°C during summer and fall, to 23°C during winter and spring; on the eastern coast, during winter, the minimum temperature can reach 21°C (Banzon et al. 2016).

Brazilian reef ecosystems have the least diverse but highly endemic coral fauna of all tropical provinces (16 corals hermatypic corals and five hydrocorals; ~30% endemism), being characterized by five endemic species well adapted to strong hydrodynamic conditions and a certain degree of sedimentation and water turbidity (Leão et al. 2019). The four coral endemic species of Brazil are *Mussismilia braziliensis*, *M. hispida, M. harttii, M. leptophylla,*(Leão et al. 2019). Coral bleaching is intensifying in the Indo-Pacific and the Caribbean (Hughes et al. 2017, Hoegh-Guldberg et al. 2018), however, this phenomenon does not appear, yet, to be as severe for Brazilian reefs (Mies et al. 2020). Moreover, other organisms such as calcareous algae can assume an equal or greater relevance than that of the corals themselves (Castro and Pires 2001, Leão et al. 2016).

About 711 species of fish inhabit the Brazilian reefs (Pinheiro et al. 2018). A quarter of this diversity is accountable to common and dominant species, while remaining species are rare. Low-latitude sites were more diverse in rare species (Araújo et al. 2020). Regarding taxonomy, 54.2% of these species are Perciformes, followed by Anguilliformes (7.3%) and Tetraodontiformes (5.5%). At family level we find Carangidae (35 species), followed by Gobiidae (31), Epinephelidae (25), Serranidae (25), Scorpaenidae (23), Labridae (21), Haemulidae (19) and Muraenidae (19). Most species are generalists (48%) with the ability to forage and reproduce in different habitats, reaching depths greater than 50 m (Ferreira et al. 2004, Pinheiro et al. 2018).

A subtle and constant threat: global warming

The increasing rise in ocean temperature have been affecting ecosystems more heavily in the last century (Zanna et al. 2019, Neukom et al. 2019). Globally, in the previous 200 years, biodiversity underwent abrupt changes (turnover) in its composition, with marine biomes exceeding, in alteration, terrestrial biomes by a magnitude of up to 20% (Blowes et al. 2019). In marine ecosystems, heat waves, which are likely to intensify in the future (both in intensity and frequency), are powerful disturbing agents with the ability to restructure and simplify entire ecosystems, causing coral bleaching, the decrease in biomass of macroalgae and kelp forests (Smale et al. 2019). These abrupt changes in species population dynamics of primary producers and bioconstruction organisms are likely to interrupt the supply of ecological goods and services by marine ecosystems in the coming decades (Trisos et al. 2020).

These changes are consequence of non-linear relationships between water temperature and species physiology. In this sense, animals have specific temperature limits and tolerance ranges (thermal niche), which determine their latitudinal distribution and sensitivity to global warming (Sunday et al. 2012, Sully et al. 2019). Principles potentially related to this pattern include the dependence of physiological rates on temperature and on oxygen demand (Pörtner 2002, Pörtner and Knust 2007). Thermal tolerance also changes during the species' life cycle (Pörtner and Peck 2010), meaning that the adult reproductive and embryo stages have narrower thermal tolerance ranges than larvae and non-reproductive adults (Dahlke et al. 2020). These results indicate that fish reproduction is highly sensitive to changes in sea water temperature, defining a high vulnerability to global marine fauna (Pörtner 2019).

Sea water temperature can also influence trophic (prey-predator) interactions between aquatic organisms (Bartley et al. 2019, Gibert 2019). It is known that the relationship between temperature and consumption per unit of time is unimodal and non-linear, being maximized at intermediate

temperatures in the thermal range of each species (Uiterwaal and DeLong 2020). In a complementary sense, the maximum size of the fish species and its feeding habit are important variables to predict somatic growth, especially in reef fish (Morais and Bellwood 2018). Several studies with predictive models show that even small changes in the size of fish species, such as a 4% reduction over 50 years, can lead to increased mortality and even a 30% reduction in biomass and productivity (Jørgensen and Fiksen 2010, Audzijonyte et al. 2013). A differential effect of temperature has recently been demonstrated on the specific maximum size of 335 species of reef fish in the Pacific, with positive or negative relationships (Audzijonyte et al. 2020). For the Western Atlantic, projections for the next 30 years point to a general reduction in the intensity of trophic relations in the tropical region, which may happen in other extratropical regions, changing the structure and functioning of the old ecosystems and creating new ones (Inagaki et al. 2020). The confirmation of these results at local and regional scale will imply that the standing biomass and the production of large marine predators will probably increase with the increase of oceanic temperatures, while the biomass and production of smaller prey species will decrease, affecting the structure and functioning of the reef ecosystems.

It is important to note that the persistence and productivity of marine organisms are influenced by a series of abiotic and biotic factors, with emphasis on temperature and trophic interactions. In the future, many of these species will be increasingly affected by climate change and its consequences (global warming, ocean acidification, oxygen reduction, nutrient redistribution and decrease in primary production, eutrophication, among others; Roessig et al. 2004, Hollowed et al. 2013, Pörtner 2019).

Therefore, obtaining a mechanistic and physiological-based understanding of how ocean warming affects (or can affect) marine flora and fauna is essential to generate reliable projections of the future effects of climate change (Koenigstein et al. 2016). Studies examining the consequences of ocean warming on marine organisms have mainly focused on the Indian-Pacific Oceans (Vergés et al.

2016, Brandl et al. 2018, Day et al. 2018, Rodgers et al. 2018), with much less studies conducted in the Atlantic Ocean (Bryndum−Buchholz et al. 2019, Lotze et al. 2019).

Thesis Objectives

Based on the theoretical background described above, this PhD dissertation aims to shed light on the non-linear relationship between abiotic (temperature) and biotic (resource-consumer interactions) factors that may affect Western Atlantic reef fish' biomass. The primary aims of this thesis are:

1 To determine whether consumer dependence through interference is likely to be a mechanism that affects the per capita consumption rate of an herbivorous fish species at typically observed consumer densities in a pristine tropical reef ecosystem. We tested the alternative hypotheses that the per capita consumption rate depends on either the resource density alone or both the algae and fish densities.

2 To test how ocean warming impact tropical reef food webs through shifts in standing biomass and energy flow in a pristine tropical reef ecosystem. Specifically, we hypothesize that local increases or decreases in functional groups/species' standing biomass during warming can be predicted by their thermal range (TR).We expect that the species with a reduced TR will be the ones that most have impacted their standing biomass compared to those species that have a wide TR (i.e., more than 2° C). Moreover, we expect that under ocean warming, the fraction of energy (e.g., biomass) transferred from one trophic level to the next will decrease, leading to less efficient and slower biomass transfers in the new reef ecosystem state.

3 (1) To describe empirical relationships between seawater temperature (SST) and mean fish body size across marine fish from temperate to tropical western Atlantic's reef ecosystems; (2) to test whether relationships between seawater temperature and mean fish body size depend on fish species. Specifically, we hypothesize that if SST affects fish body size, large-bodied species (maximum observed length > 35 cm) will be more likely to increase in mean body size with warming.

Thesis outline

Chapter 1: **Consumer-dependent functional response of a herbivorous reef fish in a field experiment**

In this chapter, using an experimental field approach, we tested if the consumer dependence through interference is likely to be a mechanism that affects the food intake rates of herbivore fish at typically observed consumer densities in a pristine tropical reef ecosystem. We tested the alternative hypothesis that the per capita consumption rate depends on the resource density alone or on the consumer and resource densities. We fitted functional response models, with or without consumer dependence, adopting a Bayesian inference approach. Based on the fitting models' results, we concluded that the per capita herbivore fish' consumption rate is consumer-dependent and that there is evidence of mutual interference among consumers. Our findings have an important influence on when and why herbivorous fish-algae populations fluctuate, how they are likely to evolve, and how they respond to environmental changes.

Chapter 2: **Ocean warming will reduce standing biomass in a tropical Western Atlantic reef ecosystem**

In this chapter, we modelled the food web of a tropical near-pristine reef ecosystem. We analyzed changes in standing biomass and energy flux across trophic levels as a response to climate change over the 21st century. By the end of the century, total living biomass would decrease by 1%, 8%, and 44% under the low, medium, and high ocean warming scenarios, respectively. This most extreme ocean warming scenario will dramatically reduce the biomass, forcing shifts in trophic composition, which will affect energy flow through the entire food web by declining the trophic transfer efficiency (TTE) and the biomass residence time (BTE), leading to a general degradation of the food web. Such food web degradation alters the dominant energy flow jeopardizing biomass replenishment, resulting in a

less productive ecosystem with increasing dependency on pelagic energy subsidies, reducing the resilience of tropical reef ecosystems.

Chapter 3: **Fish body size and temperature relationship: new insights from the Western Atlantic Ocean**

In this chapter we study whether fish body size increases or decreases along temperature gradient between marine fish species from 34°N and 27°S in the Western Atlantic Ocean (From North Carolina in Eastern USA to Santa Catarina in South Brazil). The effects of sea water temperature on fish body size are studied using 1,133 underwater video surveys made in between 2011 and 2014, representing 19 species in 17 locations across 61° of latitude of the Western Atlantic Ocean. We found no clear indication that seawater temperature is affecting the mean body length of reef fish across species. We provide comprehensive evidence that 31% of species (n= 6) were smaller in warmer waters, while 15% (n = 3) were bigger in warmer waters throughout the species' natural distribution. We also found no relationship between the species' maximum observed length and the sensitivity to increasing sea water temperature in the spatial distribution range observed for each species. The ecological and fitness implications of these results are difficult to predict but may impair predator-prey interactions and reshape food webs in the expected warmer Atlantic Ocean. Moreover, the non-linear and quantifiable connection between mean fish body size and sea-surface temperature provides new power to test and predict the response of fish to changing environmental conditions in the Western Atlantic Ocean reef ecosystems.

References

Abrams, P. A. 2000. The Evolution of Predator-Prey Interactions: Theory and Evidence. Annual Review of Ecology and Systematics 31:79–105.

Araújo, M. E. de, F. M. G. de Mattos, F. P. L. de Melo, L. de C. T. Chaves, C. V. Feitosa, D. L. Lippi, F. C. Félix Hackradt, C. W. Hackradt, J. L. S. Nunes, Z. M. de A. N. Leão, R. K. P. de Kikuchi, A. V. Ferreira Junior, P. H. C. Pereira, C. H. R. Macedo, C. L. S. Sampaio, and J. L. L. Feitosa. 2020. Diversity patterns of reef fish along the Brazilian tropical coast. Marine Environmental Research 160:105038.

Arditi, R., J.-M. Callois, Y. Tyutyunov, and C. Jost. 2004. Does mutual interference always stabilize predator–prey dynamics? A comparison of models. Comptes Rendus Biologies 327:1037–1057.

Arditi, R., and L. R. Ginzburg. 1989. Coupling in predator-prey dynamics: Ratio-Dependence. Journal of Theoretical Biology 139:311–326.

Arditi, R., and L. R. Ginzburg. 2012. How Species Interact: Altering the Standard View on Trophic Ecology. Oxford University Press, Oxford, New York.

Audzijonyte, A., A. Kuparinen, R. Gorton, and E. A. Fulton. 2013. Ecological consequences of body size decline in harvested fish species: positive feedback loops in trophic interactions amplify human impact. Biology letters 9:20121103.

Audzijonyte, A., S. A. Richards, R. D. Stuart-Smith, G. Pecl, G. J. Edgar, N. S. Barrett, N. Payne, and J. L. Blanchard. 2020. Fish body sizes change with temperature but not all species shrink with warming. Nature Ecology & Evolution 4:809–814.

Aued, A. W., F. Smith, J. P. Quimbayo, D. V. Cândido, G. O. Longo, C. E. L. Ferreira, J. D. Witman, S. R. Floeter, and B. Segal. 2018. Large-scale patterns of benthic marine communities in the Brazilian Province. PLOS ONE 13:e0198452.

Banzon, V., T. M. Smith, T. M. Chin, C. Liu, and W. Hankins. 2016. A long-term record of blended satellite and in situ sea-surface temperature for climate monitoring, modeling and environmental studies. Earth System Science Data 8:165–176.

Bartley, T. J., K. S. McCann, C. Bieg, K. Cazelles, M. Granados, M. M. Guzzo, A. S. MacDougall, T. D. Tunney, and B. C. McMeans. 2019. Food web rewiring in a changing world. Nature Ecology & Evolution 3:345–354.

Baum, J. K., and B. Worm. 2009. Cascading top-down effects of changing oceanic predator abundances. Journal of Animal Ecology 78:699–714.

Berryman, A. A. 1992. The Orgins and Evolution of Predator-Prey Theory. Ecology 73:1530–1535.

Blowes, S. A., S. R. Supp, L. H. Antão, A. Bates, H. Bruelheide, J. M. Chase, F. Moyes, A. Magurran, B. McGill, I. H. Myers-Smith, M. Winter, A. D. Bjorkman, D. E. Bowler, J. E. K. Byrnes, A. Gonzalez, J. Hines, F. Isbell, H. P. Jones, L. M. Navarro, P. L. Thompson, M. Vellend, C. Waldock, and M. Dornelas. 2019. The geography of biodiversity change in marine and terrestrial assemblages. Science 366:339–345.

Brandl, S. J., C. H. R. Goatley, D. R. Bellwood, and L. Tornabene. 2018. The hidden half: ecology and evolution of cryptobenthic fishes on coral reefs. Biological Reviews 93:1846–1873.

Bryndum‐Buchholz, A., D. P. Tittensor, J. L. Blanchard, W. W. L. Cheung, M. Coll, E. D. Galbraith, S. Jennings, O. Maury, and H. K. Lotze. 2019. Twenty-first-century climate change impacts on marine animal biomass and ecosystem structure across ocean basins. Global Change Biology 25:459–472.

Carr, M. H., T. W. Anderson, and M. A. Hixon. 2002. Biodiversity, population regulation, and the stability of coral-reef fish communities. Proceedings of the National Academy of Sciences 99:11241–11245.

Castro, C. B., and D. O. Pires. 2001. Brazilian coral reefs: What we already know and what is still missing. Bulletin of Marine Science 69:357–371.

Dahlke, F. T., S. Wohlrab, M. Butzin, and H.-O. Pörtner. 2020. Thermal bottlenecks in the life cycle define climate vulnerability of fish. Science 369:65–70.

Darling, E. S., N. A. Graham, F. A. Januchowski-Hartley, K. L. Nash, M. S. Pratchett, and S. K. Wilson. 2017. Relationships between structural complexity, coral traits, and reef fish assemblages. Coral Reefs 36:561–575.

Day, P. B., R. D. Stuart‐Smith, G. J. Edgar, and A. E. Bates. 2018. Species' thermal ranges predict changes in reef fish community structure during 8 years of extreme temperature variation. Diversity and Distributions 24:1036–1046.

DeAngelis, D. L., R. A. Goldstein, and R. V. O'Neill. 1975. A Model for Tropic Interaction. Ecology 56:881–892.

Detmer, T. M., J. H. McCutchan, and W. M. Lewis. 2017. Predator driven changes in prey size distribution stabilize secondary production in lacustrine food webs. Limnology and Oceanography 62:592–605.

Ferreira, C. E. L., S. R. Floeter, J. L. Gasparini, B. P. Ferreira, and J. C. Joyeux. 2004. Trophic structure patterns of Brazilian reef fishes: a latitudinal comparison. Journal of Biogeography 31:1093–1106.

Fox, M. D., G. J. Williams, M. D. Johnson, V. Z. Radice, B. J. Zgliczynski, E. L. A. Kelly, F. L. Rohwer, S. A. Sandin, and J. E. Smith. 2018. Gradients in Primary Production Predict Trophic Strategies of Mixotrophic Corals across Spatial Scales. Current Biology 28:3355-3363.e4.

Gibert, J. P. 2019. Temperature directly and indirectly influences food web structure. Scientific Reports 9:1–8.

Hatcher, B. G. 1988. Coral reef primary productivity: A beggar's banquet. Trends in Ecology & Evolution 3:106–111.

Hawlena, D., M. S. Strickland, M. A. Bradford, and O. J. Schmitz. 2012. Fear of Predation Slows Plant-Litter Decomposition. Science 336:1434–1438.

Hernández-León, S., R. Koppelmann, E. Fraile-Nuez, A. Bode, C. Mompeán, X. Irigoien, M. P. Olivar, F. Echevarría, M. L. Fernández de Puelles, J. I. González-Gordillo, A. Cózar, J. L. Acuña, S. Agustí, and C. M. Duarte. 2020. Large deep-sea zooplankton biomass mirrors primary production in the global ocean. Nature Communications 11:6048.

Heron, S. F., R. van Hooidonk, J. Maynard, K. Anderson, J. C. Day, E. Geiger, O. Hoegh-Guldberg, T. Hughes, P. Marshall, D. O. Obura, and C. M. Eakin. 2018. Impacts of Climate Change on World

Heritage Coral Reefs: Update to the First Global Scientific Assessment. UNESCO World Heritage Centre, Paris.

Hoegh-Guldberg, O., E. V. Kennedy, H. L. Beyer, C. McClennen, and H. P. Possingham. 2018. Securing a Long-term Future for Coral Reefs. Trends in Ecology & Evolution 33:936–944.

Hollowed, A. B., M. Barange, R. J. Beamish, K. Brander, K. Cochrane, K. Drinkwater, M. G. Foreman, J. A. Hare, J. Holt, and S. Ito. 2013. Projected impacts of climate change on marine fish and fisheries. ICES Journal of Marine Science 70:1023–1037.

Hughes, T. P., M. L. Barnes, D. R. Bellwood, J. E. Cinner, G. S. Cumming, J. B. C. Jackson, J. Kleypas, I. A. van de Leemput, J. M. Lough, T. H. Morrison, S. R. Palumbi, E. H. van Nes, and M. Scheffer. 2017. Coral reefs in the Anthropocene. Nature 546:82–90.

Inagaki, K. Y., M. G. Pennino, S. R. Floeter, M. E. Hay, and G. O. Longo. 2020. Trophic interactions will expand geographically but be less intense as oceans warm. Global Change Biology n/a.

Ivlev, V. S. 1961. Experimental Ecology of the Feeding of Fishes. Yale University Press.

Jennings, S., and K. J. Warr. 2003. Smaller predator-prey body size ratios in longer food chains. Proceedings of the Royal Society of London. Series B: Biological Sciences 270:1413–1417.

Jørgensen, C., and Ø. Fiksen. 2010. Modelling fishing-induced adaptations and consequences for natural mortality. Canadian Journal of Fisheries and Aquatic Sciences 67:1086–1097.

Kendall, B. E., C. J. Briggs, W. W. Murdoch, P. Turchin, S. P. Ellner, E. McCauley, R. M. Nisbet, and S. N. Wood. 1999. Why Do Populations Cycle? A Synthesis of Statistical and Mechanistic Modeling Approaches. Ecology 80:1789–1805.

Knowlton, N., R. E. Brainard, R. Fisher, M. Moews, L. Plaisance, and M. J. Caley. 2010. Coral reef biodiversity. Life in the world's oceans: diversity distribution and abundance:65–74.

Koenigstein, S., F. C. Mark, S. Gößling‐Reisemann, H. Reuter, and H.-O. Poertner. 2016. Modelling climate change impacts on marine fish populations: process-based integration of ocean warming, acidification and other environmental drivers. Fish and Fisheries 17:972–1004.

Leão, Z. M. A. N., R. K. P. Kikuchi, B. P. Ferreira, E. G. Neves, H. H. Sovierzoski, M. D. M. Oliveira, M. Maida, M. D. Correia, R. Johnsson, Z. M. A. N. Leão, R. K. P. Kikuchi, B. P. Ferreira, E. G.

Neves, H. H. Sovierzoski, M. D. M. Oliveira, M. Maida, M. D. Correia, and R. Johnsson. 2016. Brazilian coral reefs in a period of global change: A synthesis. Brazilian Journal of Oceanography 64:97–116.

Leão, Z. M. A. N., R. K. P. Kikuchi, and M. D. M. Oliveira. 2019. The Coral Reef Province of Brazil. Pages 813–833 *in* C. Sheppard, editor. World Seas: an Environmental Evaluation (Second Edition). Academic Press.

Lotka, A. J. 1925. Elements of Physical Biology. Williams and Wilkins Company.

Lotze, H. K., D. P. Tittensor, A. Bryndum-Buchholz, T. D. Eddy, W. W. L. Cheung, E. D. Galbraith, M. Barange, N. Barrier, D. Bianchi, J. L. Blanchard, L. Bopp, M. Büchner, C. M. Bulman, D. A. Carozza, V. Christensen, M. Coll, J. P. Dunne, E. A. Fulton, S. Jennings, M. C. Jones, S. Mackinson, O. Maury, S. Niiranen, R. Oliveros-Ramos, T. Roy, J. A. Fernandes, J. Schewe, Y.-J. Shin, T. A. M. Silva, J. Steenbeek, C. A. Stock, P. Verley, J. Volkholz, N. D. Walker, and B. Worm. 2019. Global ensemble projections reveal trophic amplification of ocean biomass declines with climate change. Proceedings of the National Academy of Sciences 116:12907–12912.

May, R. 1973. Stability and Complexity in Model Ecosystems. Princeton University Press, Princeton, NJ, USA.

Mies, M., R. B. Francini-Filho, C. Zilberberg, A. G. Garrido, G. O. Longo, E. Laurentino, A. Z. Güth, P. Y. G. Sumida, and T. N. S. Banha. 2020. South Atlantic Coral Reefs Are Major Global Warming Refugia and Less Susceptible to Bleaching. Frontiers in Marine Science 7.

Morais, R. A., and D. R. Bellwood. 2018. Global drivers of reef fish growth. Fish and Fisheries 19:874–889.

Morais, R. A., and D. R. Bellwood. 2019. Pelagic Subsidies Underpin Fish Productivity on a Degraded Coral Reef. Current Biology 29:1521-1527.e6.

Neukom, R., N. Steiger, J. J. Gómez-Navarro, J. Wang, and J. P. Werner. 2019. No evidence for globally coherent warm and cold periods over the preindustrial Common Era. Nature 571:550–554.

Odum, H. T., and E. P. Odum. 1955. Trophic Structure and Productivity of a Windward Coral Reef Community on Eniwetok Atoll. Ecological Monographs 25:291–320.

Pinheiro, H. T., L. A. Rocha, R. M. Macieira, A. Carvalho‐Filho, A. B. Anderson, M. G. Bender, F. D. Dario, C. E. L. Ferreira, J. Figueiredo‐Filho, R. Francini‐Filho, J. L. Gasparini, J.-C. Joyeux, O. J. Luiz, M. M. Mincarone, R. L. Moura, J. de A. C. C. Nunes, J. P. Quimbayo, R. S. Rosa, C. L. S. Sampaio, I. Sazima, T. Simon, D. A. Vila‐Nova, and S. R. Floeter. 2018. South-western Atlantic reef fishes: Zoogeographical patterns and ecological drivers reveal a secondary biodiversity centre in the Atlantic Ocean. Diversity and Distributions 24:951–965.

Pörtner, H. O. 2002. Climate variations and the physiological basis of temperature dependent biogeography: systemic to molecular hierarchy of thermal tolerance in animals. Comparative Biochemistry and Physiology Part A: Molecular & Integrative Physiology 132:739–761.

Pörtner, H.-. O. 2019. Special Report on the Ocean and Cryosphere in a Changing Climate.

Pörtner, H. O., and R. Knust. 2007. Climate Change Affects Marine Fishes Through the Oxygen Limitation of Thermal Tolerance. Science 315:95–97.

Pörtner, H. O., and M. A. Peck. 2010. Climate change effects on fishes and fisheries: towards a cause-and-effect understanding. Journal of fish biology 77:1745–1779.

Reaka-Kudla, M. L. 1997. The global biodiversity of coral reefs: a comparison with rain forests. Biodiversity II: Understanding and protecting our biological resources 2:551.

Rodgers, G. G., J. M. Donelson, M. I. McCormick, and P. L. Munday. 2018. In hot water: sustained ocean warming reduces survival of a low-latitude coral reef fish. Marine Biology 165:73.

Roessig, J. M., C. M. Woodley, J. J. Cech, and L. J. Hansen. 2004. Effects of global climate change on marine and estuarine fishes and fisheries. Reviews in fish biology and fisheries 14:251–275.

Rosenzweig, M. L., and R. H. MacArthur. 1963. Graphical Representation and Stability Conditions of Predator-Prey Interactions. The American Naturalist 97:209–223.

Scharf, F. S., F. Juanes, and R. A. Rountree. 2000. Predator size-prey size relationships of marine fish predators: interspecific variation and effects of ontogeny and body size on trophic-niche breadth. Marine Ecology Progress Series 208:229–248.

Schmitz, O. J., D. Hawlena, and G. C. Trussell. 2010. Predator control of ecosystem nutrient dynamics. Ecology Letters 13:1199–1209.

Sinclair, A. R. E., S. Mduma, and J. S. Brashares. 2003. Patterns of predation in a diverse predator–prey system. Nature 425:288–290.

Smale, D. A., T. Wernberg, E. C. J. Oliver, M. Thomsen, B. P. Harvey, S. C. Straub, M. T. Burrows, L. V. Alexander, J. A. Benthuysen, M. G. Donat, M. Feng, A. J. Hobday, N. J. Holbrook, S. E. Perkins-Kirkpatrick, H. A. Scannell, A. Sen Gupta, B. L. Payne, and P. J. Moore. 2019. Marine heatwaves threaten global biodiversity and the provision of ecosystem services. Nature Climate Change 9:306–312.

Sorokin, Y. I. 1993. Coral Reef Ecology. Springer Science & Business Media.

Sully, S., D. E. Burkepile, M. K. Donovan, G. Hodgson, and R. van Woesik. 2019. A global analysis of coral bleaching over the past two decades. Nature Communications 10:1–5.

Sunday, J. M., A. E. Bates, and N. K. Dulvy. 2012. Thermal tolerance and the global redistribution of animals. Nature Climate Change 2:686–690.

Trisos, C. H., C. Merow, and A. L. Pigot. 2020. The projected timing of abrupt ecological disruption from climate change. Nature:1–6.

Turchin, P. 2003. Complex Population Dynamics: A Theoretical/Empirical Synthesis. Princeton University Press.

Uiterwaal, S. F., and J. P. DeLong. 2020. Functional responses are maximized at intermediate temperatures. Ecology 101:e02975.

Vergés, A., C. Doropoulos, H. A. Malcolm, M. Skye, M. Garcia-Pizá, E. M. Marzinelli, A. H. Campbell, E. Ballesteros, A. S. Hoey, A. Vila-Concejo, Y.-M. Bozec, and P. D. Steinberg. 2016. Long-term empirical evidence of ocean warming leading to tropicalization of fish communities, increased herbivory, and loss of kelp. Proceedings of the National Academy of Sciences 113:13791–13796.

Volterra, V. 1926. Fluctuations in the Abundance of a Species considered Mathematically. Nature 118:558–560.

Zanna, L., S. Khatiwala, J. M. Gregory, J. Ison, and P. Heimbach. 2019. Global reconstruction of historical ocean heat storage and transport. Proceedings of the National Academy of Sciences 116:1126–1131.

Chapter 1

Title

Consumer-dependent functional response of a herbivorous reef fish in a field experiment

Leonardo Capitani[1,2,*], Natalia Roos[1,2], Guilherme Ortigara Longo[1,2], Ronaldo Angelini[1,3], Luca Schenone[4]

[1] Post-Graduate Program in Ecology, Bioscience Institute, Universidade Federal do Rio Grande do Norte, Natal, 59072-970, Brazil

[2] Marine Ecology Laboratory, Department of Oceanography and Limnology, Universidade Federal do Rio Grande do Norte, Natal, RN, 59014-002, Brazil

[3] Department of Civil Engeneering, Universidade Federal do Rio Grande do Norte, Natal, 59078-970, Brazil

[4] Laboratorio de Limnología, INIBIOMA (CONICET-UNCo), Quintral 1250, San Carlos de Bariloche (8400), Río Negro, Argentina

* Corresponding Author. Email: leonardocapitani@icloud.com.

OIKOS

Consumer-dependent functional response of a herbivorous reef fish in a field experiment

Journal:	*Oikos*
Manuscript ID	OIK-08502
Wiley - Manuscript type:	Research
Keywords:	consumer-resource interactions, mutual interference, Acanthurus chirurgus, consumer-dependence, field experiment, Digenea simplex

Abstract:	In theoretical ecology, the quantity of resource consumed by a consumer per unit of time, defined as functional response, is of paramount importance. To better understand how species interact and vary over time, it is necessary to analyze whether consumer's functional response depends on resource density alone (which is the reference assumption) or on both resource and consumer densities. There are few field studies that, by varying the resource and consumer densities, provide solid empirical evidence on which is the most suitable model of functional response in complex systems, such as coral reefs. We performed a field experiment with a herbivorous surgeonfish and their resource, a red seaweed, in a near-pristine reef ecosystem. We measured algal consumption while varying densities of consumers and resources. We fit nine alternative functional response models, which either included or excluded consumer-dependence. The model selection and the parameter estimation indicated that the functional response of the herbivorous surgeonfish depended on both resource and consumer densities. These results imply that, within a given density, surgeonfishes can share resources but individual's consumption rate decreased with higher fish densities. These results also suggest that mutual intraspecific interference exists at herbivorous fish densities generally observed in the field and it should be considered in predicting consumption rates by herbivorous reef fishes. Finally, this study implies that models incorporating consumer-dependence must be considered for understanding herbivorous fish and algae population dynamics when placed in the context of the most biodiverse ecological communities, such as reef ecosystems.

Abstract

In theoretical ecology, the quantity of resource consumed by a consumer per unit of time, defined as functional response, is of paramount importance. To better understand how species interact and vary over time, it is necessary to analyze whether consumer's functional response depends on resource density alone (which is the reference assumption) or on both resource and consumer densities. There are few field studies that, by varying the resource and consumer densities, provide solid empirical evidence on which is the most suitable model of functional response in complex systems, such as coral reefs. We performed a field experiment with a herbivorous surgeonfish and their resource, a red seaweed, in a near-pristine reef ecosystem. We measured algal consumption while varying densities of consumers and resources. We fit nine alternative functional response models, which either included or excluded consumer-dependence. The model selection and the parameter estimation indicated that the functional response of the herbivorous surgeonfish depended on both resource and consumer densities. These results imply that, within a given density, surgeonfishes can share resources but individual's consumption rate decreased with higher fish densities. These results also suggest that mutual intraspecific interference exists at herbivorous fish densities generally observed in the field and it should be considered in predicting consumption rates by herbivorous reef fishes. Finally, this study implies that models incorporating consumer-dependence must be considered for understanding herbivorous fish and algae population dynamics when placed in the context of the most biodiverse ecological communities, such as reef ecosystems.

Key words: consumer-resource interactions, mutual interference, *Acanthurus chirurgus*, *Digenea simplex*, field experiment, consumer-dependence, Bayesian inference

Introduction

In consumer-resource interaction theory, predation is quantified by determining the average consumption rate per consumer, known as the consumer's functional response (Turchin 2003). Functional response plays an important role in consumer-resource interactions because it connects individual behavioral-level processes (e.g., foraging behavior) and community-level processes (e.g., consumers can only be produced from the resources they consume; Pimm 1982, Polis and Winemiller 1996). Mathematical models on functional response have been used since the 1920s (Lotka 1925, Volterra 1926), leading to many new formalizations of ecological processes, such as disease epidemics, food web dynamics, and other important biological phenomena (Murray 2002, McCann 2012, Weitz 2015). A large part of our ability to explain how ecosystems are structured and how ecosystems function is thus directly linked to our ability to define which functional response model adequately captures the observed predation patterns (May 1973, Drossel et al. 2004, Kalinkat et al. 2013).

Since the 1950s, functional response models considered two main ecological factors: (1) the resource density and (2) the density of consumers (but see Turchin 2003). In resource-dependent models, functional response is assumed to be a function of resource density alone (e.g., Holling 1959). On the other hand, ratio-dependent models represent a special case of consumer dependence in which the consumption rate depends on the resource-to-consumer ratio (Arditi and Ginzburg 1989). In the last 50 years, more complex models have been proposed to account for the role of interference among consumers by mechanically defining it with further parameters (Ivlev 1961, Hassell and Varley 1969, Arditi and Akçakaya 1990). These models defined as "consumer-dependent" have had empirical validation in various studies in the

laboratory and in the field (Zimmermann et al. 2015, Prokopenko et al. 2017, Novak and Stouffer 2020). Nowadays, both resource and consumer densities are known to be important to describe the consumer's functional response, in terrestrial and aquatic ecosystems (Abrams and Ginzburg 2000, Skalski and Gilliam 2001, DeLong and Vasseur 2011).

Functional response models comparison has only been explored concerning a few herbivore-resource interactions, with no clear empirical evidence supporting either functional response form (Crawley 1997, Fortin et al. 2004, Fussmann et al. 2005). Many empirical herbivore-plant studies used experimental designs that made it impossible to detect anything other than resource dependence because the consumption experiments were carried out with a single herbivore individual (Hobbs et al. 2003, Morozov 2010, Xu et al. 2016). Therefore, a modelling shortcoming remains over which of the two classic functional response forms represents ecosystem dynamics where herbivores interact directly or indirectly while foraging.

Marine herbivorous fishes are critical in determining the structure and dynamics of shallow reef ecosystems and play a key role in carbon and nutrient fluxes (Clements et al. 2009, Bonaldo et al. 2014, Plass−Johnson et al. 2015). Empirical evidence has indicated a negative relationship between herbivore fish per capita energy reserves (i.e., liver mass/total mass index) and total fish density, suggesting that resource availability and consumer density determine individuals' physiological condition (Tootell and Steele 2016). However, social foraging (e.g., a group formed by more than one fish individual) is indicated as a biological mechanism that increases the per capita resource intake by enhancing the ability of herbivorous fish to locate specific food items, especially when resources are either scarce or patchily distributed (Michael et al. 2013). In the southwestern Atlantic Ocean, agonistic interactions were more frequent where herbivorous

fish were most abundant but there was no clear relationship between interference competition and foraging patterns (Francini-Filho et al. 2010). It is important to consider that these agonistic interactions can strongly affect the amount of algae consumed by the fish and the resulting rate at which the fish move energy and materials through the reef ecosystem (Gil and Hein 2017). Despite considerable efforts and debate seeking to disentangle how herbivores shape reef marine ecosystems (Steneck et al. 2017), few field experimental studies have quantified the role of intraspecific interactions on the herbivore fish per capita consumption rate (Lewis and Wainwright 1985, Vergés et al. 2009).

We combined field experiments and mathematical modelling to determine whether consumer dependence through interference affects the per capita consumption rates of herbivorous fishes in southwestern Atlantic Ocean's reef ecosystems. We used the herbivorous surgeonfish, *Acanthurus chirurgus* (Perciformes, Acanthuridae), and the red seaweed, *Digenea simplex* (Rhodophyta, Rhodomelaceae), as an experimental consumer-resource pair in the field and tested the alternative hypotheses that the per capita consumption rate depends on either the resource density alone or both the resource and consumer densities. We fitted nine functional response models, which either included or excluded consumer dependence, adopting a Bayesian inference approach (Ellison 2004). Specifically, our goal was to examine whether the herbivorous fish' functional response was resource-, ratio- or consumer-dependent. Our field experiment and modelling analysis suggest that consumer dependence is likely to be an important factor influencing the effects of herbivorous fish on the structure and dynamics of reef ecosystems.

Methods

Model organisms and study location

We measured the per capita consumption rate of the surgeonfish (*A. chirurgus*) feeding on the red seaweed (*D. simplex*), its primary diet item (Longo et al. 2015), in a tide pool in Rocas Atoll (32º 00' W to 34º 00' W longitude and 03º 30'S to 04º 30' S latitude, Figure 1). The area of the pool where the study was conducted was about 595 m^2.

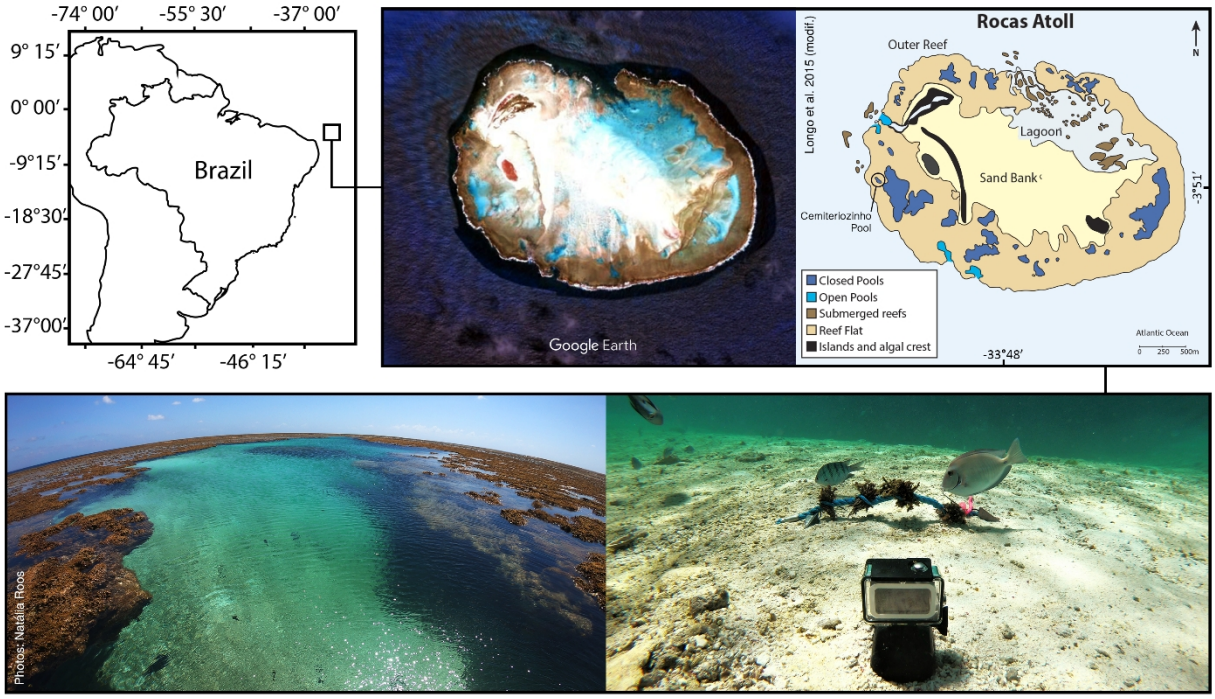

Figure 1 Study area location for the functional response underwater video experiments in the Rocas Atoll, Brazil. Top right panel: exact location of the closed pool "Cemiteriozinho" where experiments were made (area = 595 m^2); Left bottom: photograph shows the emerged part of the "Cemiteriozinho" pool. Right bottom: photograph shows the experiment setup with GoPro camera and *Acanthurus chirurgus* individual in frame. Photographs credits: Dr. Natalia Roos. Maps of the Rocas Atoll were retrieved and adapted from Google Maps and Longo et al. 2015.

In this pool, hardly any *D. simplex* were available for fish to eat, as they were mostly covered by sand. The surgeonfish *A. chirurgus* is a diurnal grazer that mostly feeds on algae and organic detritus found on compacted sand and rocky bottoms (Choat et al. 2002, Ferreira and Gonçalves 2006, Longo et al. 2015). Since its intense feeding activity reduces spatial

147 competition between corals and algae, *A. chirurgus* is widely recognized as a critical functional
148 species on reef ecosystems (Marshell and Mumby 2015, Longo et al. 2019). The red seaweed *D.*
149 *simplex* is a common tropical to warm-temperate species with a disjunct distribution in the
150 tropical to warm-temperate Atlantic and Pacific Oceans (Pakker et al. 1996). In Rocas Atoll *D.*
151 *simplex* is uncommon within tide pools but it is very abundant in the reef plateau where it finds
152 shelter against herbivores, since it is the most consumed seaweed by herbivorous fishes in this
153 area (Longo et al. 2015). Rocas Atoll has a 7.5 km^2 of emerged area and is the only atoll
154 formation in the southwestern Atlantic Ocean (Claudino-Sales 2019). It is considered a near-
155 pristine reef ecosystem because it presents unique environmental and geomorphologic
156 conditions, being the first marine protected area established in Brazil since 1979 where the only
157 human activity allowed on site is scientific research (Amado-Filho et al. 2016).

158 *Functional response experiments*
159
160 The experiments consisted in 15-minute manipulative field trials in which algae was offered in
161 five different densities to a constant number of herbivorous fishes (Figure 2).

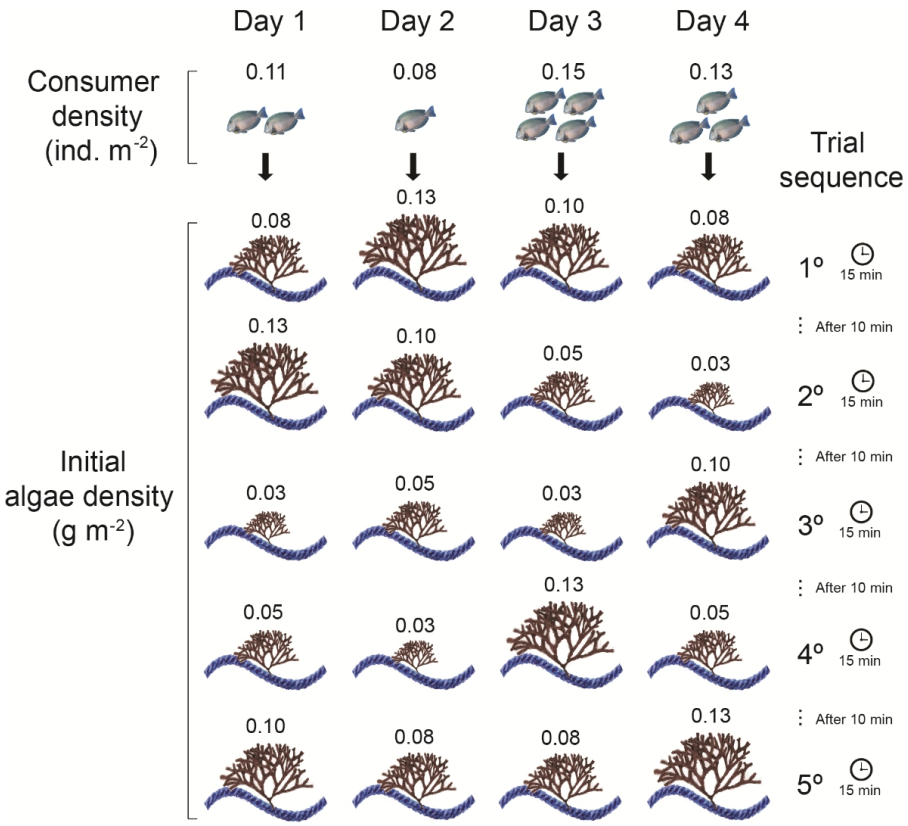

Figure 2. Experimental design used in the present study. Five trials per day were conducted in randomized orders over four different days. Each trial was recorded for 15 min with 10 min intervals between them. Per capita algae consumption rate was measured at factorial combinations of four consumer densities and five resource densities. Fishes and seaweeds are not to scale in this figure.

We conducted twenty trials over four non-consecutive days (i.e., five trials per day). Fish density was naturally controlled during low tides, because fishes get trapped in tide pools with no communication with the outer side of the Atoll ring (Longo et al. 2015). We assessed the number of *A. chirurgus* before the beginning of the trials through underwater visual censuses, which were conducted using the time-swim method in which the same expert diver identified and counted the fish in the pool for three minutes in each trial day. The *A. chirurgus* abundances observed in each day were 0.08, 0.11, 0.13 and 0.15 individuals·m^{-2} (50, 63, 79 and 90 individuals·pool^{-1} respectively). We collected *D. simplex* from the reef flat, placed in a mesh bag

and rotated ten times to remove the excess water before being weighted on a high precision scale (according to Longo et al. 2015). The algae densities offered were 0.03, 0.05, 0.08, 0.10, and 0.13 $g \cdot m^{-2}$ (15, 30, 45, 60, and 75 $g \cdot pool^{-1}$ respectively). Each algae density was then attached to 0.5 m length ropes and transported separately inside Ziploc bags to the experiment pool. Each rope had a control replicate that was placed in a cage of 1 cm mesh size to control for biomass loss due to hydrodynamics and handling procedures.

We conducted each feeding trial at low tide during the same period of the day (10:00 h to 14:00 h). Each trial was separated by a 10-minute break period. An underwater video camera (GoPro Hero model 7, 12 megapixels; 60 frames/s, GoPro Inc., San Mateo, California, USA) was positioned in front of each rope, approximately 1 m from the trial, to record the feeding activity of *A. chirurgus* on the algae and surrounding substrate (Figure 1). After this period, the rope and control were removed from the pool and stored in the Ziploc bags for posterior weighing after all trials were concluded. We analyzed the videos in slow motion to estimate the number of *A. chirurgus* individuals feeding on *D. simplex* per minute in each trial and the number of bites per minute in each trial.

Data processing

Grazing rates were determined on the basis of two measurements: (i) how much algae was grazed from each rope over the 15-minute trials (relative to the amount lost on the control rope), and (ii) the number of grazing bites observed over the same time period counted in 1 minute increments using the video recordings. First, the amount of algae consumed per trial (*AC*, g) was calculated as:

$$AC = \frac{W_i - W_f}{Wc_i \cdot Wc_f} \quad (1)$$

where W_i and W_f are the initial and final algae biomass in the trial rope, respectively, while Wc_i and Wc_f are the initial and final algae biomass in the control rope, respectively. Then, we estimated the consumption rate per minute (F_t, g min^{-1}) as:

$$F_t = \frac{AC}{TB} \cdot B \quad (2)$$

where TB is the total number of bites observed per trial and B is the number of bites observed per minute t (bites min^{-1}).

To account for algae depletion during the 15-minute trial, we use F_t to calculate changes in the algae density over time (N_t, g·m^{-2}):

$$N_t = \frac{N_{t-1} - F_t}{A} \quad (3)$$

where the total algae biomass at the minute t correspond to the previous biomass minus the biomass of algae consumed at minute t. To account for algae density, we divided the algae biomass by the total area of the tide pool (595 m^2). Finally, we calculated the per capita consumption rate (f_t, g ind^{-1} min^{-1}) as:

$$f_t = \frac{F_t}{Z_t} \quad (4)$$

where Z_t is the number of *A. chirurgus* individuals observed feeding on algae in that minute.

Models description

Nine functional response models (FR) were chosen to explain the observed per capita consumption rates f_t by herbivorous fish (Table 1): (1) a model consisted of a constant, density-

213 independent consumption rate (termed the "null model"), (2 to 4) the resource-dependent models
214 (Holling type I, type II and the simplified Ivlev model), (5 to 7) the pure ratio-dependent models
215 (Arditi-Ginzburg type I, type II and the Ivlev ratio-dependent model), and (8 and 9) the
216 consumer-dependent models that incorporate consumer-dependence through the use of an
217 additional parameter (Hassell and Varley 1969, Arditi and Akçakaya 1990).

218 **Table 1** Equations for the different functional response models: the null, the resource-dependent
219 (Holling type I and type II and Ivlev), the ratio-dependent (Arditi-Ginzburg type I and type II)
220 and the consumer-dependent (Hassell–Varley and Arditi-Akcakaya) models. N: resource
221 density; P: consumer density; a: attack rate, h: handling time; c: consumer maximum intake rate;
222 d: consumer satiation coefficient; m: consumer mutual interference coefficient.

Model name	Shape	Equation form (FR)	References
Null model	Constant	$f(N) = \alpha$	-
Resource-dependent models			
Holling type I (H1)	Linear	$f(N) = a \cdot N$	Holling 1959
Holling type II (H2)	Hyperbolic	$f(N) = a \cdot N / 1+(a \cdot h \cdot N)$	Holling 1959
Ivlev (IV)	Hyperbolic	$f(N) = c \cdot (1 - \exp[-d \cdot N])$	Ivlev 1961
Ratio-dependent models			
Arditi-Ginzburg type I (R1)	Linear	$f(N, P) = a \cdot (N/P)$	Arditi and Ginzburg 1989
Arditi-Ginzburg type II (R2)	Hyperbolic	$f(N, P) = a \cdot N / 1 + a \cdot h \cdot N/P$	Arditi and Ginzburg 1989
Ivlev (IVR)	Hyperbolic	$f(N) = c \cdot (1 - \exp[-d \cdot N/P])$	Ivlev 1961
Consumer-dependent models			
Hassell-Varley (P1)	Linear	$f(N, P) = a \cdot N \cdot P^{-m}$	Hassell and Varley 1969
Arditi-Akcakaya (P2)	Hyperbolic	$f(N, P) = a \cdot N/1 + a \cdot h \cdot N \cdot P^{-m}$	Arditi and Akçakaya 1990

223

In these models, we used as predictor variables: N_{t-1} which represents the changing density of the algae during the trial (particularly we use the density at the previous minute) and P , which represents the density of the herbivorous fish in the tide pool (i.e., total number of fishes divided by the area of the tide pool). Parameter a is the consumer's searching efficiency and it can be defined as the proportion of the resource encountered per consumer per unit of searching time (Turchin 2003). Parameter h is the handling time, assuming that consumers waste time handling the resource (Turchin 2003). For Ivlev models, c is the maximum consumer intake rate and d is the consumer satiation coefficient (Ivlev 1961). Finally, parameter m is the mutual interference between consumers, it generally designates the fact that increasing consumer density depresses the average individual consumer food intake (Arditi and Ginzburg 1989, 2012).

Model fitting and selection

We adopted a Bayesian framework to fit the functional response models, where the unknown parameters were treated as random variables (Ellison 2004). We assigned a prior distribution to the parameters to express our prior knowledge about them. Since consumption rate cannot take negative values, we choose positive half-normal distributions for the full probability model of our experimental data:

$$f_t \sim Normal\left(\mu, \sigma^2\right) T(0,) \tag{5}$$

where the mean (μ) was modelled with the functional response equations (FR) of Table 1 and a random intercept (b, Equation 6) to account the effect of the order in which the field experiments were carried out ("Sequence" in Equation 7). Finally, we choose a positive Cauchy distribution for the standard deviation (σ) of the full probability model (Equation 8).

$$\mu = b + FR \tag{6}$$

$$b \sim Sequence \quad (7)$$

$$\sigma \sim Cauchy(0,1) \quad (8)$$

We chose weakly informative priors for the functional response parameters, also defined on the positive reals. We chose the standard deviations of the parameters to only cover realistic values with enough prior uncertainty to be mostly informed by our data. Prior probability distributions for functional response parameters can be found in the supporting information (Appendix 1, Table S1).

We fitted the models using the *brm* function in the brms package within R (version 4.0.3, R Core Team 2020). The brms package provides an interface to fit generalized (non-)linear multivariate models using Stan performing full Bayesian inference (Carpenter et al. 2017, Bürkner 2017). Markov chain Monte Carlo sampling (MCMC) was run with 3 chains of 1500 iterations each, of which the first 500 were discarded as the burn-in. The last 1000 were used to generate posterior probability density ranges. The convergence of the MCMC chains was assessed by visually inspecting the chains and was tested using the Gelman-Rubin statistic (Gelman and Rubin 1992). Finally, we compared the fit accuracy of the functional response models using leave-future-out cross-validation (LFOCV), which is the recommended method for Bayesian model comparison when the data has temporal structure (Bürkner et al. 2020). The leave-future-out cross-validation method can be performed from the log-likelihood values of the posterior samples by using the loo package within R (Vehtari et al. 2017). The best model in terms of fit accuracy to our data was identified by applying Bayesian "stacking" weights based on their expected log-posterior predictive density (ELPD) according to Yao et al. (2018).

Results

Individuals of *A. Chirgurus* were observed to feed on the algae *D. simplex* throughout the entire time in all 20 trials and the seaweed was not fully consumed in any of them. The effect of the order of algae offered to the fish (random intercept *b* in Equation 7) showed similar posterior values for all the functional response models, indicating it was not a strong determinant of the per capita consumption rate (Appendix 1, Table S2).

The hyperbolic consumer-dependent model P2 provided the best fit accuracy to our data (weight = 0.52), followed by the linear consumer-dependent P1 model (weight = 0.48) (Table 2). The P2 functional response indicated that the maximum consumption rate (h^{-1}) was ~1.2 grams of algae consumed per minute (fitted parameters: a = 0.06 m^2 min^{-1}, 95% CI [0.01, 0.19], h = 0.83 minutes, 95% CI [0.04, 2.26]). On the other hand, the mutual interference parameter m for both P1 and P2 models were higher than 1 (1.59[1.11, 2.12] and 1.61[1.09, 2.21], respectively, Appendix 1, Table S2). Ratio-dependent functional response models (R1, R2 and IVR) showed an intermediate fit accuracy to data (lower ELPDs than consumer-dependent models). Finally, resource-dependent functional response models (H1, H2, and IV) and the null model showed a poor fit to data compared to the ratio and consumer-dependent models (lowest ELPDs, Table 2).

Table 2 Performance of herbivore fish functional response models relative to resource density (*Digenea simplex*) and consumer density (*Acanthurus chirurgus*). ELPD: expected log-posterior predictive density (higher values indicate a better fit to data); Grey rows identifies the best-fit models according to model weights; Boldface type identifies our selected best model.

Model	Parameters	Form	Variables	ELPD	Weights
P2	**3**	**Hyperbolic**	**Consumer-dependent**	**-39.96**	**0.52**
P1	2	Linear	Consumer-dependent	-39.93	0.48
R1	1	Linear	Ratio-dependent	-41.03	0

Model	Parameters	Form	Variables	ELPD	Weights
R2	2	Hyperbolic	Ratio-dependent	-41.11	0
IVR	2	Hyperbolic	Ratio-dependent	-41.19	0
IV	2	Hyperbolic	Resource-dependent	-46.69	0
H1	1	Linear	Resource-dependent	-46.83	0
H2	2	Hyperbolic	Resource-dependent	-46.85	0
Null	1	Constant	-	-52.06	0

From our field experiments, the per capita consumption rates of *A. chirgurus* on *D. simplex* were higher at intermediate to high algae densities (Figure 3a boxplots) and low fish densities (Figure 3b boxplots). The per capita consumption rate estimated by the best model (P2) was positively related to algae density (Figure 3a solid line) and negatively related to fish density (Figure 3b solid line). We also observed a pronounced increase in the per capita consumption rates with higher ratios between algae and fish densities (Figure 3c boxplots). Our best model predicted higher per capita consumption rates as the amount of algae per fish increases (Figure 3c solid line).

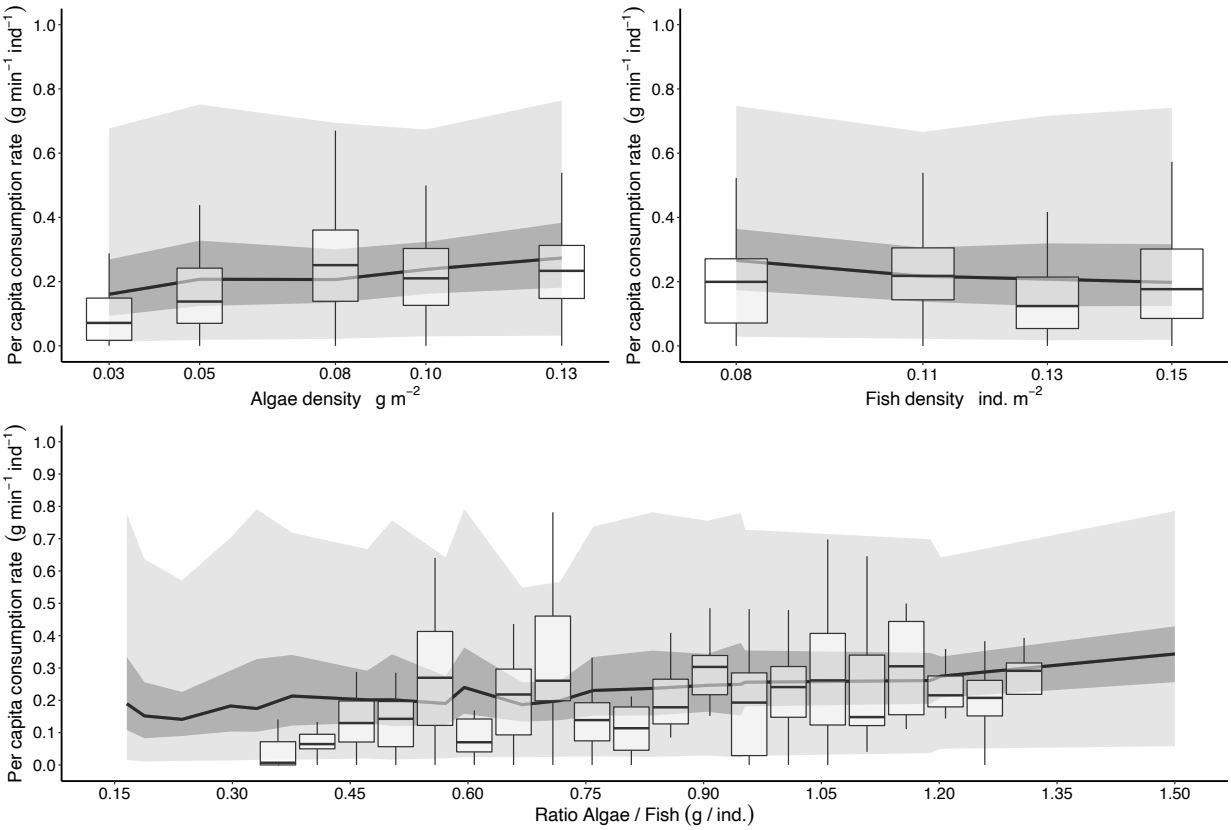

Figure 3 Observed functional response of *Acanthurus chirurgus* on *Digenea simplex* and prediction of the best-fit model P2 (hyperbolic consumer-dependent). a: per capita consumption rate versus algae density; b: per capita consumption rate versus fish density; c: per capita consumption rate versus the ratio between algae and fish densities. Boxplots represent the results from our field experiments (here, the line in the middle shows the median), while the solid line is the Bayesian posterior mean model prediction and the shaded regions are the 50% and 95% posterior credible intervals.

Discussion

To our knowledge, this study provides the first empirical evidence of consumer-dependence for the functional response of a marine herbivorous fish in its natural environment. We found that the consumer-resource interaction between the herbivorous fish *A. chirurgus* and the red seaweed *D. simplex* is best described by the consumer-dependent models, indicating that mutual interference reduces fish per capita consumption rate when their density is high. Such mutual interference exists at surgeonfish densities generally observed in the field (Vincent et al. 2011,

16

308 Morais et al. 2017, Hernández-Landa and Aguilar-Perera 2019). Therefore, mutual interference
309 by consumers should be considered as a biological mechanism by which herbivorous fish density
310 depresses individual consumption performance.

311 The hyperbolic functional responses are the most common forms in natural consumer-
312 resource interactions (Turchin 2003, Uiterwaal and DeLong 2020). Hyperbolic functional
313 response includes a handling time parameter (h), which biologically represents consumer's
314 satiation and mathematically represents an upper asymptote in the per capita consumption rate
315 (Holling 1959). We found that both the linear (P1) and the hyperbolic (P2) consumer-dependent
316 models showed a similar fit accuracy to our experimental data., which may be related to the
317 duration of our experimental trials. Our 15-minute trials represented less than 10% of the of
318 surgeonfish' residence time in the pool during the low-tide period (~4 h). Therefore, we suggest
319 that the hyperbolic P2 model would outperform the linear P1 model in the full low-tide period.
320 Nevertheless, despite the shape of the functional response, mutual interference is a crucial factor
321 to explain our experimental data better than pure resource- and ratio-dependent models, since
322 both P1 and P2 models are consumer-dependent.

323 Mutual interference between consumers arises from both behavioral and environmental
324 conditions (Cosner et al. 1999, Abrams and Ginzburg 2000, Francini-Filho et al. 2010). We
325 observed surgeonfish aggregation patterns around the algae during our field experiments, which
326 suggests that surgeonfish density is positively associated with algae density (Lawson et al. 1999).
327 Consumers should compete for resource-rich patches, meaning that resource spatial clustering
328 can further reduce consumption rates by increasing the opportunity for fish-fish interactions
329 (Levin et al. 2000, Osório et al. 2006). Mutual interference also emerges when the consumer's

individual home ranges are relatively large compared to the area available for foraging (Ginzburg and Jensen 2008). In our experimental system, fish are constrained to search for patchily distributed algae over a discrete area during a discrete time period (low tide). In such a situation, home ranges tend to overlap, and mutual interference may take place, leading to consumer density dependence in the herbivorous fish' per capita consumption rate (Nash et al. 2012, Welsh and Bellwood 2012).

Overall, our results add to a growing body of evidence supporting the idea that predator's consumption rate can be modelled by using resource and consumer density as explicative variables in ecosystem functioning (Arditi and Ginzburg 2012, Hossie and Murray 2016, Chan et al. 2017). Since the density of fish changes daily in our study system, we acknowledge that interference could shift from low to high levels as the herbivorous fish population size increases. This shift in mutual interference strength and, consequently, in consumer dependence may stabilize the biomass dynamics across trophic levels, consistent with field and theoretical predictions (Arditi et al. 2004, Griffen and Delaney 2008). Our results imply that functional response models that do not consider how herbivorous fish respond to one another could mischaracterize the consequent dynamics of fish and algae populations. These considerations fall among the scarce scientific studies that emphasize the role of intraspecific interactions among reef fish as an important explanatory variable for the flux of energy and materials through ecosystems (Hixon and Jones 2005, Gil and Hein 2017, Eurich et al. 2018).

The consumption of algae by herbivorous fish and the consequent excretion of essential nutrients such as N and P are fundamental ecological processes for the functioning and health of reef ecosystems around the world (Shantz et al. 2015, Robinson et al. 2018, Munsterman et al.

2021). By combining field experiments with a modelling approach, we found that the functional response of a herbivorous fish in heterogeneous reef ecosystem is consumer-dependent and that the final outcome of consumption is constrained by mutual interference. We suggest that future work investigate whether and how traits, such as body size, resource quality, movement rates, search strategies, and water temperature, affect mutual interference. The accumulation of evidence will allow clear mechanistic explanations of the effect of herbivory in one of the most complex and biodiverse marine ecosystems on Earth.

Acknowledgments

We thank Kevin McCann, Roger Arditi, Thierry Spataro, Eurico Noleto, Lucas Del Bianco Faria and Paulo Inácio de Knegt López de Prado who provided highly constructive comments on earlier versions of this manuscript. We thank Stefano Morselli for his help with the English revision and the Atol das Rocas Biological Reserve staff for fundamental logistical support. This study was financed in part by the Coordenação de Aperfeiçoamento de Pessoal de Nível Superior-Brasil (CAPES) - Finance Code 001(awarded to LC) and by the Brazilian Oceanic Long Term Monitoring Program PELD/ILOC (CNPq 441241/2016-6 to CEL Ferreira). NCR is currently a post-doctoral fellow supported by Serrapilheira Institute (Grant Number Serra-1708-15364 awarded to GOL). GOL is also grateful to a research productivity scholarship provided by CNPq (grant number 310517/2019-2).

Authors' contributions

Leonardo Capitani: Conceptualization (lead); Data curation (lead); Formal analysis (lead); Writing – original draft (lead); Writing – review and editing (lead).

Luca Schenone: Data curation (equal); Formal analysis (equal); Writing – original draft (equal); Writing – review and editing (equal).

Natalia Roos: Methodology: data collection (lead); Writing – original draft (supporting); Writing – review and editing (supporting).

Guilherme Ortigara Longo: Conceptualization (equal); Writing – original draft (supporting); Writing – review and editing (supporting).

Ronaldo Angelini: Conceptualization (equal); Writing – original draft (supporting); Writing – review and editing (supporting).

Data availability statement

Raw data and the R code for data analysis that support the findings of this study are free available from gitHub repository, https://github.com/leomarameo7/FR_herbivore_fish. Videos footages showing mutual interference behavior in surgeonfish *A. chirurgus* while eating algae are available from gitHub repository too, https://github.com/leomarameo7/FR_herbivore_fish. Complete high-quality video of the experimental trials are available on request to corresponding author.

References

Abrams, P. A. and Ginzburg, L. R. 2000. The nature of predation: prey dependent, ratio dependent or neither? - Trends in Ecology & Evolution 15: 337–341.

Amado-Filho, G. M. et al. 2016. Mesophotic ecosystems of the unique South Atlantic atoll are composed by rhodolith beds and scattered consolidated reefs. - Mar Biodiv 46: 933–936.

Arditi, R. and Ginzburg, L. R. 1989. Coupling in predator-prey dynamics: Ratio-Dependence. - Journal of Theoretical Biology 139: 311–326.

Arditi, R. and Akçakaya, H. R. 1990. Underestimation of mutual interference of predators. - Oecologia 83: 358–361.

Arditi, R. and Ginzburg, L. R. 2012. How Species Interact: Altering the Standard View on Trophic Ecology. - Oxford University Press.

Arditi, R. et al. 2004. Does mutual interference always stabilize predator–prey dynamics? A comparison of models. - Comptes Rendus Biologies 327: 1037–1057.

Bonaldo, R. M. et al. 2014. The ecosystem roles of parrotfishes on tropical reefs. - Oceanography and Marine Biology: An Annual Review 52: 81–132.

Bürkner, P.-C. 2017. brms: An R Package for Bayesian Multilevel Models Using Stan. - Journal of Statistical Software 80: 1–28.

Bürkner, P.-C. et al. 2020. Approximate leave-future-out cross-validation for Bayesian time series models. - Journal of Statistical Computation and Simulation 90: 2499–2523.

Carpenter, B. et al. 2017. Stan: A Probabilistic Programming Language. - Journal of Statistical Software 76: 1–32.

Chan, K. et al. 2017. Improving the assessment of predator functional responses by considering alternate prey and predator interactions. - Ecology 98: 1787–1796.

Choat, J. et al. 2002. The trophic status of herbivorous fishes on coral reefs. - Marine Biology 140: 613–623.

Claudino-Sales, V. 2019. Brazilian Atlantic Islands: Fernando de Noronha and Atol das Rocas, Brazil. - In: Claudino-Sales, V. (ed), Coastal World Heritage Sites. Coastal Research Library. Springer Netherlands, pp. 217–223.

Clements, K. D. et al. 2009. Nutritional ecology of marine herbivorous fishes: ten years on. - Functional Ecology 23: 79–92.

Cosner, C. et al. 1999. Effects of Spatial Grouping on the Functional Response of Predators. - Theoretical Population Biology 56: 65–75.

Crawley, M. J. 1997. Plant–Herbivore Dynamics. - In: Plant Ecology. John Wiley & Sons, Ltd, pp. 401–474.

DeLong, J. P. and Vasseur, D. A. 2011. Mutual interference is common and mostly intermediate in magnitude. - BMC Ecology 11: 1.

Drossel, B. et al. 2004. The impact of nonlinear functional responses on the long-term evolution of food web structure. - Journal of Theoretical Biology 229: 539–548.

Ellison, A. M. 2004. Bayesian inference in ecology. - Ecology Letters 7: 509–520.

Eurich, J. G. et al. 2018. Direct and indirect effects of interspecific competition in a highly partitioned guild of reef fishes. - Ecosphere 9: e02389.

Ferreira, C. E. L. and Gonçalves, J. E. A. 2006. Community structure and diet of roving herbivorous reef fishes in the Abrolhos Archipelago, south-western Atlantic. - Journal of Fish Biology 69: 1533–1551.

Fortin, D. et al. 2004. Multi-Tasking by Mammalian Herbivores: Overlapping Processes During Foraging. - Ecology 85: 2312–2322.

Francini-Filho, R. B. et al. 2010. Foraging activity of roving herbivorous reef fish (Acanthuridae and Scaridae) in eastern Brazil: influence of resource availability and interference competition. - Journal of the Marine Biological Association of the United Kingdom 90: 481–492.

Fussmann, G. F. et al. 2005. A Direct, Experimental Test of Resource Vs. Consumer Dependence. - Ecology 86: 2924–2930.

Gelman, A. and Rubin, D. B. 1992. Inference from Iterative Simulation Using Multiple Sequences. - Statistical Science 7: 457–472.

Gil, M. A. and Hein, A. M. 2017. Social interactions among grazing reef fish drive material flux in a coral reef ecosystem. - PNAS 114: 4703–4708.

Ginzburg, L. and Jensen, C. 2008. From controversy to consensus: the indirect interference functional response. - Proceedings of the International Association of Theoretical and Applied Limnology 30: 297–301.

Griffen, B. and Delaney, D. 2008. Species invasion shifts the importance of predator dependence. - Ecology 88: 3012–21.

Hassell, M. P. and Varley, G. C. 1969. New Inductive Population Model for Insect Parasites and its Bearing on Biological Control. - Nature 223: 1133–1137.

Hernández-Landa, R. C. and Aguilar-Perera, A. 2019. Structure and composition of surgeonfish (Acanthuridae) and parrotfish (Labridae: Scarinae) assemblages in the south of the Parque Nacional Arrecife Alacranes, southern Gulf of Mexico. - Mar Biodiv 49: 647–662.

Hixon, M. A. and Jones, G. P. 2005. Competition, Predation, and Density-Dependent Mortality in Demersal Marine Fishes. - Ecology 86: 2847–2859.

Hobbs, N. T. et al. 2003. Herbivore Functional Response in Heterogeneous Environments: A Contest among Models. - Ecology 84: 666–681.

Holling, C. S. 1959. The Components of Predation as Revealed by a Study of Small-Mammal Predation of the European Pine Sawfly. - The Canadian Entomologist 91: 293–320.

Hossie, T. J. and Murray, D. L. 2016. Spatial arrangement of prey affects the shape of ratio-dependent functional response in strongly antagonistic predators. - Ecology 97: 834–841.

Ivlev, V. S. 1961. Experimental Ecology of the Feeding of Fishes. - Yale University Press.

Kalinkat, G. et al. 2013. Body masses, functional responses and predator–prey stability. - Ecology Letters 16: 1126–1134.

Lawson, G. L. et al. 1999. Size-related habitat use and schooling behavior in two species of surgeonfish (Acanthurus bahianus and A. coeruleus) on a fringing reef in Barbados, West Indies. - Environmental Biology of Fishes 54: 19–33.

Levin, P. S. et al. 2000. Integrating individual behavior and population ecology: the potential for habitat-dependent population regulation in a reef fish. - Behavioral Ecology 11: 565–571.

Lewis, S. M. and Wainwright, P. C. 1985. Herbivore abundance and grazing intensity on a Caribbean coral reef. - Journal of Experimental Marine Biology and Ecology 87: 215–228.

Longo, G. O. et al. 2015. Between-Habitat Variation of Benthic Cover, Reef Fish Assemblage and Feeding Pressure on the Benthos at the Only Atoll in South Atlantic: Rocas Atoll, NE Brazil. - PLOS ONE 10: e0127176.

Longo, G. O. et al. 2019. Trophic interactions across 61 degrees of latitude in the Western Atlantic. - Global Ecology and Biogeography 28: 107–117.

Lotka, A. J. 1925. Elements of Physical Biology. - Williams and Wilkins Company.

Marshell, A. and Mumby, P. J. 2015. The role of surgeonfish (Acanthuridae) in maintaining algal turf biomass on coral reefs. - Journal of Experimental Marine Biology and Ecology 473: 152–160.

May, R. 1973. Stability and Complexity in Model Ecosystems. - Princeton University Press.

McCann, K. S. 2012. Food Webs. - Princeton University Press.

Michael, P. J. et al. 2013. Identity and behaviour of herbivorous fish influence large-scale spatial patterns of macroalgal herbivory in a coral reef. - Marine Ecology Progress Series 482: 227–240.

Morais, R. A. et al. 2017. Spatial patterns of fish standing biomass across Brazilian reefs. - Journal of Fish Biology 91: 1642–1667.

Morozov, A. Y. 2010. Emergence of Holling type III zooplankton functional response: bringing together field evidence and mathematical modelling. - J. Theor. Biol. 265: 45–54.

Munsterman, K. S. et al. 2021. A View From Both Ends: Shifts in Herbivore Assemblages Impact Top-Down and Bottom-Up Processes on Coral Reefs. - Ecosystems in press.

Murray, J. D. 2002. Mathematical Biology: I. An Introduction. - Springer-Verlag.

Nash, K. L. et al. 2012. Influence of habitat condition and competition on foraging behaviour of parrotfishes. - Marine Ecology Progress Series 457: 113–124.

Novak, M. and Stouffer, D. B. 2020. Systematic bias in studies of consumer functional responses. - Ecology Letters in press.

Osório, R. et al. 2006. Territorial defence by the Brazilian damsel Stegastes fuscus (Teleostei: Pomacentridae). - Journal of Fish Biology 69: 233–242.

Pakker, H. et al. 1996. Evolutionary and Ecological Differentiation in the Pantropical to Warm-Temperate Seaweed Digenea Simplex (rhodophyta)1. - Journal of Phycology 32: 250–257.

Pimm, S. L. 1982. Food Webs. - Chapman and Hall.

Plass‐Johnson, J. G. et al. 2015. Fish herbivory as key ecological function in a heavily degraded coral reef system. - Limnology and Oceanography 60: 1382–1391.

Polis, G. A. and Winemiller, K. O. 1996. Food Webs: Integration of Patterns & Dynamics. - Springer Science & Business Media.

Prokopenko, C. et al. 2017. Evaluation of alternative prey-, predator- and ratio-dependent functional response models in a zooplankton microcosm. - Canadian Journal of Zoology in press.

Robinson, J. P. W. et al. 2018. Environmental conditions and herbivore biomass determine coral reef benthic community composition: implications for quantitative baselines. - Coral Reefs 37: 1157–1168.

Shantz, A. A. et al. 2015. Fish-derived nutrient hotspots shape coral reef benthic communities. - Ecological Applications 25: 2142–2152.

Skalski, G. T. and Gilliam, J. F. 2001. Functional Responses with Predator Interference: Viable Alternatives to the Holling Type II Model. - Ecology 82: 3083–3092.

Steneck, R. S. et al. 2017. Herbivory in the marine realm. - Current Biology 27: R484–R489.

Tootell, J. S. and Steele, M. A. 2016. Distribution, behavior, and condition of herbivorous fishes on coral reefs track algal resources. - Oecologia 181: 13–24.

Turchin, P. 2003. Complex Population Dynamics: A Theoretical/Empirical Synthesis. - Princeton University Press.

Uiterwaal, S. F. and DeLong, J. P. 2020. Functional responses are maximized at intermediate temperatures. - Ecology 101: e02975.

Vehtari, A. et al. 2017. Practical Bayesian model evaluation using leave-one-out cross-validation and WAIC. - Stat Comput 27: 1413–1432.

Vergés, A. et al. 2009. Role of fish herbivory in structuring the vertical distribution of canopy algae Cystoseira spp. in the Mediterranean Sea. - Marine Ecology Progress Series 375: 1–11.

Vincent, I. et al. 2011. Biomass and Abundance of Herbivorous Fishes on Coral Reefs off Andavadoaka , Western Madagascar. - Western Indian Ocean Journal of Marine Science 10: 83–98.

Volterra, V. 1926. Fluctuations in the Abundance of a Species considered Mathematically. - Nature 118: 558–560.

Weitz, J. S. 2015. Quantitative Viral Ecology: Dynamics of Viruses and Their Microbial Hosts. - Princeton University Press.

Welsh, J. Q. and Bellwood, D. R. 2012. How far do schools of roving herbivores rove? A case study using Scarus rivulatus. - Coral Reefs 31: 991–1003.

Xu, M. et al. 2016. Comparative Functional Responses Predict the Invasiveness and Ecological Impacts of Alien Herbivorous Snails. - PLOS ONE 11: e0147017.

Yao, Y. et al. 2018. Using Stacking to Average Bayesian Predictive Distributions (with Discussion). - Bayesian Anal. 13: 917–1007.

Zimmermann, B. et al. 2015. Predator-dependent functional response in wolves: from food limitation to surplus killing. - Journal of Animal Ecology 84: 102–112.

Supporting information:
Appendix 1

Table S1 Definition and prior distributions for functional response models' parameters tested in this study.

Model	Parameter name	Prior distribution (mean, s.d.)
Null	α: constant maximum intake rate	Gaussian(0, 0.5)[0,]
all	Sequence	Gaussian(0, 0.5)
all	Res. Stand. Dev.	Cauchy(0, 0.1)
H1, H2, R1, R2, P1, P2	*a*: attack rate	Gaussian(0, 0.5)[0,]
H2, R2, P2	*h*: handling time	Gaussian(0, 2)[0,]
P1, P2	*m*: mutual interference	Gaussian(1, 0.5)
IV, IVR	*c*: maximum intake rate	Gaussian(0, 0.5)[0,]
IV, IVR	*d*: satiation coefficient	Gaussian(0, 2)[0,]

Table S2. Posterior summary and convergence statistics for all functional response models fitted. Res. Stand. Dev. = Residual Standard Deviation; Estimate = Posterior mean and [95% Bayesian credible interval]; ESS = Effective sample size; R̂hat = Gelman-Rubin Statistic.

Model	Parameter	Estimate	R̂hat	ESS
Null	α: constant maximum intake rate	0.32 [0.01; 0.86]	1	1047
Null	Sequence	-0.11 [-0.65; 0.21]	1	935
Null	Res. Stand. Dev.	0.44 [0.41; 0.48]	1	1813
H1	*a*: attack rate	1.08 [0.7; 1.45]	1	1434
H1	Sequence	0.13 [0.07; 0.19]	1	922
H1	Res. Stand. Dev.	0.42 [0.39; 0.46]	1	2236
H2	*a*: attack rate	1.14 [0.69; 1.63]	1	1507
H2	Sequence	0.13 [0.07; 0.2]	1	859
H2	*h*: handling time	0.8 [0.02; 2.46]	1	1429
H2	Res. Stand. Dev.	0.42 [0.39; 0.46]	1	2129
R1	*a*: attack rate	0.16 [0.13; 0.2]	1	1323
R1	Sequence	0.09 [0.05; 0.13]	1	791
R1	Res. Stand. Dev.	0.39 [0.36; 0.43]	1	2498
R2	*a*: attack rate	0.22 [0.14; 0.4]	1.01	884
R2	Sequence	0.08 [0.02; 0.12]	1	754

R2	*h*: handling time	0.8 [0.03; 2.22]	1.01	1006
R2	Res. Stand. Dev.	0.4 [0.36; 0.43]	1	2034
P1	*a*: attack rate	0.05 [0.01; 0.14]	1	1193
P1	Sequence	0.1 [0.06; 0.14]	1	982
P1	*m*: mutual interference	1.6 [1.06; 2.16]	1	1207
P1	Res. Stand. Dev.	0.39 [0.36; 0.42]	1	2082
P2	*a*: attack rate	0.06 [0.01; 0.19]	1	1308
P2	Sequence	0.09 [0.04; 0.14]	1	1114
P2	*h*: handling time	0.83 [0.04; 2.26]	1	1360
P2	*m*: mutual interference	1.61 [1.09; 2.21]	1	1493
P2	Res. Stand. Dev.	0.39 [0.36; 0.42]	1	2656
IV	*c*: maximum intake rate	0.66 [0.32; 1.23]	1	1588
IV	Sequence	0.11 [0.05; 0.18]	1	1022
IV	*d*: satiation coefficient	2.44 [0.99; 4.84]	1	1528
IV	Res. Stand. Dev.	0.42 [0.39; 0.46]	1	2401
IVR	*c*: maximum intake rate	0.61 [0.31; 1.15]	1	1238
IVR	Sequence	0.08 [0.02; 0.12]	1	1540
IVR	*d*: satiation coefficient	0.44 [0.15; 1.04]	1	1258
IVR	Res. Stand. Dev.	0.4 [0.37; 0.43]	1	1810

In this study we used Markov chain Monte Carlo (MCMC) techniques to draw samples from the Bayesian posterior probabilities. We ended up with a collection of parameter values, and the frequencies of these values correspond to the posterior plausibilities. We then did a picture of the posterior from the histogram of these samples. It is crucial to investigate whether the model fitting algorithm converged to its target, that is, the parameters' posterior distribution for fully Bayesian models. There are multiple ways to investigate convergence. We could do so graphically by looking at trace plots (Figure S1, Figure S2 for the best functional response models P2 and P1).

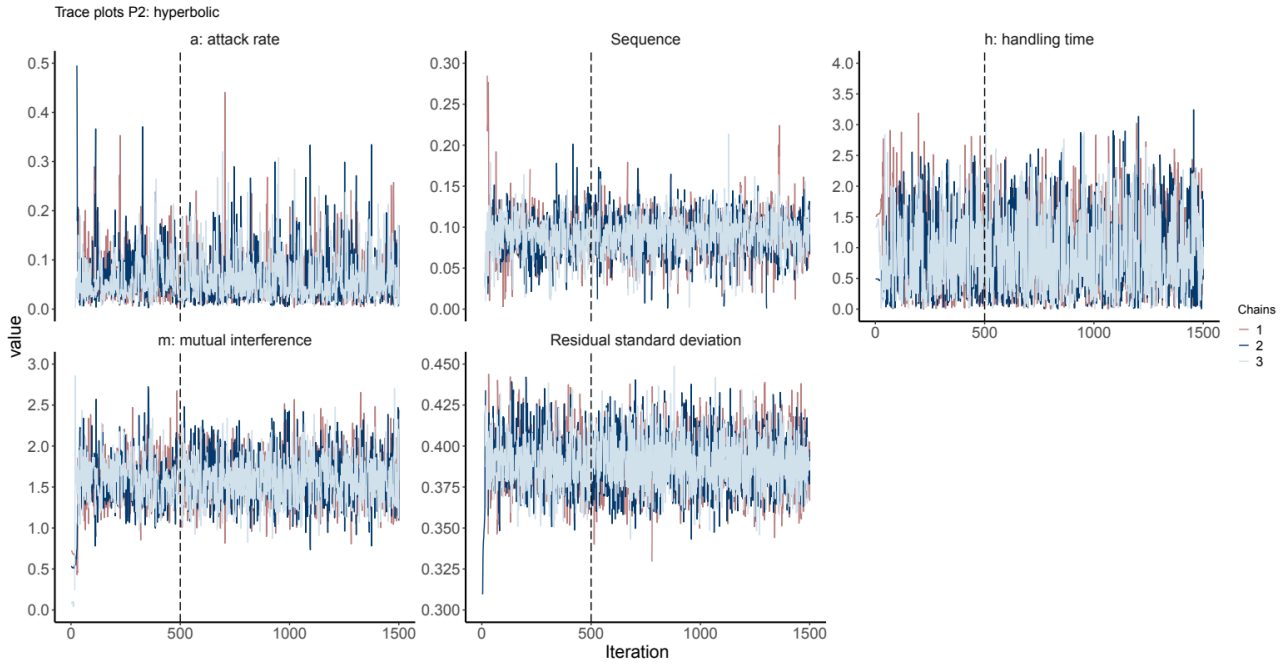

Figure S1. Trace plots of all relevant parameters of the hyperbolic consumer-dependent functional response model (P2). The first 500 draws (dashed line) in each chain are part of an adaptation phase that MCMC uses to tune the sampling algorithm and are discarded.

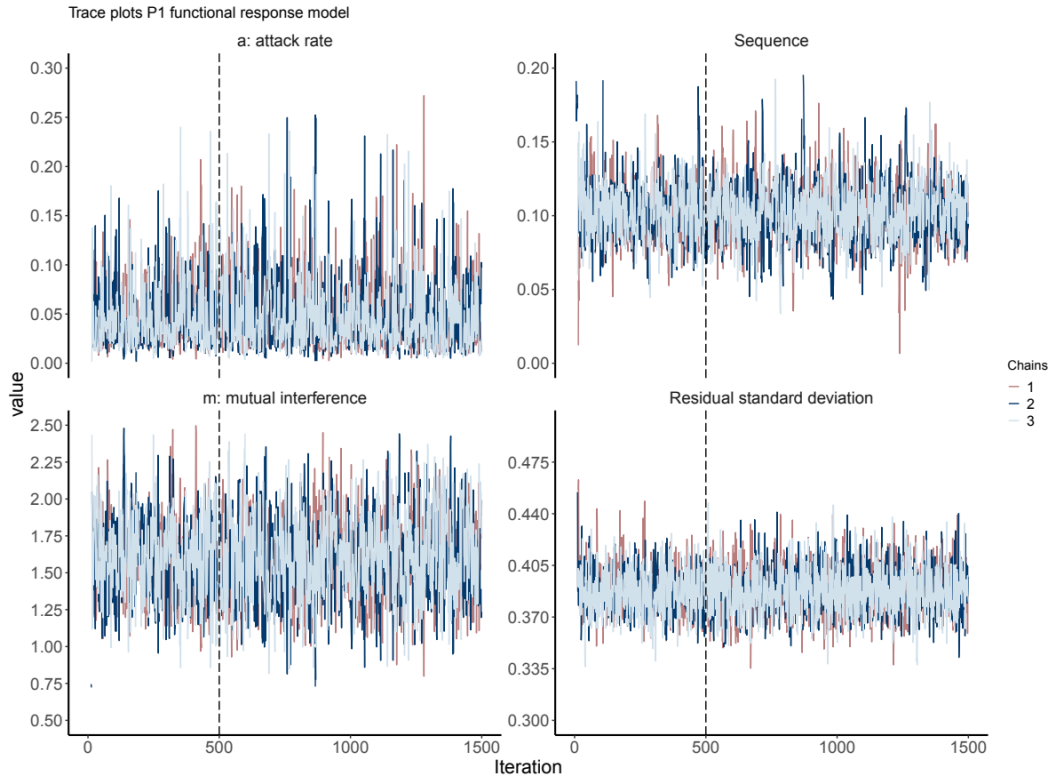

Figure S2. Trace plots of all relevant parameters of the linear consumer-dependent functional response model (R1). The first 500 draws (dashed line) in each chain are part of an adaptation phase that MCMC uses to tune the sampling algorithm and are discarded.

Chapter 2

Title: Ocean warming will reduce standing biomass in a tropical Western Atlantic reef ecosystem

Shortened version: Tropical reef biomass reduced by ocean warming

Leonardo Capitani[1,2,*], Julio Neves de Araujo[3], Edson A. Vieira[1,2], Ronaldo Angelini[1,4], Guilherme O. Longo[1,2].

[1] Post-Graduate Program in Ecology, Bioscience Center, Universidade Federal do Rio Grande do Norte, Natal, 59072-970, Brazil

[2] Marine Ecology Laboratory, Department of of Oceanography and Limnology, Universidade Federal do Rio Grande do Norte, Natal, 59014-002, Brazil

[3] Department of Oceanography, Universidade Federal do Espírito Santo, Vitória, 29075-910, Brazil

[4] Department of Civil Engeneering, Universidade Federal do Rio Grande do Norte, Natal, 59078-970, Brazil

Corresponding author

*Leonardo Capitani, Post-Graduate Program in Ecology, Bioscience Center, Natal, Brazil. Email: leonardocapitani@icloud.com

Telephone number: +55 84 981750704

Author contributions

LC, RA and GOL conceived the idea. LC, RA and JNA developed the Ecopath food web model and implement functional groups-specific temperature response functions. EV designed the figures. LC led the writing of the manuscript. All authors contributed critically to the draft and gave the final approval for publication. RA and GOL equally share the senior authorship of this study.

Abstract

Ocean warming is altering life on Earth from individuals to ecosystems. The impacts on standing biomass and food webs functioning are less evident due to the paucity of data and difficulty to generate reliable models. We modelled the food web of a tropical near-pristine reef ecosystem and analysed changes on living biomass across trophic levels as a response to ocean warming over the 21st century. By the end of the century, total standing biomass will decrease by 1%, 8 % and 44% under different ocean warming scenarios (from reduced RCP 2.6 emission scenario to business-as-usual RCP 8.5 scenario). As total biomass decreases, the ecosystem structure shifts favouring invertivorous fishes, suspension feeding zooplankton, and algal turfs while corals collapse. The mean trophic transfer efficiency is expected to decrease by ~2% between 2012 and 2100 under the RCP 8.5, while biomass residence time (mean time that a unit of biomass remains in the ecosystem) will decrease by ~10%. Such food web degradation can alter the dominant biomass flow jeopardizing biomass replenishment, resulting in a less productive ecosystem with increasing dependency on pelagic energy subsidies, reducing the resilience of tropical reef ecosystems.

Keywords: Predator-prey interactions, marine ecosystem, climate change, food web, modelling, atoll

Introduction

Human-induced warming is affecting ecosystems in all oceans (McCauley and others 2015; Lotze and others 2019). Rising temperatures will transform marine ecosystems into new configurations, towards more homogeneous and less stable biological communities (Sydeman and others 2015; Nolan and others 2018). The predicted ocean warming under high greenhouse-gas emissions scenarios will severely affect species distribution, abundance and extinction rates (Bryndum−Buchholz and others 2019; Pörtner and others 2019). Ocean warming will also affect trophic interactions and entire food webs that control the dynamics and stability of biological communities, as well as energy and matter flow within and across ecosystems (Zhang and others 2017; Gibert 2019; Inagaki and others 2020). Despite overlooked due to lack of data and difficulties in generating reliable models, predicting changes in food webs can help us understand the structure and dynamics of these novel and simplified ecosystems that are likely to emerge under ocean warming scenarios (Blanchard and others 2012).

The food web modelling approach allows, through the identification of species, the estimation of their biomass and their trophic relationships, to generate holistic descriptions on the functioning of the ecosystem studied (Polis and Winemiller 1996; Belgrano and others 2005). In the marine field, for example, since the 90s more than 400 studies have been described relating the functioning of the food web, disturbing factors such as fishing and climate change (Colléter and others 2015). A recent study notes that the trophodynamics of coastal marine ecosystems have already changed and are expected to amplify their rate of change in the coming decades (Pontavice and others 2020). Another study indicates that under a high ocean warming, total marine animal biomass declined by an ensemble mean of 15%-30% in the North and South Atlantic and Pacific, and the Indian Ocean by 2100, whereas polar ocean basins experienced at 20%-80% increase (Bryndum−Buchholz and others 2019). Thus, the food web modelling approach can help in defining which drivers, the importance of them and if and how there will be changes in the structure and functioning of marine ecosystems.

Coral reefs are among the most diverse and sensitive ecosystems on the planet, with multiple reports of severe impacts by ocean warming (Hughes and others 2017; Williams and others 2019). Major impacts on these ecosystems include coral bleaching leading to loss of structural complexity and diversity (Magel and others 2019), shifts in species distribution (Robinson and others 2019) and changes in the ecosystem trophic structure with increasing algal cover leading to an increase in the importance of microbes in the energy flow (i.e., microbialization; Haas and others 2016). Such deleterious impacts of ocean warming on ectotherms will be amplified if food intake is reduced, either because warming reduces standing food resources or because it restricts foraging time (Huey and Kingsolver 2019). Besides ecosystem functioning, the degradation of coral reefs threatens important services, including fisheries and tourism, on which millions of humans rely (Rogers and others 2018; Curnock and others 2019).

To understand the impacts of ocean warming on reef ecosystems, we investigated the potential future effects of human-induced ocean warming on standing biomass in reef food webs using a near-pristine tropical reef ecosystem in the Southwestern Atlantic Ocean as a model. Specifically, we hypothesize that local increases or decreases in the standing biomass of species during warming can be predicted by their thermal range (TR). We assume that the species with a reduced TR (i.e., less than 2° C) will be the ones that will have their standing biomass most impacted when compared to those species that have a wide TR (i.e., more than 2° C) (Burrows and others 2020; Fredston-Hermann and others 2020). We constructed and fitted a food web model based on primary data obtained in the field along a seven-year time series complemented with data from the literature. Then, we explored the temporal evolution of the ecosystem trophic structure through comparisons of standing biomass and transfer efficiency indicators. In the Ecopath model we incorporated species-specific thermal ranges and functional responses in order to test the impact of ocean warming under three projected scenarios predicted by the Intergovernmental Panel on Climate Change (IPCC; Pörtner and others 2019). Finally, we calculated biomass' transfer efficiency

indicators to assess the modifications in the structure and functioning of the Rocas Atoll's reef ecosystem under future ocean warming.

Methods

Study area

Rocas atoll is the only atoll formation in South Atlantic Ocean, laying approximately 230 km off the NE coast of Brazil (03°50'S, 33°49'W) as part of a seamount chain in the E-W direction known as the fracture zone of Fernando de Noronha. It has a surface area of 7.5 km^2 with large and shallow inner lagoon and reef flat areas (Supplementary Material, Figure S1; Longo and others 2015). The Rocas Atoll was established as a marine reserve in 1978 and effectively enforced since 1991 and is one of the few reef ecosystems in the western South Atlantic Ocean in a near-pristine condition (no local fishing, tourism or pollution). Since 2013, Rocas Atoll is annually monitored through the Brazilian Long-Term Ecological Research program (PELD-ILOC; http://peldiloc.sites.ufsc.br/) and is considered a natural laboratory to assess ocean warming impacts with minimal local direct anthropogenic impact. Our model includes the entire reef flat and pools that are formed during high and low tide (Supplementary Material, Figure S1).

Food web modelling

The model was built on the Ecopath with Ecosim (EwE) software version 6.6 (Christensen and Pauly 1993; Walters and others 1997, 2000). The equations and algorithms underlying the EwE framework are documented in Supplementary materials and extensively in the scientific literature (Christensen and Walters 2004; Heymans and others 2016). The model consisted of 28 functional groups: ranging from primary producers to herbivores and carnivores, but with the 13 fish species considered as individual model species. We included one non-living group (detritus). All functional groups were defined as adult ontogenetic phase. We aggregated several species into functional groups with other species of similar life history traits, diet composition and shared predators in the interest of keeping the model results easy to deal (Supplementary Material, Table S1). The functional groups are regulated by gains (consumption, production, and immigration) and losses

(natural mortality and emigration), which are linked to each other by trophic interactions (Supplementary Material, Table S2).

Model parameterization

We used the following input parameters: biomass (*B*), production per unit of biomass (*P/B*), consumption per unit of biomass (*Q/B*), diet matrix, and the model-estimated ecotrophic efficiency (*EE*) to build the food web models. *EE* describes the fraction of the productivity that is used in the system. Ecopath sets up a series of linear equations to solve for unknown values establishing mass-balance in the same operation.

All data were converted to biomass per unit area of reef ($g \cdot m^{-2}$) using conversion factors from the literature for fish and most mobile invertebrates, and our own determinations of coral and algal biomass per unit surface area (Longo and others 2015). Abundance-by-length estimates for fish species were taken from underwater visual censuses (UVC) between 2012 and 2018 and converted to biomass using length–weight relationships estimated with the local samples. Because there are no biomass estimates for benthic macro invertebrates and micro invertebrates in Rocas Atoll, we used the Ecotrophic Efficiency (EE), based on Heymans and others (2016), set to 0.9 and 0.85 for macro and micro invertebrates, respectively. For functional groups with multiple species, their biomasses were summed and then divided by the atoll area (7.5 km^2). For species that only occupy part of the area, the biomass parameter was pro-rated by area. Estimates of P/B and Q/B of fish were obtained from empirical equations (Pauly 1980; Palomares and Pauly 1998). For invertebrates, estimates for P/B and Q/B ratios were obtained from another South Atlantic Ecopath model (Araújo and others 2017).

Trophic relationships

Data on diet was obtained from stomach contents analysis, stable isotopes analysis, and primary literature (Supplementary Material, Tables S1 and Table S2). To help visualize the results, fish species were assigned to trophic guilds based on their diet and feeding behavior, including the way they capture, store, and transfer energy across trophic levels (Madin and others 2016). We have

defined four trophic guilds: reef sharks, generalist fish predators, invertivorous fish, herbivorous and detritivorous fish.

Fish biomass accumulation

Biomass accumulation values for fish species (Supplementary Material, Table S3) were calculated as the biomass in one year minus previous biomass averaged over six years (2012-2018).

Model fitting

The Rocas Atoll Ecopath model for the reference year 2012 was fitted to the time series data on fish biomass (14 species, period 2012-2018) using the temporal dynamic module of the Ecopath, named Ecosim (Walters and others 1997). Vulnerability parameters, for each predator/prey diet combination, are estimated using an optimization search routine in Ecosim (i.e., stepwise method), which reduces the sum of squares difference between the predicted and observed data (Scott and others 2016). The best-fit model is found and determined by the minimum difference between model predictions to time-series observations using the weighted sum of squared differences (SS) and the Akaike Information Criterion (AIC) (Akaike 1974), which penalizes for fitting too many parameters based on the number of time series available for estimating the SS. The best-fitted model (*status quo*) was able to reproduce the historical trends (Supplementary Material, Table S4 and Figure S3).

Biomass dynamics projections under ocean warming scenarios

We ran simulations (using the Ecosim module) on biomass dynamics based on fish time-series data and using temperature projections from 2018 to 2100. We present species-specific biomass dynamics and compare each ocean warming scenario relative to a hypothetical future with no changes in sea temperature by 2100 (status quo scenario) using the average percent variation of the relative biomass.

Three Representative Concentration Pathways (RCP 2.6, RCP 4.5, and RCP 8.5) were used for projections of the future ocean warming in the Coupled Model Intercomparison Project Phase 5 (Taylor and others 2012). They are identified by their approximate anthropogenic radiative forcing

178 (in $W \cdot m^{-2}$, relative to 1750) by 2100 (Pörtner and others 2019). Future sea surface temperature
179 values were extracted from the Royal Netherlands Meteorological Institute Climate Explorer portal
180 (http://climexp.knmi.nl) within the study area location. Thirty-two model outputs were extracted for
181 the study area with temperatures fluctuating around their mean. Current average seawater
182 temperature in Rocas Atoll's is 27.3º C, which by 2100, is expected to rise 0.5º C, 1.3º C and 3º C
183 under the low (RCP 2.6), medium (RCP 4.5) and high (RCP 8.5) ocean warming scenarios,
184 respectively (Supplementary Material, Figure S2).

185 Optimal temperatures and thermal ranges were defined for each modelled functional group
186 using 5th and 95th percentiles estimates for minimum and maximum preferable and
187 survivable temperatures from AquaMaps (Kaschner and others 2019) (Figure 1). We checked
188 the reliability of the AquaMaps data based on expert knowledge about species-specific
189 thermal ranges and habitat usage. For functional groups with multiple species, temperature
190 ranges were averaged and weighted by biomass. In Ecosim, optimal temperatures and
191 temperature ranges were included as species temperature Gaussian response functions as has
192 already been done in other research using the EwE approach in analysing the temporal
193 dynamics of fish biomass under increasing sea temperature (Bentley and others 2017; Serpetti
194 and others 2017; Corrales and others 2018). Species thermal performance followed the classic
195 bell shape supported by field data (Payne and others 2016; Childress and Letcher 2017;
196 Waldock and others 2019) and physiological models (Angilletta 2009; Neubauer and
197 Andersen 2020). The thermal performance curves were then used to modify the feeding rate of
198 each functional group/species within the model, where the maximum feeding rate occurred at
199 the optimum temperature, and feeding rates declined as temperature departed from the
200 optimum. It follows that reduced feeding rates would lead to reduced biomass. The intercept
201 between each species-specific thermal performance curves and the annual average sea water
202 temperature were used to calculate a factor to modify the predator consumption rates with a
203 maximum multiplier of 1 for optimum temperature (Bentley and others 2017). The multiplier

declines as the average sea water temperature deviates from the optimum at a rate determined by the thermal performance curve standard deviations (Bentley and others 2017; Serpetti and others 2017; Corrales and others 2018).

Therefore, for each predator-prey interaction, consumption rates were calculated as (1):

$$Q_{ij} = \frac{a_{ij} \cdot v_{ij} \cdot B_i \cdot P_j \cdot T_j \cdot M_{ij} / D_j}{v_{ij} + (v_{ij} \cdot T_i \cdot M_{ij}) + (a_{ij} \cdot M_{ij} P_i \cdot T_j / D_j)} \cdot f(Env_{function}, t) \quad (1)$$

where a_{ij} is the rate of effective search for prey (i) by predator (j), v_{ij} is the vulnerability parameter, T_i represents prey relative feeding time, T_j is the predator relative feeding time, B_i is prey biomass, P_j is the predator biomass, M_{ij} is the mediation forcing effects, and D_j represents effects of handling time as a limit to consumption rate. Environmental response functions ($Env_{function}$, t) represent the tolerance of a species to an environmental parameter (here based on the minimum and maximum levels and on the 5th and 95th percentiles; Figure 1). We used the Environmental response function to account for changes in sea surface temperature over time.

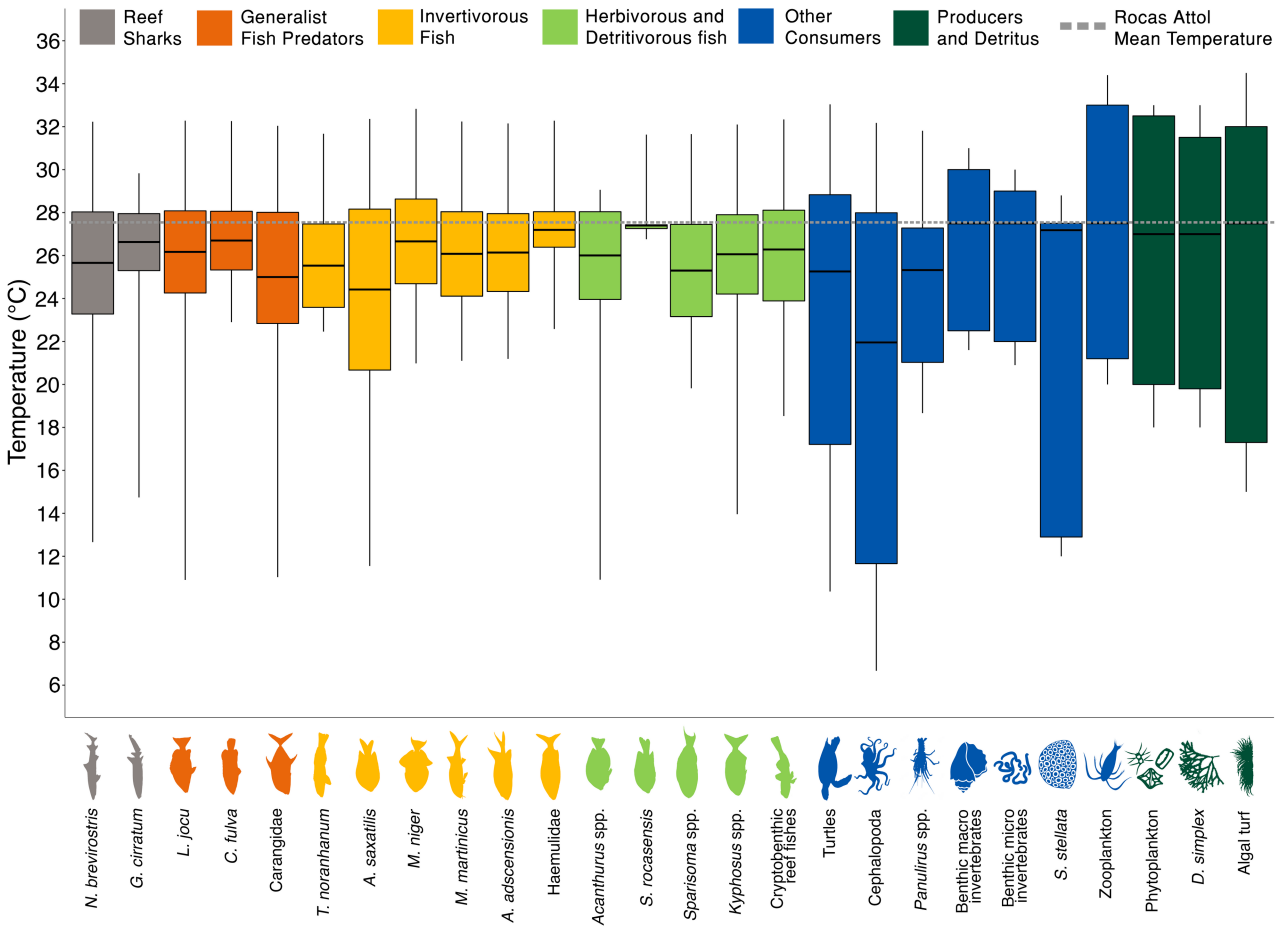

Figure 1 Functional groups/species temperature ranges for functional groups/species in the Rocas Atoll reef ecosystem food web model. Box plots represent optimum temperature (bold black line), the lower and upper hinges correspond to the 5th and 95th percentiles and the end of the whiskers as maximum and minimum temperatures for each functional group/species.

Assessing uncertainty

The Monte Carlo routine in Ecosim was used to perform sensitivity analyses for projections of biomass dynamics under ocean warming (Steenbeek and others 2018). This routine tests the sensitivity of Ecosim's output to Ecopath input parameters by drawing input parameters from a uniform distribution centered on the base Ecopath value with the coefficients of variation (CV) set to default 0.1 (Christensen and Walters 2004; Steenbeek and others 2018). In our study, we set coefficients of variation as 0.1 for B (biomass per unit area), P/B (Production/Biomass), Q/B (Consumption/Biomass), and Biomass Accumulation parameters for the functional groups/species of which we do not have detailed information over at least three years of local sampling. For the functional groups/species of which we had time series observed data, we defined the CV as the ratio between the standard deviation and the mean value of each fish standing biomass time series (Supplementary Material, Table S5). We ran 250 Monte Carlo simulations for each scenario based on coefficients of variation to determine the 95% confidence intervals.

Trophic Transfer Efficiency (TTE) and Biomass Residence Time (BRT) indicators

To describe the impacts of ocean warming on the Rocas Atoll's reef ecosystem structure we used two time-dependent indicators that summarize biomass transfer efficiency through the food web and are expected to change in a warming ocean: the trophic transfer efficiency (TTE) and the Biomass Residence Time (BRT) (Pontavice and others 2020). The TTE indicator (%) is the fraction of biomass production transferred from one trophic level (TL) to the next and summarizes all the food web losses at each TL. The BRT indicator (years) is the average amount of time that a biomass unit spends at a given TL before trophic transfer to higher TLs in the food web through predation. The BRT is inversely proportional to the speed of biomass transfer across TLs. Five input parameters were used to estimate the trophic transfer efficiency (TTE) and the biomass residence time (BRT):

P/B (Production to Biomass), P/Q (Production to Consumption), Q/B (Consumption to Biomass), BA (Biomass accumulation rate) and EE (Ecotrophic Efficiency). For each functional group/species, the parameters P/B, Q/B, P/Q, BA and EE were extracted from the deterministic dynamic simulations of Ecosim every 10 years, from 2012 to 2100 for each RCP scenario. Then, for each functional group/species the parameters P/B, Q/B and P/Q were distributed over a range of trophic classes (following a lognormal distribution and using classes with a width of 0.1 TL) according to an established methodology implemented in the R package EcoTroph (Colléter and others 2015). In our analysis, we estimated TTE and BRT indicators from trophic level TL= 2 to TL= 4. Thus, the values of TTE and BRT reflect mean estimates from trophic levels 2–3 and from trophic levels 3–4, every 10 years of ocean warming simulation scenarios. We refer to the detailed description on how to calculate the TTE and BRT indicators in the publication of Pontvice and others 2020 and the specific R code associated with the repository of this study https://github.com/leomarameo7/Atoll_Rocas_project.

Results

Simulated biomass changes under ocean warming scenarios

Total standing biomass through the food web was severely reduced under warming (Figure 2 and Figure 3A). Qualitative visual food web analysis suggest that ocean warming weakened many trophic interactions, especially in trophic level 2 due to the severe reduction of macro and micro invertebrates and cryptobenthic reef fishes (Figure 2B). Total standing biomass (1090 $g \cdot m^{-2}$), is expected to decrease by 1% under RCP 2.6, by 8 % under RCP 4.5, and by 44 % under RCP 8.5 (Figure 3A).

Regarding the biomass dynamics, the RCP 4.5 and RCP 8.5 scenarios began to diverge from RCP 2.6 and status quo scenarios in 2040 (Figure 3A). There was a continuous overlap of the confidence intervals of total biomass dynamics among all scenarios until 2075, when a steep decline started to occur under the RCP 8.5, which deviated from the other scenarios (Figure 3A). Under RCP 8.5, we projected a severe loss of Trophic Transfer Efficiency, from 4% to 2.4% (Fig. 3B) and a 0.3 year

decrease in Biomass Residence Time, from 2.1 to 1.8 years (Fig. 3C) over the period 2012-2100. After 2030, TTE and BRT remain stable in scenario RCP 2.6. For the RCP 4.5 scenario, there is no clear trend for TTE, and the initial (4.07%) mean values are practically the same.

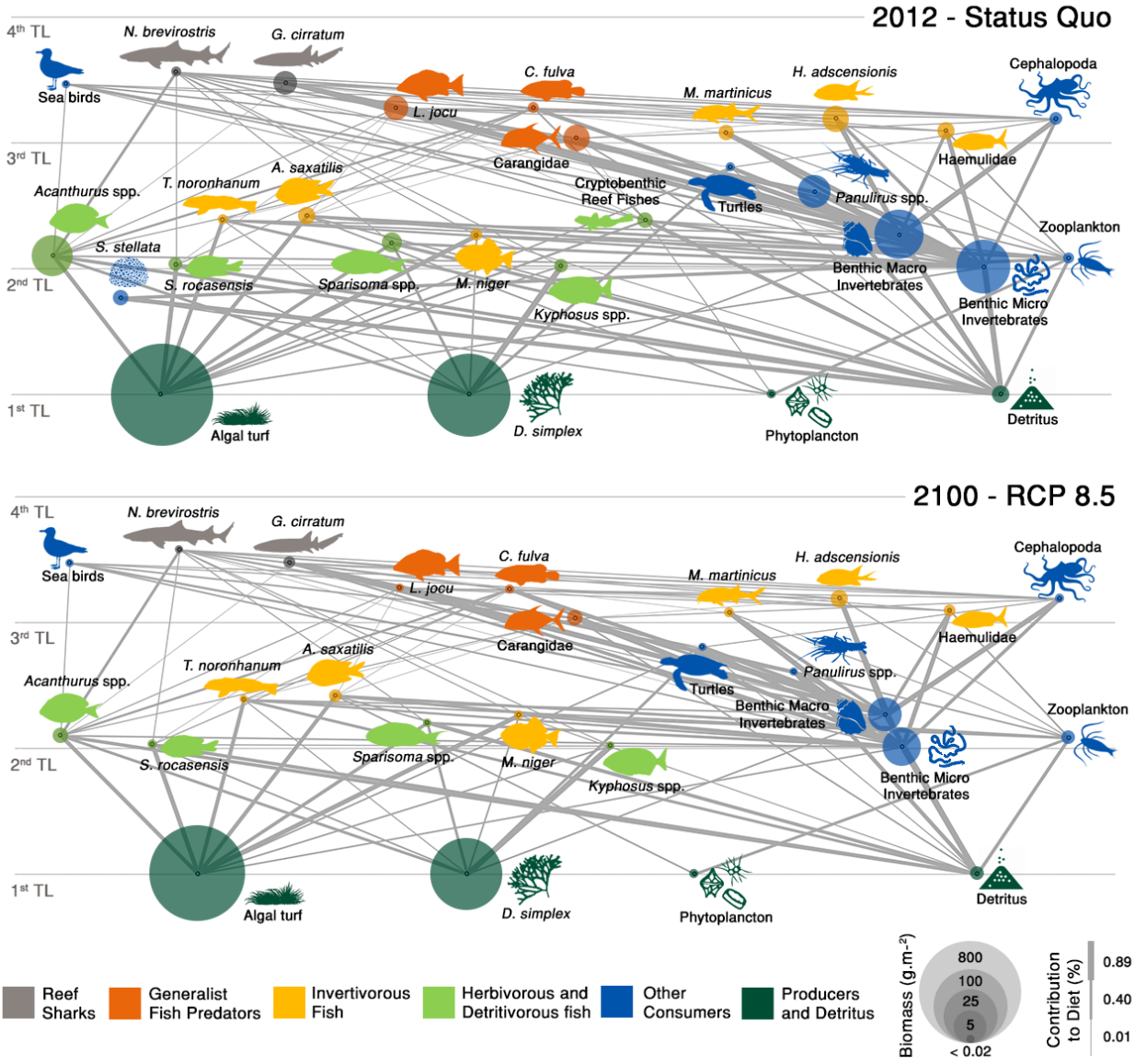

Figure 2 Alteration of standing biomass and trophic flows within the Rocas Atoll's food web under ocean warming. **A**: Food web of the Rocas Atoll ecosystem (year 2012). **B:** Food web of the Rocas Atoll ecosystem under RCP 8.5 ocean warming scenario (year 2100). Each functional group/species is shown as a circle and its size is proportional to the biomass' square root. The food web's groups are represented by their trophic levels (TL, y-axis) and linked by predator-prey relationships showed as lines representing the relative prey's contribution in the predator's diet. Organisms' shapes are not to scale.

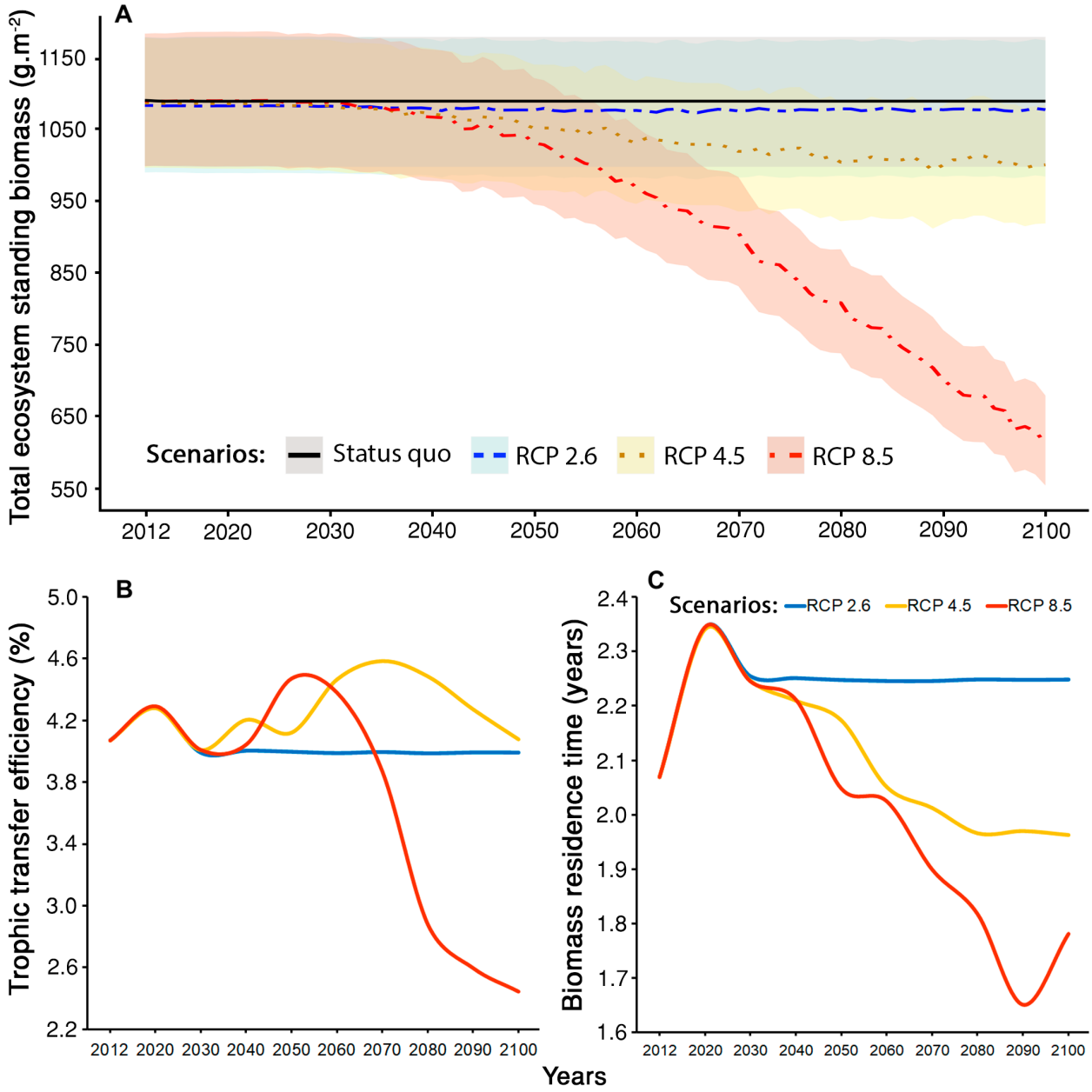

Figure 3 Response of total fish standing biomass to ocean warming. **A**: Projections of the total fish standing biomass under ocean warming scenarios, low (RCP 2.6) medium (RCP 4.5) and high (RCP 8.5). 95% confidence intervals around the mean are shown for trend lines. **B**: Projections of trophic transfer efficiency (TTE) and **(C)** projections of biomass residence time (BRT) between 2012 and 2100 under three ocean warming scenarios, RCP 2.6, RCP 4.5 and RCP 8.5 in blue, yellow and red, respectively. The lines are the mean values of both biomass' transfer efficiency indicators.

Under the status quo scenario, total fish biomass reached an average of 27.2 g·m^{-2} by 2100, which was close to that predicted under the RCP 2.6 scenario (Figure 4). The RCP 4.5 scenario predicted an average decrease of 17.3%, and the RCP 8.5 predicted an 86% decrease in total fish biomass which is estimated to reach 3.7 g·m^{-2} (Figure 4B). In addition to declines in biomass, model simulations also predict alterations on the trophic structure of the fish assemblage in 2100 (Figure

294 4C). Herbivores and detritivores (currently ~ 49% of total fish biomass) will experience the major
295 declines under RCP 8.5 reaching ~19% of fish total biomass (Figure 4C). Invertivorous fishes
296 (currently representing 22.5% of total fish biomass) increased their relative proportion to ~51%
297 under RCP 8.5, despite the decrease in their standing biomass (Figure 4C and Figure 5). Under the
298 RCP 8.5 scenario, the trophic composition of the reef fish assemblages changed from an
299 herbivorous/detritivorous-dominated assemblage to an invertivorous-dominated assemblage by
300 2100 (Figure 4C).

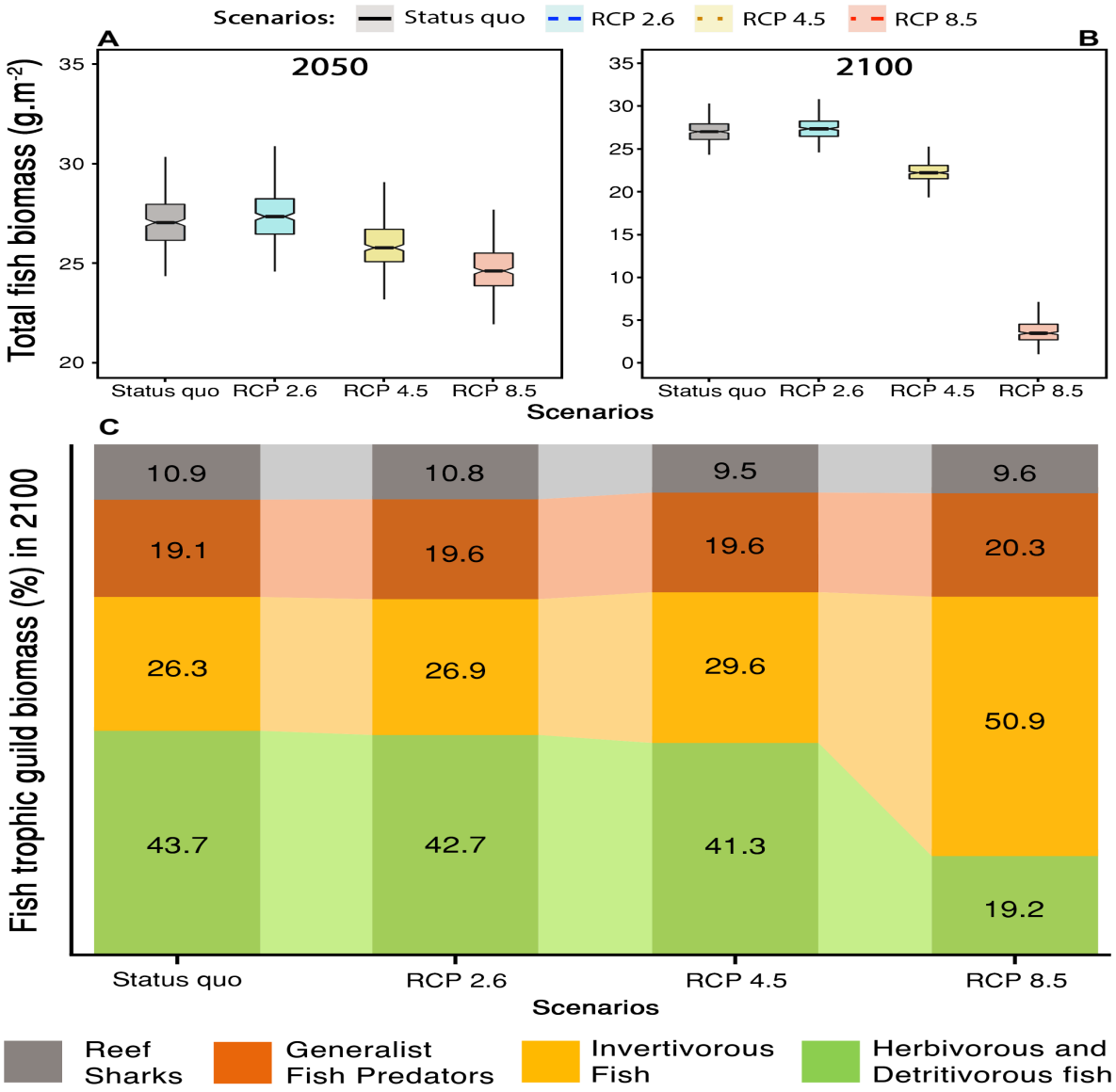

302 **Figure 4** Projected ocean warming effect (RCP 2.6, RCP 4.5, RCP 8.5) vs Status quo scenario in
303 (**A**) 2050 and (**B**) 2100 for fish functional group/species standing biomass. Box plots display the
304 median (horizontal line), the lower and upper hinges correspond to the first and third quartiles (the

25th and 75th percentiles). The lower whisker extends from the hinge to the smallest value at most 1.5 * interquartile range of the hinge. The red dotted line represents the Status quo scenario median value for reference. **C:** Bar graphics represent trophic guild mean percent relative contribution for total fish biomass under ocean warming scenarios by 2100 year.

Generalist predators and reef sharks maintained similar biomass proportions under all scenarios (Figure 4C) but also with a reduction in their standing biomass (Figure 5). Under RCP 4.5 and RCP 8.5 respectively, standing biomass decreased by 28% and 88% for reef sharks, 15% and 8.5% for generalist predators, 7% and 74% for invertivorous fish, 23% and 94% for herbivorous/detritivorous fishes (Figure 5, but see also Figure S4 and Figure S6 in Supplementary Materials).

Standing biomass of almost all non-fish functional groups also decreased under RCP 4.5 and RCP 8.5 scenarios, but with variable magnitudes (Figure 6; but see also Figure S5 and Figure S7 in Supplementary Materials). For instance, *Siderastrea stellata* corals decreased by 61% under RCP 4.5 scenario, with prevision to be ecologically extinct by 2075 under high emission scenarios. The biomass of primary producers, lobsters, sea turtles, seabirds, and invertebrates also declined in all scenarios (Figure 6). Conversely, zooplankton standing biomass remained unchanged under the RCP 2.6 but experienced a 37% increase under RCP 4.5 and 111% increase under RCP 8.5.

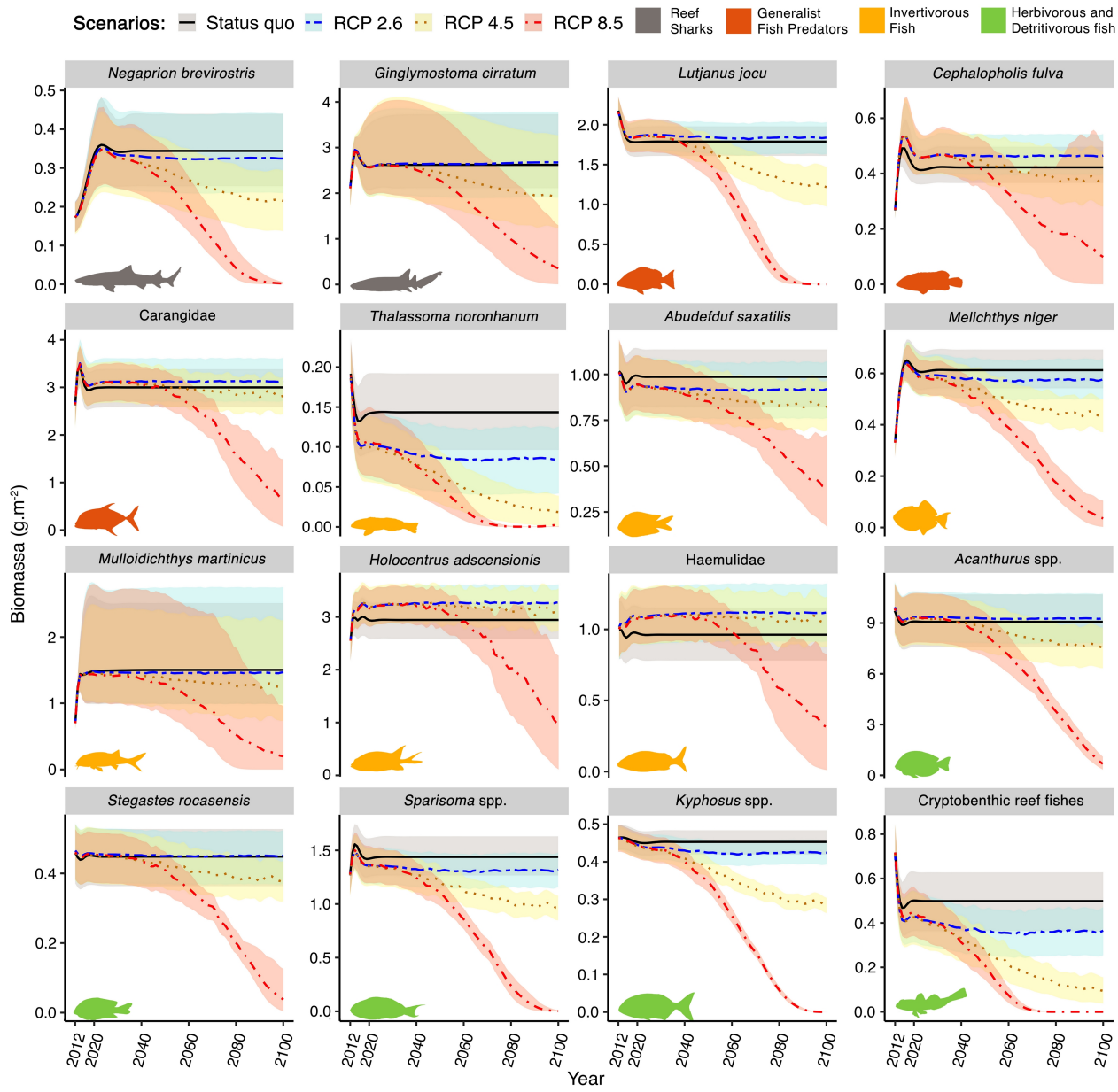

Figure 5 Projections of fish functional group/species biomass dynamics in the Rocas Atoll reef ecosystem under ocean warming scenarios. Shadows represent the 5% and 95% percentiles obtained using the Monte Carlo routine.

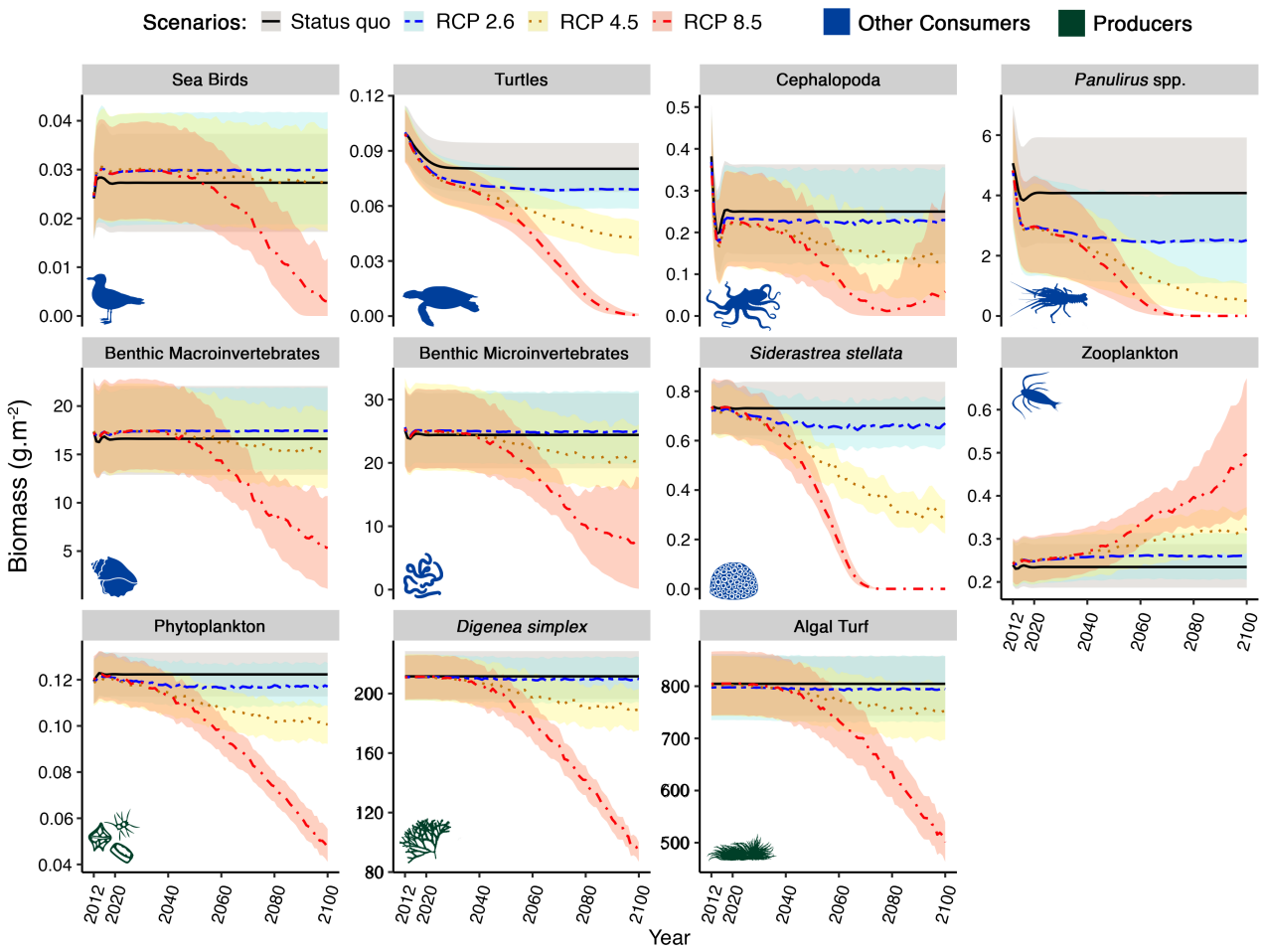

Figure 6 Projections of non-fish functional group/species biomass dynamics in the Rocas Atoll reef ecosystem under ocean warming scenarios. Shadows represent the 5% and 95% percentiles obtained using the Monte Carlo routine.

Discussion

We found that under the most extreme ocean warming scenario (RCP 8.5), most taxa are likely to experience dramatic declines in standing biomass. Ecosystem trophic composition will shift by 2075, affecting energy flow through the entire food web by declining the trophic transfer efficiency (TTE) and the biomass residence time (BTE). This change may lead to a general degradation of the food web, reducing the resilience of tropical reefs. Moreover, the most dramatic changes predicted in our projections will occur by 2075, when climate conditions will exceed the current thermal niche of most functional groups/species. This will jeopardize biomass replenishment resulting in a less productive ecosystem with increasing dependency on pelagic energy subsidies given the severe declines in benthic producers (algal turfs and seaweeds). Our findings are consonant with recent studies indicating that marine food webs are at risk of collapse due to ocean warming (Blowes and

others 2019; Bryndum−Buchholz and others 2019), particularly in reef ecosystems where synergistic human impacts have caused drastic changes (Hughes and others 2017; Beyer and others 2018).

Our results may have broader implications for tropical reefs worldwide because many of the key components of change (e.g. decrease of nominally herbivorous fishes, decline of corals and algal turfs) are congruent with previous studies across the Pacific and South Atlantic Oceans (Pratchett and others 2011; Richardson and others 2018; Inagaki and others 2020; Morais and others 2020). Herbivorous fishes transfer nutrients as excreta, gametes, or somatic tissue to contribute to food chains elsewhere on the reef, including detrital food chains in back reef or lagoon environments (Vermeij and others 2013; Bellwood and others 2018). Grazing fish stimulate algal turfs' productivity by selecting for fast-growing species and growth forms, removing senescent material, reducing self-shading effects, and enhancing the availability of nutrients (Carpenter 1986; Klumpp and Mckinnon 1992; Marshell and Mumby 2015). Increased nutrient load and reduced herbivory have resulted in long sediment-laden turfs as an alternative and stable community state in degraded reefs (Goatley and others 2016). Therefore, the projected simultaneous decline of algal turfs and herbivore fish standing biomass may trigger a severe disruption of the major reef energetic pathway that supports higher-level food chains of the reef ecosystem, leading to novel states in these reefs (Inagaki and others 2020).

Shifts in the ecosystem trophic structure such as that generated by the loss of secondary consumers can alter primary production and, potentially, the functioning of reef ecosystems (Dulvy and others 2004; Inagaki and others 2020). Sea turtles, sea birds, and reef sharks can connect open oceans and reefs by vectoring organic matter and nutrients between them (Bouchard and Bjorndal 2000; Otero and others 2018; Williams and others 2018). Research has shown that, in reef environments, sharks and fish are a vital nutrient reservoir; primary production is enhanced by fish storing nutrients (in biomass) and egesting them (Allgeier and others 2014; Mourier and others 2016). Fishing on high trophic levels reduces nearly half of reef fish communities' capacity to store and recycle nutrients

(Allgeier et al., 2016). The loss of sea bird colonies as those present in the Rocas Atoll would severely affect biogeochemical cycles. Seabirds are important global drivers in the nitrogen and phosphorus cycles, enhancing islands' primary production (Graham and others 2018). Therefore, the expected loss of secondary consumers such as sea birds, sharks, and sea turtles are likely to indicate lower fish production in the future reef state with repercussions for the functioning of the entire reef ecosystem.

Ocean warming this century is likely to lead to a decline in tropical phytoplankton diversity and biomass (Thomas and others 2012; Lotze and others 2019). This general trend can be explained by warming causing increased ocean stratification, which reduces nutrient availability in the upper ocean, leading to decreased primary production and lower energy supply for higher trophic levels (Bopp and others 2013; Kwiatkowski and others 2019). In oligotrophic gyres of the tropical ocean, islands and atolls can enhance phytoplankton biomass and create hotspots of productivity and biodiversity (e.g., island mass effect, IME) (Gove and others 2016; James and others 2020). For example, phytoplankton enhancement is a long-term, near-ubiquitous feature among Pacific coral reef islands and atolls. Similarly, in Rocas Atoll, the increase of phytoplankton biomass is also caused by the IME and not by upwelling (Jales and others 2015). We argue that reef biota may be constrained by ocean warming due to decreases in their primary trophic resources caused by bottom-up forcing and stratification in the water column, which changes the mixed layer depth resulting in lower nutrients and primary production. Also, our models indicated that zooplankton shall experience notable biomass increase because of decreasing predation pressure by invertivorous fish which would contribute to phytoplankton decline. As a result, we predict that tropical reef ecosystems such as Rocas Atoll will be severely threaded, mainly if there are no energetic subsidies in the form of plankton or inorganic nutrients provided by upwelling of pelagic deeper waters.

Sea water temperature drives biomass transfers through the food web in tropical marine ecosystems (Pontavice and others 2020), which are characterized by lower trophic transfer efficiency and fast

biomass transfers (lower BRT) in comparison to temperate and polar ecosystems (Eddy and others 2021).The projected decrease in transfer efficiency at the global scale over the 21st century is expected to amplify impacts at higher trophic levels, leading to a 21% decrease in abundance of marine predators (Pontavice and others 2021). Our study indicates that the Rocas Atoll's reef ecosystem will experience a decline in trophic transfer efficiency and biomass residence time indicators under the most extreme ocean warming scenario. This fact may be related to a severe decline in fish standing biomass, especially at high trophic levels and a species composition defined by less efficient and fast-growing species (Maureaud and others 2017). Thus, we expect that in the next 50 years the sustained increase in ocean temperature will alter the Rocas Atoll's reef ecosystem functioning towards a faster and less efficient state.

Our approach also comprises caveats that need to be acknowledged. Despite the robust direction of change, the substantial spread in our projections' magnitude illustrate considerable uncertainty in functional groups/species' parameters estimates (e.g., micro and macro invertebrate's biomass, production and consumption). We strictly checked for thermodynamic and ecological principles for balancing a food web model (*sensu* Heymans and others 2016). Moreover, we dealt with the uncertainty associated with the model parameters estimates via Monte Carlo statistical routine (Steenbeek and others 2018). This procedure ascertains important trophic interactions through model fitted to time series data, which provides a good idea of the range of outputs available based on the uncertainty surrounding the input data, as seen by the 5th and 95th percentile values plotted. Additionally, we evaluated the influence of temperature on functional group-specific consumption rates but not on functional groups' production rate and functional groups physiological adaptations. Marine vertebrates with slow growth, late maturity, and low annual fecundity, such as sea birds, sea turtles, and sharks, are expected to be evolutionarily less resilient to rapid ocean warming, although they have substantial adaptive plasticity (Sydeman and others 2015). Adaptation could be impeded if there were negative genetic correlations between performance in warmer conditions and changes in other environmental parameters (Munday and others 2013; Sunday and others 2014). An

additional element of uncertainty is the use of the food web models to predict fish biomass dynamics in the absence of globally comprehensive observations of species thermal ranges and assuming a unimodal-gaussian thermal performance curve. AquaMaps database is the only source of thermal ranges for all functional groups in our model, so we have decided to keep a single source of data to avoid greater uncertainty deriving from consulting multiple sources derived from different methods. However, we performed a scrupulous check of each thermal range, comparing it with the maximum and minimum temperature values observed in the western Atlantic Ocean, using NOAA Optimum Interpolation 1/4 Degree Daily Sea Surface Temperature model data as reference (Reynolds and Banzon 2008), which demonstrated a good level of agreement. Thus, our results can be considered conservative in the magnitude of the projected impacts on functional groups biomass dynamics but assertive in the direction of changes. Progress in the development of global species-specific datasets for environmental variables other than the temperature would enable more comprehensive investigations in the future. Each of the assumptions explored here can be converted into testable hypotheses and then examined in model sensitivity analyses. It would provide insights into how much detail is needed and what can be ignored, reducing the uncertainty in the relationship between temperature and trophic interactions to predict the biological impacts of ocean warming.

Conclusions

Considering the projected decrease of up to 44% of standing biomass by 2100 under the high ocean warming scenario, increases in ocean warming frequency and intensity on tropical reef ecosystems will cause synchronous and severe changes in reef biodiversity, ecosystem structure and functioning. Our projections suggest that tropical reef ecosystems will be severely impacted by increasing temperatures through standing biomass declines, mainly of reef fish and invertebrates, which are predicted to occur by the end of the 21st century both under the RCP 4.5 and the RCP 8.5 scenarios. These changes will lead to a less productive and diverse ecosystem, potentially hampering the services provided by reef ecosystems worldwide. Delaying the crossing of this ecological reef state scenario may be possible but requires rapid reductions in greenhouse gas

emissions. Our results also highlight the urgency of including monitoring sites in tropical marine regions and investigating the potential of migration and adaptation in marine biota. Ocean acidification, disturbance in nutrient cycles, pollution, and fisheries are also important threats that could be further explored to improve predictions of the future of tropical reef ecosystems.

Data accessibility

The raw data and the R code for data analysis that support the findings of this study are freely available in the GitHub repository: https://github.com/leomarameo7/Atoll_Rocas_project. Biological parameters can be consulted in Fishbase website (https://www.fishbase.org) and AquaMaps (https://www.aquamaps.org/). Ecopath model file is available on request to the corresponding author.

Funding

This work was supported by Serrapilheira Institute (grant number Serra-1708-15364 awarded to GOL) and PELD/ILOC (CNPq 441241/2016-6 awarded to CEL. Ferreira). Our work was supported in part by the Coordenação de Aperfeiçoamento de Pessoal de Nível Superior-Brazil (CAPES) - Finance Code 001 (PhD scholarship to LC and postdoctoral scholarship to EAV). GOL is also grateful to a research productivity scholarship provided by CNPq (grant number 310517/2019-2).

Acknowledgments

We thank Renato Morais for highly constructive comments on earlier version of this manuscript. We further thank Dr. Terry Done and anonymous reviewers for their suggestions and improvements.

476 **References**

Akaike H. 1974. A new look at the statistical model identification. IEEE Transactions on Automatic Control 19:716–23.

Angilletta MJ. 2009. Thermal adaptation: a theoretical and empirical synthesis. Oxford University Press

Araújo JN, Martins AS, Bonecker ACT, Esteves AM, Tenenbaum DR, Gonzalez-rodriguez E, Reis ER, Lavrado HP, Lima LM, Costa PAS, Paranhos R, Bonecker SLC, Disaró ST, Rodrigues SV. 2017. Modelos Ecopath da plataforma continental e do talude da Bacia de Campos: análise das propriedades ecossistêmicas e do efeito da sazonalidade. In: Modelagem Ecossistêmica para integração e manejo na Bacia de Campos (Atlântico sudoeste). Vol. 8. Rio de janeiro: Elsevier Brazil. pp 131–87.

Belgrano A, Scharler U, Dunne J, Ulanowicz R. 2005. Aquatic Food Webs: An Ecosystem Approach.

Bentley JW, Serpetti N, Heymans JJ. 2017. Investigating the potential impacts of ocean warming on the Norwegian and Barents Seas ecosystem using a time-dynamic food-web model. Ecological Modelling 360:94–107.

Beyer HL, Kennedy EV, Beger M, Chen CA, Cinner JE, Darling ES, Eakin CM, Gates RD, Heron SF, Knowlton N, Obura DO, Palumbi SR, Possingham HP, Puotinen M, Runting RK, Skirving WJ, Spalding M, Wilson KA, Wood S, Veron JE, Hoegh−Guldberg O. 2018. Risk-sensitive planning for conserving coral reefs under rapid climate change. Conservation Letters 11:e12587.

Blanchard JL, Jennings S, Holmes R, Harle J, Merino G, Allen JI, Holt J, Dulvy NK, Barange M. 2012. Potential consequences of climate change for primary production and fish production in large marine ecosystems. Philosophical Transactions of the Royal Society B: Biological Sciences 367:2979–89.

Blowes SA, Supp SR, Antão LH, Bates A, Bruelheide H, Chase JM, Moyes F, Magurran A, McGill B, Myers-Smith IH, Winter M, Bjorkman AD, Bowler DE, Byrnes JEK, Gonzalez A, Hines J, Isbell F, Jones HP, Navarro LM, Thompson PL, Vellend M, Waldock C, Dornelas M. 2019. The geography of biodiversity change in marine and terrestrial assemblages. Science 366:339–45.

Bryndum‐Buchholz A, Tittensor DP, Blanchard JL, Cheung WWL, Coll M, Galbraith ED, Jennings S, Maury O, Lotze HK. 2019. Twenty-first-century climate change impacts on marine animal biomass and ecosystem structure across ocean basins. Global Change Biology 25:459–72.

Burrows MT, Hawkins SJ, Moore JJ, Adams L, Sugden H, Firth L, Mieszkowska N. 2020. Global-scale species distributions predict temperature-related changes in species composition of rocky shore communities in Britain. Global Change Biology 26:2093–105.

Childress ES, Letcher BH. 2017. Estimating thermal performance curves from repeated field observations. Ecology 98:1377–87.

Christensen V, Pauly D. 1993. Trophic models of aquatic ecosystems. Manila, Philippines: ICLARM Conf. Proc.

Christensen V, Walters CJ. 2004. Ecopath with Ecosim: methods, capabilities and limitations. Ecol Model 172:109–39.

Colléter M, Valls A, Guitton J, Gascuel D, Pauly D, Christensen V. 2015. Global overview of the applications of the Ecopath with Ecosim modeling approach using the EcoBase models repository. Ecological Modelling 302:42–53.

Corrales X, Coll M, Ofir E, Heymans JJ, Steenbeek J, Goren M, Edelist D, Gal G. 2018. Future scenarios of marine resources and ecosystem conditions in the Eastern Mediterranean under the impacts of fishing, alien species and sea warming. Scientific Reports 8:1–16.

Curnock MI, Marshall NA, Thiault L, Heron SF, Hoey J, Williams G, Taylor B, Pert PL, Goldberg J. 2019. Shifts in tourists' sentiments and climate risk perceptions following mass coral bleaching of the Great Barrier Reef. Nature Climate Change 9:535–41.

Eddy TD, Bernhardt JR, Blanchard JL, Cheung WWL, Colléter M, du Pontavice H, Fulton EA, Gascuel D, Kearney KA, Petrik CM, Roy T, Rykaczewski RR, Selden R, Stock CA, Wabnitz CCC, Watson RA. 2021. Energy Flow Through Marine Ecosystems: Confronting Transfer Efficiency. Trends in Ecology & Evolution 36:76–86.

Fredston‐Hermann A, Selden R, Pinsky M, Gaines SD, Halpern BS. 2020. Cold range edges of marine fishes track climate change better than warm edges. Global Change Biology 26:2908–22.

Gibert JP. 2019. Temperature directly and indirectly influences food web structure. Scientific Reports 9:1–8.

Haas AF, Fairoz MFM, Kelly LW, Nelson CE, Dinsdale EA, Edwards RA, Giles S, Hatay M, Hisakawa N, Knowles B, Lim YW, Maughan H, Pantos O, Roach TNF, Sanchez SE, Silveira CB, Sandin S, Smith JE, Rohwer F. 2016. Global microbialization of coral reefs. Nature Microbiology 1:1–7.

Heymans JJ, Coll M, Link JS, Mackinson S, Steenbeek J, Walters C, Christensen V. 2016. Best practice in Ecopath with Ecosim food-web models for ecosystem-based management. Ecol Model 331:173–84.

Hughes TP, Barnes ML, Bellwood DR, Cinner JE, Cumming GS, Jackson JBC, Kleypas J, van de Leemput IA, Lough JM, Morrison TH, Palumbi SR, van Nes EH, Scheffer M. 2017. Coral reefs in the Anthropocene. Nature 546:82–90.

Inagaki KY, Pennino MG, Floeter SR, Hay ME, Longo GO. 2020. Trophic interactions will expand geographically but be less intense as oceans warm. Global Change Biology n/a.

Kaschner K, Kesner-reyes K, Garilao C, Rius-Barile J, Rees T, Froese R. 2019. AquaMaps: Predicted range maps for aquatic species. World wide web electronic publication.

Longo GO, Morais RA, Martins CDL, Mendes TC, Aued AW, Cândido DV, Oliveira JC de, Nunes LT, Fontoura L, Sissini MN, Teschima MM, Silva MB, Ramlov F, Gouvea LP, Ferreira CEL, Segal B, Horta PA, Floeter SR. 2015. Between-Habitat Variation of Benthic Cover, Reef Fish Assemblage and Feeding Pressure on the Benthos at the Only Atoll in South Atlantic: Rocas Atoll, NE Brazil. PLOS ONE 10:e0127176.

Lotze HK, Tittensor DP, Bryndum-Buchholz A, Eddy TD, Cheung WWL, Galbraith ED, Barange M, Barrier N, Bianchi D, Blanchard JL, Bopp L, Büchner M, Bulman CM, Carozza DA, Christensen V, Coll M, Dunne JP, Fulton EA, Jennings S, Jones MC, Mackinson S, Maury O, Niiranen S, Oliveros-Ramos R, Roy T, Fernandes JA, Schewe J, Shin Y-J, Silva TAM, Steenbeek J, Stock CA, Verley P, Volkholz J, Walker ND, Worm B. 2019. Global ensemble projections reveal trophic amplification of ocean biomass declines with climate change. PNAS 116:12907–12.

Madin JS, Hoogenboom MO, Connolly SR, Darling ES, Falster DS, Huang D, Keith SA, Mizerek T, Pandolfi JM, Putnam HM, Baird AH. 2016. A Trait-Based Approach to Advance Coral Reef Science. Trends in Ecology & Evolution 31:419–28.

Magel JMT, Burns JHR, Gates RD, Baum JK. 2019. Effects of bleaching-associated mass coral mortality on reef structural complexity across a gradient of local disturbance. Scientific Reports 9:1–12.

Maureaud A, Gascuel D, Colléter M, Palomares MLD, Pontavice HD, Pauly D, Cheung WWL. 2017. Global change in the trophic functioning of marine food webs. PLOS ONE 12:e0182826.

McCauley DJ, Pinsky ML, Palumbi SR, Estes JA, Joyce FH, Warner RR. 2015. Marine defaunation: Animal loss in the global ocean. Science 347.

Munday PL, Warner RR, Monro K, Pandolfi JM, Marshall DJ. 2013. Predicting evolutionary responses to climate change in the sea. Ecology Letters 16:1488–500.

Neubauer P, Andersen KH. 2020. Thermal performance of fish is explained by an interplay between physiology, behaviour and ecology. Conserv Physiol 7.

Nolan C, Overpeck JT, Allen JRM, Anderson PM, Betancourt JL, Binney HA, Brewer S, Bush MB, Chase BM, Cheddadi R, Djamali M, Dodson J, Edwards ME, Gosling WD, Haberle S, Hotchkiss SC, Huntley B, Ivory SJ, Kershaw AP, Kim S-H, Latorre C, Leydet M, Lézine A-M, Liu K-B, Liu Y, Lozhkin AV, McGlone MS, Marchant RA, Momohara A, Moreno PI, Müller S, Otto-Bliesner BL, Shen C, Stevenson J, Takahara H, Tarasov PE, Tipton J, Vincens A, Weng C, Xu Q, Zheng Z, Jackson ST. 2018. Past and future global transformation of terrestrial ecosystems under climate change. Science 361:920–3.

Palomares MLD, Pauly D. 1998. Predicting food consumption of fish populations as functions of mortality, food type, morphometrics, temperature and salinity. Mar Freshwat Res 49:447–53.

Pauly D. 1980. On the interrelationships between natural mortality, growth parameters, and mean environmental temperature in 175 fish stocks. ICES J Mar Sci 39:175–92.

Payne NL, Smith JA, Meulen DE van der, Taylor MD, Watanabe YY, Takahashi A, Marzullo TA, Gray CA, Cadiou G, Suthers IM. 2016. Temperature dependence of fish performance in the wild: links with species biogeography and physiological thermal tolerance. Functional Ecology 30:903–12.

Polis GA, Winemiller KO. 1996. Food Webs: Integration of Patterns & Dynamics. Springer Science & Business Media

Pontavice H du, Gascuel D, Reygondeau G, Maureaud A, Cheung WWL. 2020. Climate change undermines the global functioning of marine food webs. Global Change Biology 26:1306–18.

Pontavice H du, Gascuel D, Reygondeau G, Stock C, Cheung WWL. 2021. Climate-induced decrease in biomass flow in marine food webs may severely affect predators and ecosystem production. Global Change Biology n/a.

Pörtner H-O, Roberts DC, Masson-Delmotte V, Zhai P, Tignor M, Poloczanska E, Mintenbeck K, Nicolai M, Okem A, Petzold J, Rama B. 2019. Summary for Policymakers. In: IPCC Special Report on the Ocean and Cryosphere in a Changing Climate.

Reynolds RW, Banzon VF. 2008. NOAA Optimum Interpolation 1/4 Degree Daily Sea Surface Temperature (OISST) Analysis, Version 2. NOAA National Centers for Environmental Information doi 10:V5SQ8XB5.

Robinson JPW, Wilson SK, Jennings S, Graham NAJ. 2019. Thermal stress induces persistently altered coral reef fish assemblages. Glob Change Biol 25:2739–50.

Rogers A, Blanchard JL, Mumby PJ. 2018. Fisheries productivity under progressive coral reef degradation. Journal of Applied Ecology 55:1041–9.

Scott E, Serpetti N, Steenbeek J, Heymans JJ. 2016. A Stepwise Fitting Procedure for automated fitting of Ecopath with Ecosim models. SoftwareX 5:25–30.

Serpetti N, Baudron AR, Burrows MT, Payne BL, Helaouët P, Fernandes PG, Heymans JJ. 2017. Impact of ocean warming on sustainable fisheries management informs the Ecosystem Approach to Fisheries. Scientific Reports 7:1–15.

Steenbeek J, Corrales X, Platts M, Coll M. 2018. Ecosampler: A new approach to assessing parameter uncertainty in Ecopath with Ecosim. SoftwareX 7:198–204.

Sunday J, Bates A, Kearney M, Colwell R, Dulvy N, Longino J, Huey R. 2014. Thermal-safety margins and the necessity of thermoregulatory behavior across latitude and elevation. Proceedings of the National Academy of Sciences of the United States of America 111.

Sydeman WJ, Poloczanska E, Reed TE, Thompson SA. 2015. Climate change and marine vertebrates. Science 350:772–7.

Taylor KE, Stouffer RJ, Meehl GA. 2012. An Overview of CMIP5 and the Experiment Design. Bulletin of the American Meteorological Society 93:485–98.

Waldock C, Stuart−Smith RD, Edgar GJ, Bird TJ, Bates AE. 2019. The shape of abundance distributions across temperature gradients in reef fishes. Ecology Letters 22:685–96.

Walters C, Christensen V, Pauly D. 1997. Structuring dynamic models of exploited ecosystems from trophic mass-balance assessments. Reviews in Fish Biology and Fisheries 7:139–72.

Walters C, Pauly D, Christensen V, Kitchell JF. 2000. Representing Density Dependent Consequences of Life History Strategies in Aquatic Ecosystems: EcoSim II. Ecosystems 3:70–83.

Williams GJ, Graham NAJ, Jouffray J-B, Norström AV, Nyström M, Gove JM, Heenan A, Wedding LM. 2019. Coral reef ecology in the Anthropocene. Functional Ecology 33:1014–22.

Zhang L, Takahashi D, Hartvig M, Andersen KH. 2017. Food-web dynamics under climate change. Proceedings of the Royal Society B: Biological Sciences 284:20171772.

Supplementary material

Ocean warming will reduce standing biomass in a tropical Western Atlantic reef ecosystem

Leonardo Capitani[1,2,*], Julio Neves de Araujo[3], Edson A. Vieira[1,2], Ronaldo Angelini[1,4], Guilherme O. Longo[1,2]

[1] Post-Graduate Program in Ecology, Bioscience Center, Universidade Federal do Rio Grande do Norte, Natal, 59072-970, Brazil

[2] Marine Ecology Laboratory, Department of of Oceanography and Limnology, Universidade Federal do Rio Grande do Norte, Natal, 59014-002, Brazil

[3] Department of Oceanography, Universidade Federal do Espírito Santo, Vitória, 29075-910, Brazil

[4] Department of Civil Engeneering, Universidade Federal do Rio Grande do Norte, Natal, 59078-970, Brazil

[*] **Corresponding author:**

Leonardo Capitani

Email: leonardocapitani@icloud.com

Telephone number: +55 84 9817590704

This supplementary material is organized into two sections. First, we present the references used to parameterize and balance the Ecopath model for 2012 (the reference year). In the second section, we provide a detailed description of the biomass dynamic simulations (Ecosim) under ocean warming.

1. Details of the Ecopath model

Individual species or groups of species were assigned into functional groups, which share similar growth and consumption rates, diet composition, and predators. The functional groups are regulated by gains (consumption, production, and immigration) and losses (natural mortality and emigration) and are linked to each other by predatory relationships (Christensen and Walters 2004). The parameterization of an Ecopath model is based on satisfying two 'master' equations. The first equation describes how the production term for each functional group can be partitioned into (1):

$$\text{Production} = \text{predation} + \text{net migration} + \text{biomass accumulation} + \text{other mortality} \quad (1)$$

The second equation is based on the principle of conservation of matter within a functional group (2):

$$\text{Consumption} = \text{production} + \text{respiration} + \text{unassimilated food} \quad (2)$$

The resulting Eq. 1 and Eq. 2 are described following the formula (3):

$$B_i * (P/B)_i * EE_i = \Sigma B_j * (Q/B)_j * Dc_{ji} + BA_i \quad (3)$$

where B_i and B_j are the biomasses of the prey species *i* and the consumers (*j*) of *i*, respectively; $(P/B)_i$ is the production/biomass ratio for *i*; EE_i is the fraction of production of *i* that is consumed within, or caught from the system (the balance being assumed to contribute to detritus); $(Q/B)_j$ is the food consumption per unit biomass of *j*; DC_{ji} is the fractional contribution by mass of *i* to the diet of *j*; and BA_i is a biomass accumulation term that describes a change in biomass over the time period studied and/or net immigration. If all four basic parameters (B, P/B, Q/B and EE) are available for

a functional group, the software can instead estimate either biomass accumulation or net migration. Ecopath sets up a series of linear equations to solve for unknown values establishing mass-balance in the same operation.

1.1 Estimate of production rates for fish functional groups

Production rate (P/B) in Ecopath is assumed to be equal to total mortality *Z*, which can be estimated as $Z = F+M2+M0$ where Z is total mortality, F – fishing mortality, M2 – natural mortality due to predation, and M0 – natural mortality due to old age, deceases, etc. Natural mortality rate (M) of fish was estimated from an empirical relationship linking M, the parameters of the von Bertalanffy Growth Function (VBGF), to mean environmental temperature (Pauly 1980) as follow:

$$M = \left(K^{0.65} L_{inf}\right) - \left(0.279\, T_c^{0.463}\right) \quad (4)$$

where, M is the natural mortality ($year^{-1}$), K is the curvature parameter of the VBGF ($year^{-1}$), L_{inf} is the asymptotic length in cm, Tc is the mean ambient temperature, in °C. A life-history routine FishBase (Froese and Pauly 2019) was used to estimate M, L_{inf} being assumed to equal L_{max}. K was determined using known relationships between L_{inf} and K within the FishBase life-history routine. Ambient temperature was assumed to be the average temperature of the Rocas Atoll Ecosystem (27°C) for the reference year 2012. When functional groups comprised several species, the group P/B was estimated as a weighted mean (weighted by each species biomass B) of the species P/Bs.

1.2 Estimate of consumption rates for fish functional groups

Consumption rates (Q/B) of fish species were estimated from empirical formulae implemented in the life-history routine of FishBase (Froese and Pauly 2019), derived by Palomares and Pauly (1998):

$$logQB = 5.847 + (0.28\, logZ) - (0.152 \log W_{inf}) - (1.36\, T') + (0.062\, A) + (0.51\, h) + (0.39\, d) \quad (5)$$

where Z is total mortality, W_{inf} is the asymptotic weight (g), T' is the mean annual temperature (expressed using T' = 1,000/Kelvin (Kelvin = °C + 273.15), A is the aspect ratio (height^2 (cm)/surface area (cm) of the caudal fin), h is a dummy variable expressing trophic category (1 for herbivores, and 0 for detritivores and carnivores), and d is a dummy variable also expressing food type (1 for detritivores, and 0 for herbivores and carnivores). For cases where Z is not available, the following relation may be used:

$$logQB = 7.964 + (0.204 \log W_{inf}) - (1.965\, T') + (0.083\, A) + (0.532\, h) + (0.398\, d) \quad (6)$$

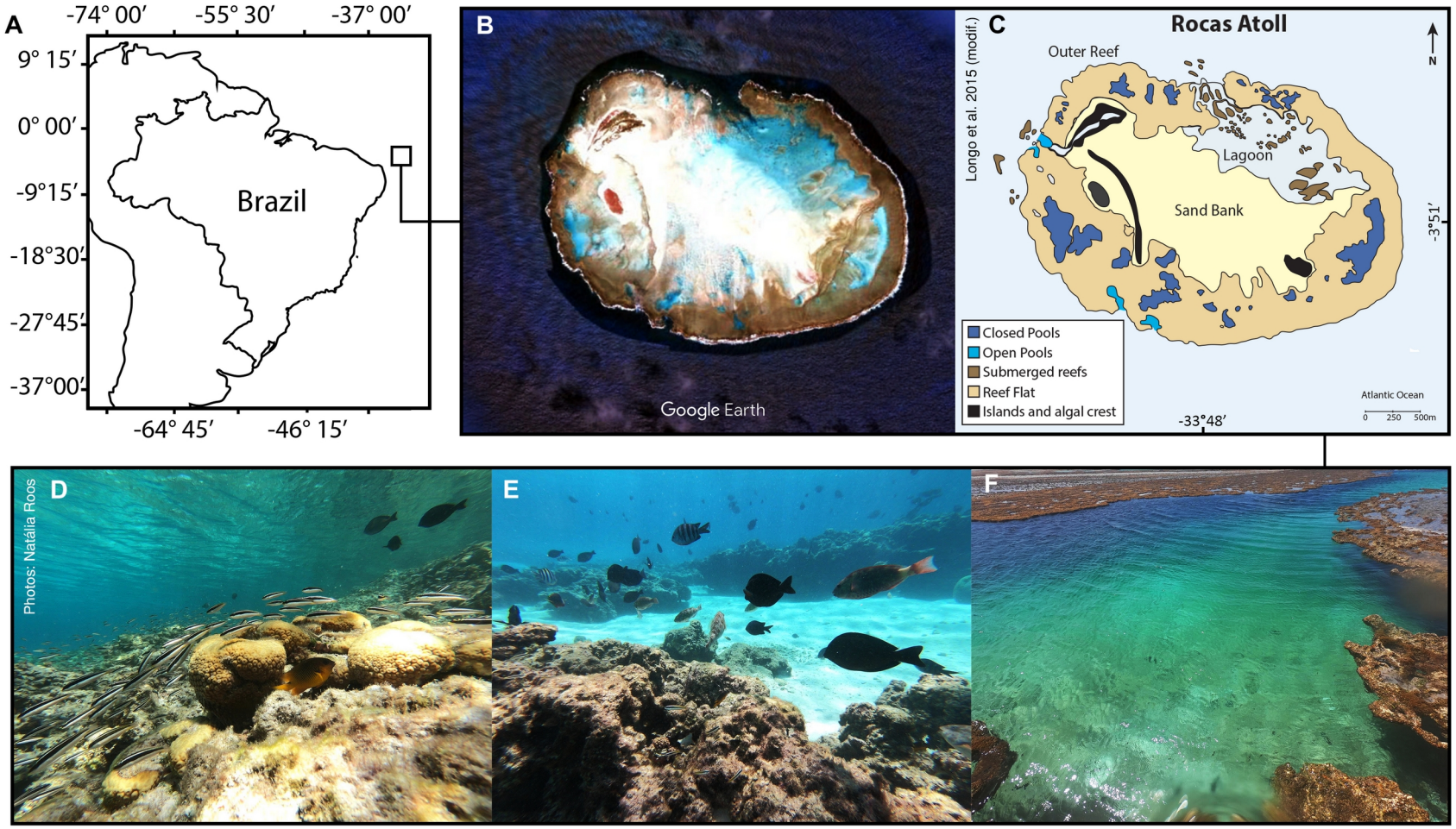

Fig. S1 The Rocas Atoll ecosystem with its different reef habitats. **A**: geographical location of the modelled ecosystem with respect to the country to which it is legally part, Brazil; **B**: satellite imagery of the modelled ecosystem retrieved from Google Earth; **C**: graphic representation of the various habitats present in the modelled ecosystem (adapted from Longo and others 2015); **D**: corals in the foreground within the reef flat; **E:** an open tidal pool within the reef flat; **F**: emerged part of a closed tidal pool within the reef flat.

Table S1. Functional groups in the Rocas Atoll Ecopath model and the data sources for the parameters for each group. Biomass is reported in $t \cdot km^{-2}$ or as the same in $g \cdot m^{-2}$. P/B is the production to biomass ratio, Q/B is the consumption to biomass ratio.

Group number	Group name	Species aggregation (in descending order of abundance)	Biomass ($g \cdot m^{-2}$)	P/B ($year^{-1}$)	Q/B ($year^{-1}$)	Diet
1	Sea birds	*Sula dactylatra*; *Sula leucogaster*; *Sula sula*; *Onychoprion fuscatus*; *Anous stolidus*; *Anous minutus; Fregata magnificens.* (Almeida et al. 2000)	From an other model. (Freire et al. 2008)	From an other model (Freire et al. 2008).	From an other model (Freire et al. 2008).	From another Ecopath model(Christensen et al. 2015)
2	*Negaprion brevirostris*	- - -	*In situ* estimate.	Empirical relationship (Pauly 1980)	Empirical relationship (Palomares and Pauly 1998).	(Cortés and Gruber 1990; Froese and Pauly 2019)
3	*Ginglymostoma cirratum*	- - -	*In situ* estimate.	Empirical relationship (Pauly 1980)	Empirical relationship (Palomares and Pauly 1998).	(Matott et al. 2005; Froese and Pauly 2019)
4	*Lutjanus jocu*	- - -	*In situ* estimate.	Empirical relationship (Pauly 1980)	Empirical relationship (Palomares and Pauly 1998).	Stomach content and isotope analysis (Andrades 2018; Froese and Pauly 2019).
5	*Cephalopholis fulva*	- - -	*In situ* estimate.	Empirical relationship (Pauly 1980).	Empirical relationship (Palomares and Pauly 1998).	Stomach content and isotope analysis (Coelho et al. 2012; Andrades 2018; Froese and Pauly 2019)
6	Carangidae	*Carangoides bartholomaei; Caranx ruber; C. crysos; C. latus; C. lugubris*	*In situ* estimate.	Empirical relationship (Pauly 1980).	Empirical relationship (Palomares and Pauly 1998).	(Silvano 2001; Sley et al. 2009; Froese and Pauly 2019)
7	*Acanthurus* spp.	*A. coeruleus; A. chirurgus; A. bahianus*	*In situ* estimate.	Empirical relationship (Pauly 1980).	Empirical relationship (Palomares and Pauly 1998).	Stomach content and isotope analysis (Longo et al. 2015; Andrades 2018; Froese and Pauly

						2019).
8	*Stegastes rocasensis*	- - -	*In situ* estimate.	Empirical relationship (Pauly 1980).	Empirical relationship (Palomares and Pauly 1998).	Stomach content and isotope analysis (Souza et al. 2011; Andrades 2018).
9	*Thalassoma noronhanum*	- - -	*In situ* estimate.	Empirical relationship (Pauly 1980)	Empirical relationship (Palomares and Pauly 1998)	Stomach content and isotope analysis (Andrades 2018; Froese and Pauly 2019)
10	*Abudefduf saxatilis*	- - -	*In situ* estimate.	Empirical relationship (Pauly 1980)	Empirical relationship (Palomares and Pauly 1998)	Stomach content and isotope analysis (Andrades 2018; Froese and Pauly 2019)
11	*Sparisoma* spp.	*S. amplum; S. axillare; S. frondosum*	*In situ* estimate.	Empirical relationship (Pauly 1980)	Empirical relationship (Palomares and Pauly 1998)	Stomach content and isotope analysis (Andrades 2018; Froese and Pauly 2019)
12	*Melichthys niger*	- - -	*In situ* estimate.	Empirical relationship (Pauly 1980)	Empirical relationship (Palomares and Pauly 1998)	(Turingan et al. 1995; Mendes et al. 2019; Froese and Pauly 2019)
13	*Kyphosus* spp.	- - -	*In situ* estimate.	Empirical relationship (Pauly 1980)	Empirical relationship (Palomares and Pauly 1998)	(Silvano and Güth 2006; Froese and Pauly 2019)
14	*Mulloidichthys martinicus*	- - -	*In situ* estimate.	Empirical relationship (Pauly 1980)	Empirical relationship (Palomares and Pauly 1998)	(Krajewski et al. 2006; Froese and Pauly 2019).
15	*Holocentrus adscensionis*	- - -	*In situ* estimate.	Empirical relationship (Pauly 1980)	Empirical relationship (Palomares and Pauly 1998)	Stomach content and isotope analysis (Andrades 2018; Froese and Pauly 2019).
16	Haemulidae	*Haemulon chrysargyreum*; *H. parra*; *Anisotremus surinamensis*; *Orthopristis ruber*	*In situ* estimate.	Empirical relationship (Pauly 1980)	Empirical relationship (Palomares and Pauly 1998)	(Pereira et al. 2015; Froese and Pauly 2019).

17	Cryptobenthic reef fishes	*Gnatholepis thompsoni*; *Coryphopterus glaucofraenum*; *Elacatinus phthirophagus*; *Labrisomus kalisherae*; *Malacoctenus spp.*; *Ophioblennius atlanticus*; *Ophioblennius trinitatis*; *Pempheris schomburgkii.* We classify reef-fish species as cryptobenthic if they have >10% individuals smaller than 50 mm maximum length. All other species are considered to be large reef fishes.(Brandl et al. 2018)	*In situ* estimate.	Empirical relationship (Pauly 1980)	Empirical relationship (Palomares and Pauly 1998)	Stomach content and isotope analysis (Andrades 2018; Froese and Pauly 2019).
18	Turtles	*Chelonia mydas, Eretmochelys imbricata*	*In situ* estimate (Grossman et al. 2019)	From another Ecopath model (Araújo et al. 2017).	From another Ecopath model (Araújo et al. 2017).	From an other Ecopath model (Araújo et al. 2017).
19	Cephalopoda	*Octopus insularis*, *Octopus vulgaris*	Sampling locally, low precision. Biomass values of 0.27 $g \cdot m^{-2}$ was increased 50% to achieve EwE assumptions. (Bouth et al. 2011)	From another Ecopath model (Freire et al. 2008).	From another Ecopath model (Freire et al. 2008).	Quantitative, detailed, isotope diet composition study (Dantas et al. 2019).

20	*Panulirus* spp.	*Panulirus echinatus, Panulirus argus, Parribacus antarticus*	Sampling locally, low precision. Master thesis. (Gaeta 2014)	From another Ecopath model. (Freire et al. 2008)	From another Ecopath model. (Freire et al. 2008)	Quantitative gut content and isotope diet composition studies (Góes and Lins-Oliveira 2009; Higgs et al. 2016)
21	Benthic macroinvertebrates	Bivalves and gastropods mostly larger than 2 mm. Mostly echinodermes, small crabs, gasteropods, scallops. (Netto et al. 2003)	Estimated by Ecopath routine.	From another Ecopath model. (Araújo et al. 2017)	From another Ecopath model. (Araújo et al. 2017)	Stable isotope analisys (Andrades 2018)
22	Benthic microinvertebrates	Amphipoda; Tanaidacea; Decapoda; Chironomidae; *Lysmata grabhami; Stenopus hispidus.* (Netto et al. 2003)	Estimated by Ecopath routine.	From another Ecopath model. (Araújo et al. 2017)	From another Ecopath model. (Araújo et al. 2017)	From another Ecopath model. (Morato et al. 2016)
23	*Siderastrea stellata* (coral)		Sampling locally, low precision. (Pinheiro et al. 2017)	From another Ecopath model. (Tan et al. 2018)	From another Ecopath model. (Tan et al. 2018)	We assumed that this species is mixotrophic, obtaining 40 % of its energy through heterotrophic means. (Leletkin 2000; Ferrier-Pagès et al. 2011)
24	Zooplankton	Tinnines, copepods, foraminifers, heliozoan, crustacean larvae, radiolarian.(Neumann-Leitão et al. 2008; Lira et al. 2014)	Sampling locally, low precision. Value of 0.11 (Lira et al. 2014) was incresed to balance the model	From another Ecopath model. (Christensen et al. 2015)	From another Ecopath model. (Christensen et al. 2015)	General knowledge of related tropical south Atlantic group/species (Bode and Hernández-León 2018).
25	Phytoplankton	*Prorocentrum balticum, P. lima, P. compressum, Coccolithus* sp.*, Pyrophacus* sp.*, Ostreopsis ovata.* (Jales 2015)	Average value over ten years 2002-2012. NOAA OceanWatch (https://oceanwatch.pifsc.noaa.gov/)	Similar species, same system, low precision. Value: 10 µg $C \cdot (L \cdot day)^{-1}$ (Buitenhuis et al. 2013)	- - -	- - -

		- - -				
26	*Digenea simplex*		Sampling locally, high precision. (Longo et al. 2015)	Same species, same system, high precision (Fonseca 2010; Fonseca et al. 2018). Conversion factor g C : g ww = 16.7 (Opitz 1996).	- - -	- - -
27	Algal turf	*Caulerpa verticillata, Canistrocarpus cervicornis, Dictyosphaeria ocellata; Dictyopteris spp.; Gelidiella acerosa; Hydrolithon pachydermum; Padina gymnospora*	Sampling locally, high precision. (Longo et al. 2015)	Same species, same system, high precision (Fonseca et al. 2018). Conversion factor g C : g ww = 16.7 (Opitz 1996).	- - -	- - -
28	Detritus	- - -	Indirect estimate. Formula: Log DE = 0.954*log (PP) + 0.863*log(Euphotic) - 2.41 DE: standing biomass detritus ($gC*m^{-2}$); PP: total primary production ($gC*m^{-2}*year^{-1}$); Euphotic: Euphotic deep (m). For the Rocas Atoll ecosystem, PP = 94.9 $gC*m^{-2}*year^{-1}$. Euphotic deep= 4 meters. Conversion factor g C : g ww = 16.7 (Opitz 1996).	- - -	- - -	- - -

Biomass estimates for fish species/functional groups

Abundance-by-length estimates for fish species were taken from underwater visual censuses (UVC) between 2012 and 2018, and converted to biomass using length–weight relationships estimated with the local samples. UVC consisted of belt transects in which a diver identified, counted, and estimated the total length of fish species inside an area of 40 m^2 (20·2 m). A total of 153 UVC were performed in March 2012 (the year of the baseline model), and the number of transects varied from 5 to 25, depending on the available reef area. We accounted for potential bias associated with counting fish swimming at the border of the transects by multiplying observed fish abundances by relative biases values for different reef fish speeds. The biases for each combination of the survey parameters (fish speed, survey time, visibility, transect width, diver speed, fish turning angle) were taken from Ward-Paige and others 2010.

Table S2. Diet composition of functional groups in the Rocas Atoll Ecopath model (reference year 2012), showing final balanced input values. The consumption of preys that are not a part of the Rocas Atoll ecosystem as it is defined, for example for species that spend fractions of the year feeding outside the area of the model, diet is characterizes as import.

Group number	Functional group	1	2	3	4	5	6	7	8	9	10	11	12	13	14	15	16	17	18	19	20	21	22	23	24
1	Sea birds																								
2	*Negaprion brevirostris*																								
3	*Ginglymostoma cirratum*																								
4	*Lutjanus jocu*		0.01	0.01	0.01	0.01																			
5	*Cephalopholis fulva*		0.10																						
6	Carangidae	0.07	0.06																						
7	*Acanthurus* spp.	0.05	0.20	0.01	0.05	0.11	0.05																		
8	*Stegastes rocasensis*		0.05		0.02	0.04																			
9	*Thalassoma noronhanum*					0.04	0.01																		
10	*Abudefduf saxatilis*				0.01	0.01	0.01																		
11	*Sparisoma* spp.		0.05																						
12	*Melichthys niger*		0.04																						
13	*Kyphosus* spp.		0.05																						
14	*Mulloidichthys martinicus*		0.02																						

15	*Holocentrus adscensionis*		0.04	0.01	0.04	0.03	0.01																		
16	Haemulidae	0.03	0.05		0.03	0.02																			
17	Cryptobenthic reef fishes	0.03	0.08		0.01	0.10	0.01																		
18	Turtles		0.01																						
19	Cephalopoda	0.05	0.05	0.10	0.03	0.01	0.04																		
20	*Panulirus* spp.			0.35																					
21	Benthic macroinvertebrates	0.12	0.03	0.29	0.39	0.35	0.19			0.10					0.25	0.70	0.30	0.05	0.35	0.70	0.20	0.05			
22	Benthic microinvertebrates	0.10	0.01	0.15	0.31	0.19	0.40	0.10	0.03	0.15	0.20	0.20	0.10	0.02	0.70	0.25	0.60	0.21	0.25	0.30	0.35	0.20	0.01		
23	*Siderastrea stellata*																								
24	Zooplankton						0.06			0.10	0.20		0.15		0.05	0.05	0.10	0.10						0.60	0.15
25	Phytoplankton										0.10							0.05							0.50
26	Digenea simplex							0.20	0.10	0.05		0.20	0.10	0.88					0.20			0.10			
27	Algal turf							0.40	0.59	0.40	0.40	0.30	0.60	0.10				0.15	0.10				0.10		
28	Detritus						0.11	0.30	0.28	0.20	0.10	0.30	0.05					0.44	0.10		0.45	0.65	0.89		
	Import	0.55	0.14	0.08	0.10	0.08	0.11																		0.35

Table S3. Basic estimates of the Rocas Atoll Ecopath model (reference year 2012). Values in bold were estimated by Ecopath balance routine. TL = trophic level; EE = ecotrophic efficiency; B = biomass ($g \cdot m^2$); P/B =production to biomass ratio ($year^{-1}$) ; Q/B = consumption to biomass ratio ($year^{-1}$); BA= biomass accumulation ($g \cdot m^2$).

Functional group number	Functional group	Trophic level	Habitat area	B ($g \cdot m^2$)	P/B	Q/B	EE	BA ($g \cdot m^2$)

1	Sea birds	**3.50**	1.00	0.02	5.40	80.00	**0.00**	
2	*Negaprion brevirostris*	**3.58**	1.00	0.17	0.23	3.70	**0.00**	
3	*Ginglymostoma cirratum*	**3.47**	1.00	1.80	0.22	3.60	**0.82**	0.31
4	*Lutjanus jocu*	**3.27**	1.00	2.22	0.52	6.30	**0.01**	-0.06
5	*Cephalopholis fulva*	**3.28**	1.00	0.20	0.65	5.51	**0.95**	0.54
6	*Carangidae*	**3.04**	1.00	2.12	0.62	13.20	**0.60**	0.44
7	*Acanthurus spp.*	**2.10**	1.00	9.86	0.83	12.90	**0.28**	-0.01
8	*Stegastes rocasensis*	**2.03**	1.00	0.46	1.25	17.10	**0.67**	-0.01
9	*Thalassoma noronhanum*	**2.71**	1.00	0.20	1.19	16.40	**0.79**	0.02
10	*Abudefduf saxatilis*	**2.63**	1.00	0.99	0.89	13.00	**0.45**	0.08
11	*Sparisoma* spp.	**2.20**	1.00	1.13	0.65	7.20	**0.20**	0.25
12	*Melichthys niger*	**2.67**	1.00	0.27	0.76	11.60	**0.52**	0.38
13	*Kyphosus* spp.	**2.02**	1.00	0.46	0.62	24.40	**0.11**	
14	*Mulloidichthys martinicus*	**3.08**	1.00	0.42	0.72	11.10	**0.60**	1.05
15	*Holocentrus adscensionis*	**3.19**	1.00	2.12	0.75	8.30	**0.98**	0.43
16	Haemulidae	**3.09**	1.00	0.96	0.79	11.60	**0.84**	0.09
17	Cryptobenthic reef fishes	**2.38**	1.00	0.79	1.87	10.57	**0.26**	-0.17

18	Turtles	**2.80**	1.00	0.02	0.29	2.35	**0.00**
19	Cephalopoda	**3.19**	1.00	0.41	6.40	36.50	**0.95**
20	*Panulirus* spp.	**2.61**	0.85	5.10	1.28	7.40	**0.36**
21	Benthic macroinvertebrates	**2.27**	1.00	**16.70**	3.80	10.00	0.90
22	Benthic microinvertebrates	**2.01**	1.00	**25.69**	4.94	16.69	0.85
23	*Siderastrea stellata*	**1.76**	0.18	0.71	1.66	9.40	**0.00**
24	Zooplankton	**2.08**	0.95	0.24	87.00	160.00	**0.94**
25	Phytoplankton	**1.00**	1.00	0.13	109.50		**0.70**
26	*Digenea simplex*	**1.00**	0.60	211.64	17.16		**0.0009**
27	Algal turf	**1.00**	0.55	802.31	15.79		**0.0004**
28	Detritus	**1.00**	1.00	381			**0.0018**

2. Details of the Ecosim module

This section provides details on the Ecosim module associated with simulations of fish biomass under increasing sea water temperature. Ecosim consists of biomass dynamics expressed through a series of coupled differential equations. The equations are derived from the Ecopath master Eq. (1) and Eq.(2), and take the form (7):

$$\frac{dB_i}{dt} = g_i \cdot \sum_j Q_{ji} - \sum_j Q_{ij} + I_i - \left(MO_i + e_i\right) \cdot B_i \quad (7)$$

where $d\mathrm{B_i}/d t$ represents the growth rate during the time interval dt of group i in terms of its biomass, B_i, g_i is the net growth efficiency estimated using the ratio between P/B and Q/B, MO_i is the non-predation ('other') natural mortality rate estimated from the ecotrophic efficiency, e_i is emigration rate, I_i is immigration rate (assumed constant over time, and hence independent of events in the ecosystem modeled). The two summations of the Eq. (7) estimate consumption rates, the first expressing the total consumption by group i, and the second the predation by all predators on the same group i.

2.1 Development of temporal simulations using the forecast temperature scenarios

In the Ecosim main equation (Eq. 7), the consumption rates, Q_{ji}, are calculated based on the 'foraging arena' concept, where B_i's are divided into vulnerable and invulnerable components (Walters and others 1997), and it is the transfer rate (v_{ij}) between these two components that determines if control is top-down, bottom-up, or of an intermediate type. The set of differential equations is solved in Ecosim using an Adams-Basforth integration routine (Butcher 2000). For each predator-prey interaction, consumption rates were calculated as (8):

$$Q_{ij} = \frac{a_{ij} \cdot v_{ij} \cdot B_i \cdot P_j \cdot T_j \cdot M_{ij} / D_j}{v_{ij} + \left(v_{ij} \cdot T_i \cdot M_{ij}\right) + \left(a_{ij} \cdot M_{ij} P_i \cdot T_j / D_j\right)} \cdot f\left(Env_{function}, t\right) \quad (8)$$

where a_{ij} is the rate of effective search for prey (i) by predator (j), v_{ij} is the vulnerability parameter, T_i represents prey relative feeding time, T_j is the predator relative feeding time, B_i is prey biomass,

P_j is the predator biomass, M_{ij} is the mediation forcing effects, and D_j represents effects of handing time as a limit to consumption rate. Environmental response functions ($Env_{function}$, t), which represent the tolerance relationship of a species to an environmental parameter (here defined with a minimum and maximum levels and the 5th and 95th percentiles) that can be used to account for changes in environmental drivers over time, in our case temperature.

Three Representative Concentration Pathways (RCPs) were used for projections of the future ocean warming in the Coupled Model Intercomparison Project Phase 5 (Taylor and others 2012). They are identified by their approximate anthropogenic radiative forcing (in $W \cdot m^{-2}$, relative to 1750) by 2100: RCP 2.6, RCP 4.5, and RCP 8.5 (Pörtner and others 2019). Future sea surface temperature values were extracted from the Royal Netherlands Meteorological Institute Climate Explorer portal (http://climexp.knmi.nl) within the study area location. Thirty-two model outputs, were extracted for the study area with temperatures fluctuating around their mean. Current average seawater temperature in Rocas Atoll's is 27.3º C, which by 2100, is expected to rise 0.5º C, 1.3º C and 3º C under the low (RCP 2.6), intermediate (RCP 4.5) and high (RCP 8.5) ocean warming scenarios, respectively (Supplementary materials, Figure S2).

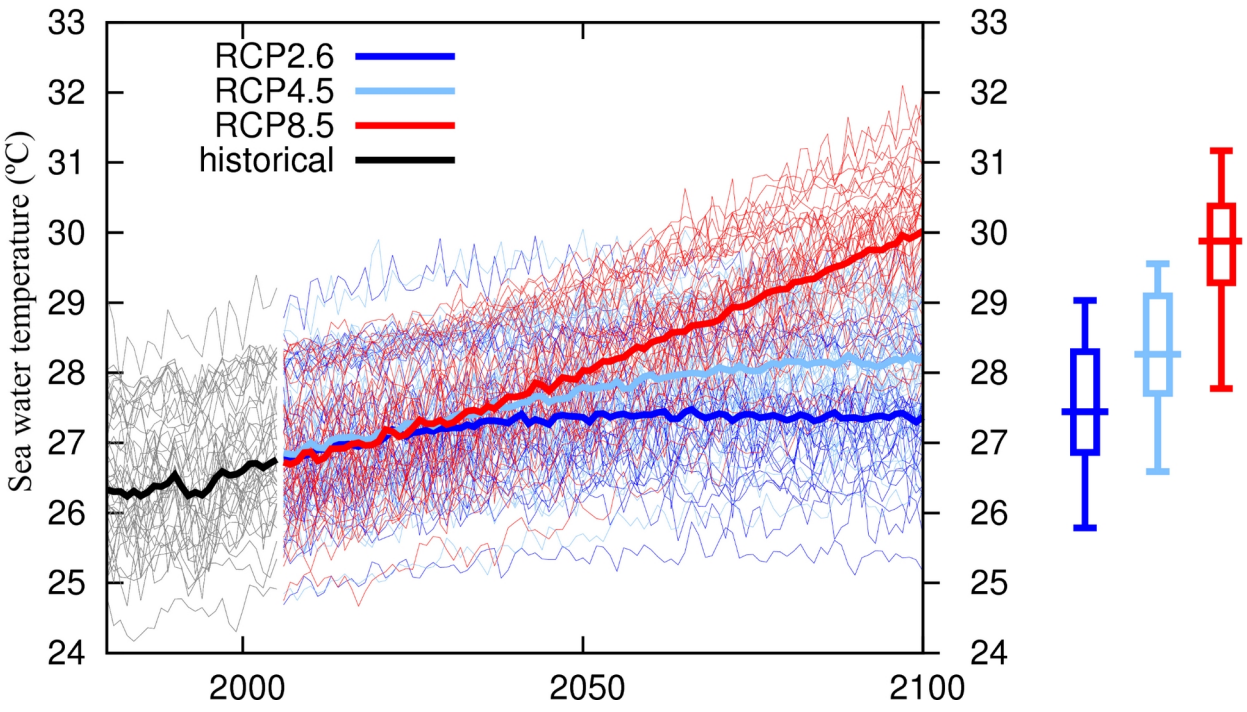

Figure S2. Future Sea Surface Water Temperature projections (1980-2100) for the Rocas Atoll reef ecosystem (03°50'S, 33°49'W, 7.5 km^2) from the ocean warming multi-model ensemble means (RCP 2.6, RCP 4.5 and RCP 8.5 greenhouse gas emissions scenarios). Box plots represents means (solid lines), the lower and upper hinges correspond to the first and third quartiles (the 25th and 75th percentiles) and the length of the whiskers as multiple 1.5 of Inter Quartile Range.

2.2 Fitting model to fish time series

The model fitting was performed using an automated stepwise fitting procedure (Scott and others 2016) to define the vulnerability values of the trophic interaction function that improve the statistical fit of predicted/observed data using the weighted sum of squared differences (SS) and the Akaike Information Criterion (AIC). The formula used for the AIC is defined as:

$$AIC = n * \log(minSS/n) + 2K \quad (9)$$

where n is calculated by the fitting procedure as the total number of observations, or time series values, from the loaded fish biomass times series. minSS is the minimum sum of squares calculated by the algorithm, and K is the number of parameters estimated. In addition, the procedure also calculates the AICc, to address small sample size. The AICc is defined as:

$$AICc = AIC + 2K \cdot (K - 1) / (n - K - 1) \quad (10)$$

All the alternative iterations that may describe the observation data in equal measure and the best-fitted model are shown in Table S1. Fitted vulnerabilities values are shown in Table S2 and time series biomass dynamics fitted by the food web model are shown in Figure S3.

Table S4. Comparison across selected stepwise fitting interactions and the model baseline iteration, showing the number of total parameters estimated (Vulnerabilities (Vs), the model sum of squares (SS), the Akaike Information Criterion (AIC) and AICc with a correction for small sample sizes. In bold the best fitted model.

Model iteration	Vs	SS	AIC	AICc
Baseline	0	13.71	-192.74	-192.74
Baseline and 1v	1	13.35	-193.25	-193.25
Baseline and 2v	2	11.88	-202.62	-202.57
Baseline and 3v	3	11.35	-204.94	-204.81
Baseline and 4v	**4**	**11.03**	**-205.58**	**-205.33**
Baseline and 5v	5	11.01	-203.56	-203.12
Baseline and 6v	6	10.74	-203.74	-203.08
Baseline and 7v	7	10.69	-201.80	-200.86
Baseline and 8v	8	10.32	-202.88	-201.62
Baseline and 9v	9	10.32	-200.47	-198.83
Baseline and 10v	10	10.21	-199.06	-196.99
Baseline and 11v	11	10.21	-196.53	-193.97
Baseline and 12v	12	10.20	-194.05	-190.94
Baseline and 13v	13	10.02	-193.06	-189.34

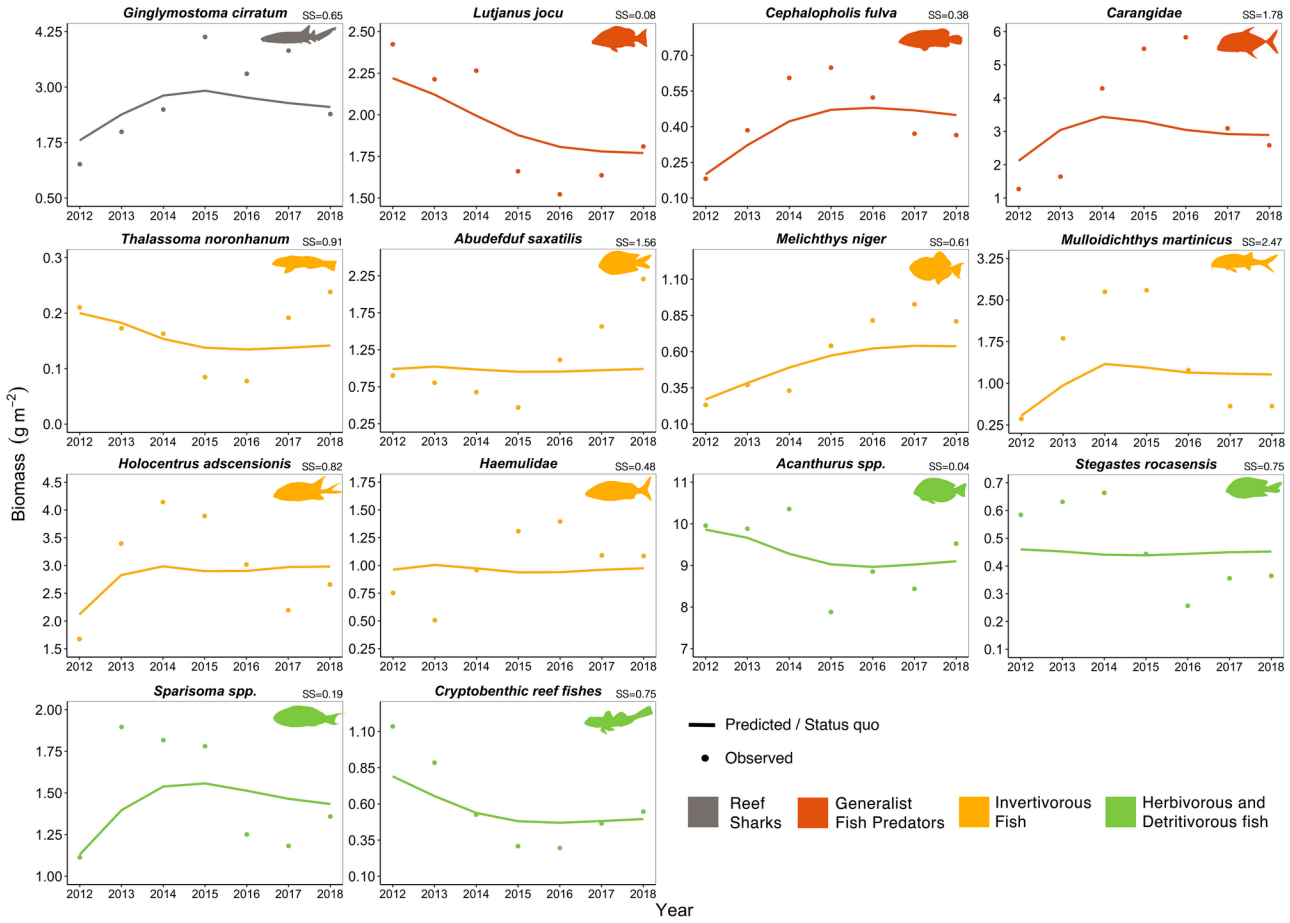

214 **Figure S3.** Observed (dots) and predicted (lines) relative biomass ($g \cdot m^{-2}$) trends for fish functional
215 groups with fitted estimated biomass data in the Rocas Atoll ecosystem model (2012-2018). The
216 sum of squares is noted next to each fish functional group name.

2.3. Assessing uncertainty in biomass dynamics under ocean warming

The Monte Carlo routine in Ecosim was used to perform sensitivity analyses for projections of biomass dynamics under ocean warming. This routine tests the sensitivity of Ecosim's output to Ecopath input parameters by drawing input parameters from a uniform distribution centered on the base Ecopath value with the coefficients of variation set to default 0.1 (Christensen and Walters 2004). In this study we set coefficients of variation as 0.1 for P/B, Q/B and Biomass Accumulation parameters. Fish biomass coefficients of variation were defined as the ratio between the standard deviation and the mean of each fish time series (Table S2). We ran 250 Monte Carlo simulations for each scenario based on coefficients of variation to determine the 95% confidence intervals. The mean of the distribution is set as the base Ecopath value of the parameter. The coefficients of variance were used to calculate the upper and lower limits of the distribution (upper limit = mean + 2*CV.*mean; lower limit = mean - 2*CV*mean).

Table S5. Upper and lower biomass coefficients of variations (CV) used for Monte Carlo analysis.

Group number	Group name	CV	Lower limit	Mean	Upper limit
1	Sea birds	0.25	0.01	0.02	0.03
2	*Negaprion brevirostris*	0.15	0.11	0.17	0.22
3	*Ginglymostoma cirratum*	0.15	1.26	1.8	2.34
4	*Lutjanus jocu*	0.05	1,998	2.22	2.44
5	*Cephalopholis fulva*	0.10	0.16	0.2	0.24
6	*Carangidae*	0.15	1.48	2.12	2.75
7	*Acanthurus spp.*	0.1	7.88	9.86	11.83
8	*Stegastes rocasensis*	0.11	0.35	0.46	0.56
9	*Thalassoma noronhanum*	0.15	0.14	0.2	0.26
10	*Abudefduf saxatilis*	0.12	0.75	0.99	1.22
11	*Sparisoma spp.*	0.11	0.88	1.13	1.37
12	*Melichthys niger*	0.13	0.19	0.27	0.34
13	*Kyphosus spp.*	0.05	0.41	0.46	0.51
14	*Mulloidichthys martinicus*	0.2	0.24	0.41	0.58
15	*Holocentrus adscensionis*	0.12	1.61	2.11	2.62
16	Haemulidae	0.15	0.67	0.96	1.25

17	Cryptobenthic reef fishes	0.11	0.61	0.79	0.96
18	Turtles	0.1	0.017	22.0	0.026
19	Cephalopoda	0.25	0.20	0.40	0.60
20	Panulirus spp.	0.25	2.55	5.1	7.65
21	Benthic macroinvertebrates	0.1	12.98	16.23	19.47
22	Benthic microinvertebrates	0.1	19.48	24.35	29.23
23	Siderastrea stellata	0.1	0.56	711	0.85
24	Zooplankton	0.15	0.16	0.23	0.30
25	Phytoplankton	0.05	0.11	0.13	0.14
26	Digenea simplex	0.05	190.47	211.63	232.80
27	Other algal turf	0.05	722.08	802.31	882.54

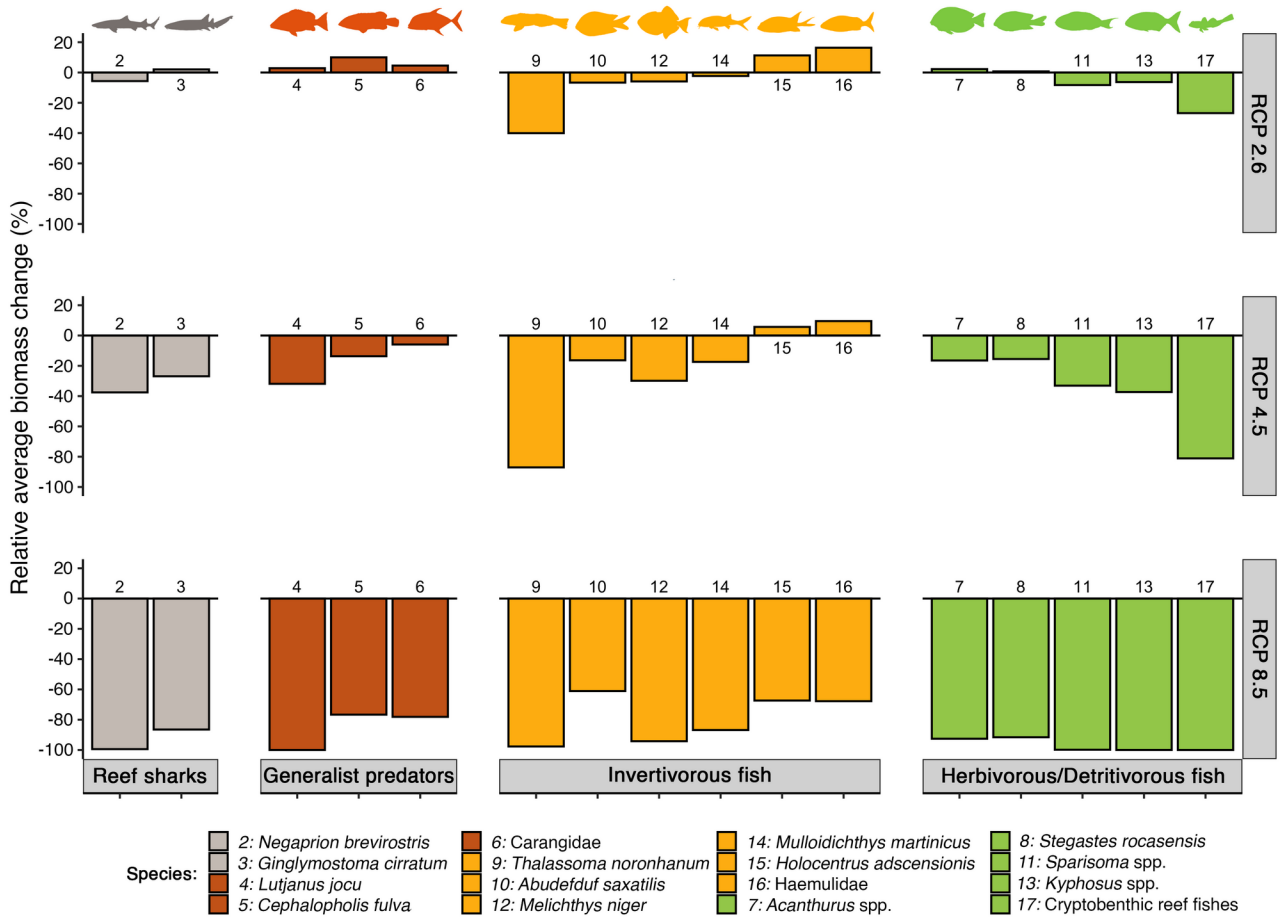

Fig. S4. Model projections for relative biomass change under ocean warming scenarios for fish functional groups of the Rocas Atoll ecosystem. All changes are expressed as % mean of the 2100 relative to the 2100 Status quo scenario projections.

Fig. S5. Model projections for relative biomass change under ocean warming scenarios for

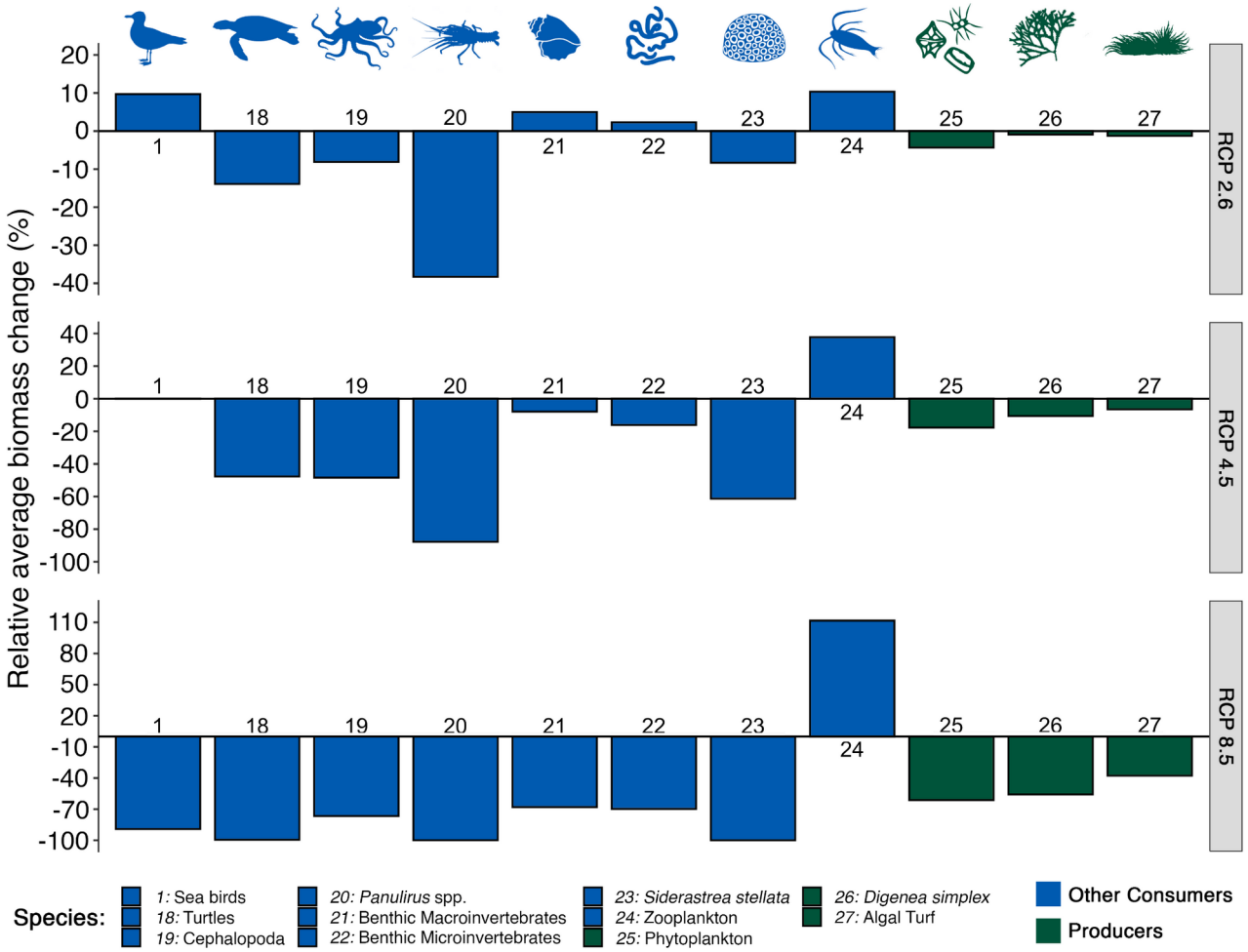

functional groups of the Rocas Atoll ecosystem that are not fish. All changes are expressed as % mean of the 2100 relative to the 2100 Status quo scenario projections.

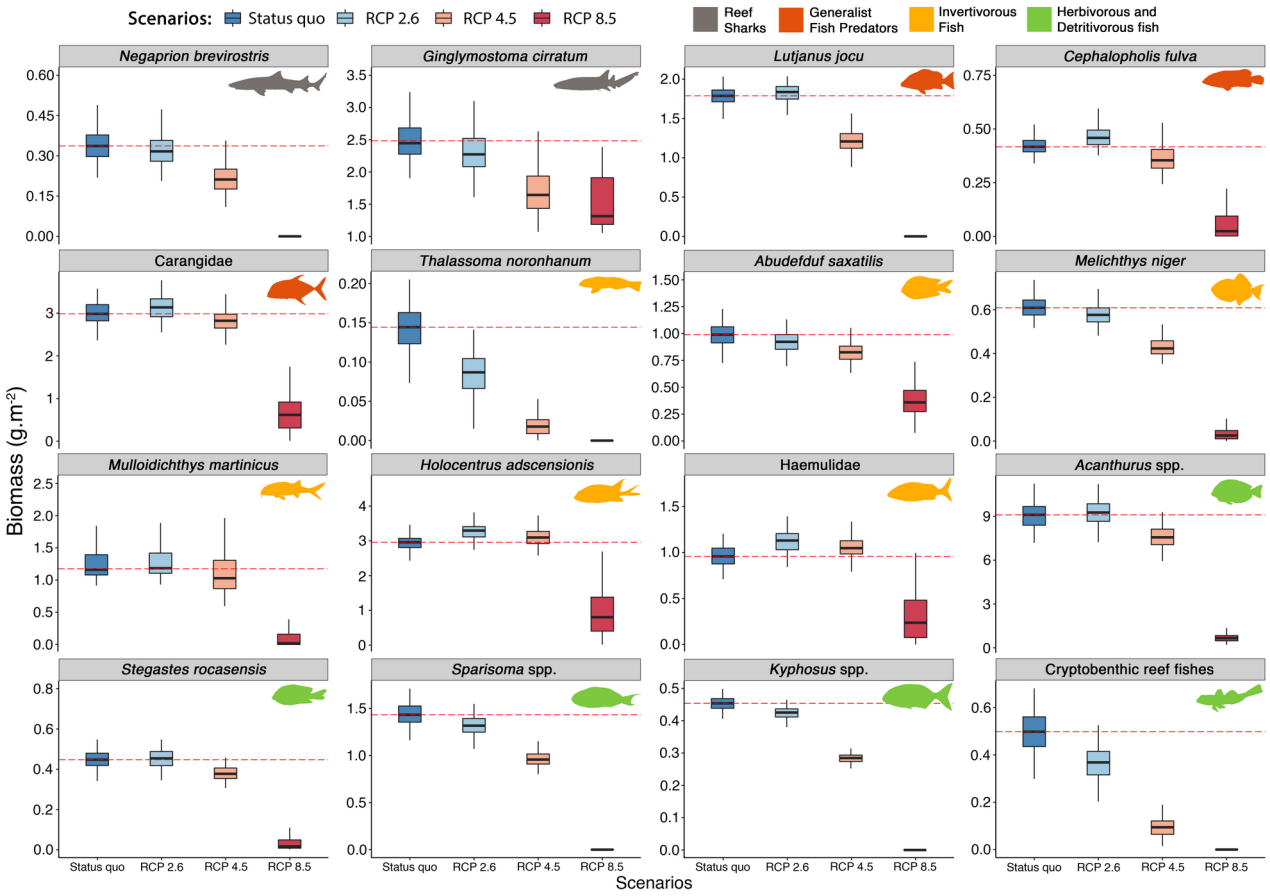

Fig. S6. Projected ocean warming effect (RCP 2.6, RCP 4.5, RCP 8.5) vs Status quo scenario in 2100 for fish functional groups biomass. Box plots display the median (horizontal line), the lower and upper hinges correspond to the first and third quartiles (the 25th and 75th percentiles). The lower whisker extends from the hinge to the smallest value at most 1.5 * interquartile range of the hinge. The red dotted line represents the Status quo scenario median value for reference.

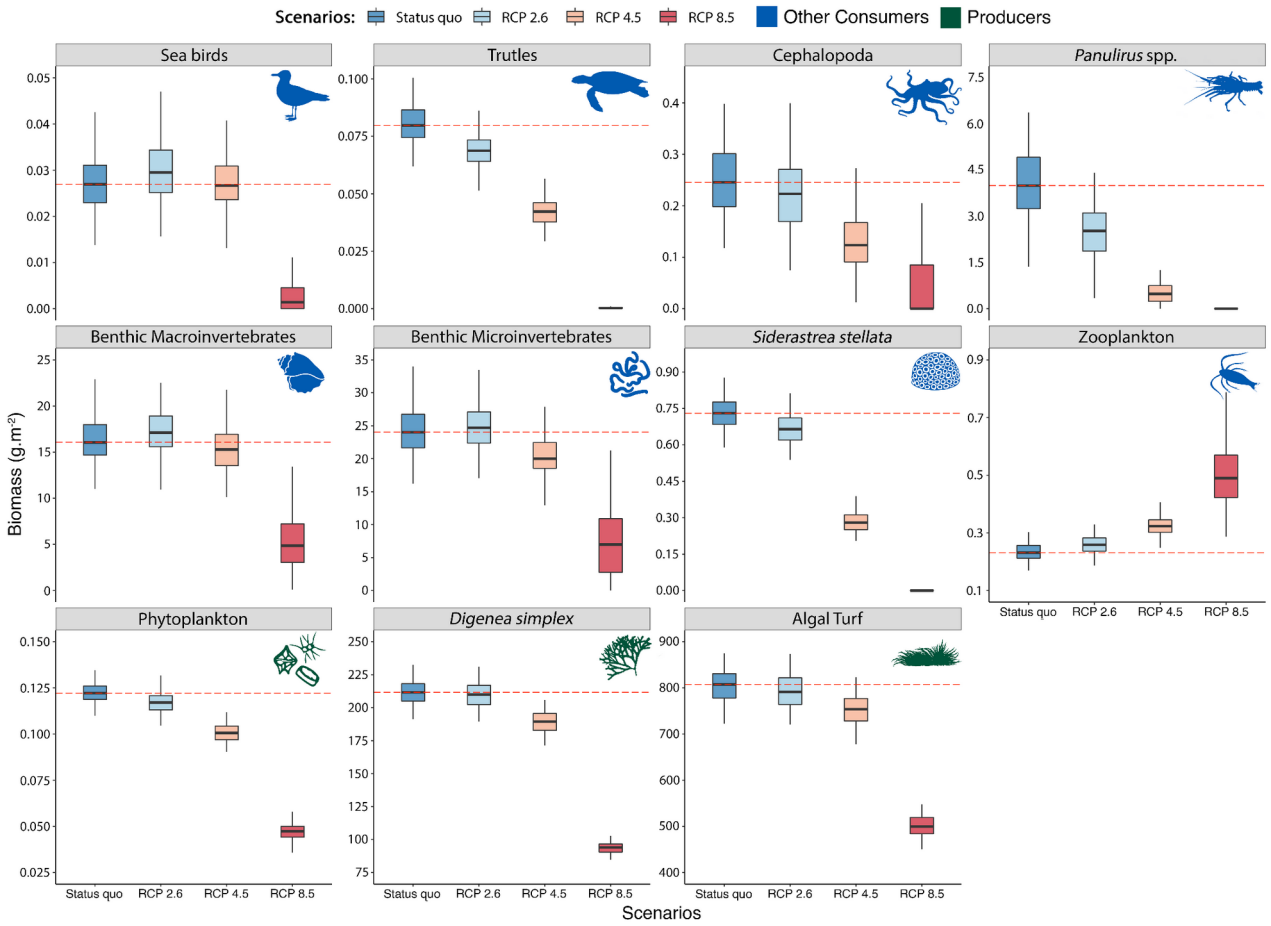

254

255 **Fig. S7.** Projected ocean warming effect (RCP 2.6, RCP 4.5, RCP 8.5) vs Status quo scenario in
256 2100 for no fish functional groups biomass. Box plots display the median (horizontal line), the
257 lower and upper hinges correspond to the first and third quartiles (the 25th and 75th percentiles).
258 The lower whisker extends from the hinge to the smallest value at most 1.5 * interquartile range of
259 the hinge. The red dotted line represents the Status quo scenario median value for reference.
260

261
262

References Section 1

Almeida CE de, Marchon-Silva V, Ribeiro R, et al (2000) Entomological fauna from Reserva Biológica do Atol das Rocas, RN, Brazil: I. Morphospecies composition. Rev Bras Biol 60:291–298. https://doi.org/10.1590/S0034-71082000000200013

Andrades RC (2018) Nicho e endemismo em ambientes entremarés recifais: uma abordagem utilizando isótopos estáveis. Doctoral Thesis, Federal University of Espirito Santo. http://repositorio.ufes.br/handle/10/9927

Araújo JN, Martins AS, Bonecker ACT, et al (2017) Modelos Ecopath da plataforma continental e do talude da Bacia de Campos: análise das propriedades ecossistêmicas e do efeito da sazonalidade. In: Modelagem Ecossistêmica para integração e manejo na Bacia de Campos (Atlântico sudoeste). Elsevier Brazil, Rio de janeiro, pp 131–187

Bode A, Hernández-León S (2018) Trophic Diversity of Plankton in the Epipelagic and Mesopelagic Layers of the Tropical and Equatorial Atlantic Determined with Stable Isotopes. Diversity 10:48. https://doi.org/10.3390/d10020048

Bouth HF, Leite TS, Lima FD de, Oliveira JEL (2011) Atol das Rocas: an oasis for Octopus insularis juveniles (Cephalopoda: Octopodidae). Zool Curitiba 28:45–52. https://doi.org/10.1590/S1984-46702011000100007

Bowie G, Mills W, Porcella D, et al (1985) Rates Constants and Kinetics Formulations in Surface Water Quality Modeling EDITION

Brandl SJ, Goatley CHR, Bellwood DR, Tornabene L (2018) The hidden half: ecology and evolution of cryptobenthic fishes on coral reefs. Biol Rev 93:1846–1873. https://doi.org/10.1111/brv.12423

Buitenhuis ET, Hashioka T, Quéré CL (2013) Combined constraints on global ocean primary production using observations and models. Glob Biogeochem Cycles 27:847–858. https://doi.org/10.1002/gbc.20074

297 Coelho F do N, Pinheiro HT, Santos RG dos, et al (2012) Spatial distribution and diet of
298 Cephalopholis fulva (Ephinephelidae) at Trindade Island, Brazil. Neotropical Ichthyol 10:383–
299 388. https://doi.org/10.1590/S1679-62252012005000010
300
301 Cortés E, Gruber SH (1990) Diet, Feeding Habits and Estimates of Daily Ration of Young Lemon
302 Sharks, Negaprion brevirostris (Poey). Copeia 1990:204–218. https://doi.org/10.2307/1445836
303
304 Christensen V, Coll M, Buszowski J, et al (2015) The global ocean is an ecosystem: simulating
305 marine life and fisheries. Glob Ecol Biogeogr 24:507–517. https://doi.org/10.1111/geb.12281
306
307 Dantas R, Silva Leite T, Queiroz de Albuquerque C (2019) The trophic role of Octopus insularis at
308 a pristine tropical atoll in southwest Atlantic: a potential keystone predator?
309 https://www.ingentaconnect.com/content/umrsmas/bullmar/pre-prints/content-bms_9543.
310
311 Ferrier-Pagès C, Hoogenboom M, Houlbrèque F (2011) The Role of Plankton in Coral
312 Trophodynamics. In: Dubinsky Z, Stambler N (eds) Coral Reefs: An Ecosystem in Transition.
313 Springer Netherlands, Dordrecht, pp 215–229
314
315 Fonseca A, Villaça R, Knoppers B (2018) Nutrients and Macroalgal Primary Production of the sole
316 Atoll in the SW-Atlantic (Atol das Rocas, Brazil). Preprint publication.
317
318 Fonseca AC (2010) Estrutura e produtividade primária das comunidades de macroalgas e dinâmica
319 de nutrientes no sistema recifal do Atol das Rocas, RN – Brasil. Doctoral Thesis, Universidade
320 Federal Fluminense. https://app.uff.br/riuff/handle/1/6138
321
322 Freire KMF, Christensen V, Pauly D (2008) Description of the East Brazil Large Marine Ecosystem
323 using a trophic model. Sci Mar 72:477–491. https://doi.org/10.3989/scimar.2008.72n3477
324
325 Froese R, Pauly D (2019) FishBase. World Wide Web electronic publication.
326
327 Gaeta J (2014) Comportamento ecologico das populaçoes de lagosta do Atol das Rocas. Master
328 thesis, Federal University of Ceará.
329 http://www.repositorio.ufc.br/bitstream/riufc/11373/1/2014_dis_jdecgaeta.pdf
330

Góes CA, Lins-Oliveira JE (2009) Natural diet of the spiny lobster, Panulirus echinatus Smith, 1869 (Crustacea: Decapoda: Palinuridae), from São Pedro and São Paulo Archipelago, Brazil. Braz J Biol 69:143–148. https://doi.org/10.1590/S1519-69842009000100018

Grossman A, Daura-Jorge FG, Silva M de B, Longo GO (2019) Population parameters of green turtle adult males in the mixed ground of Atol das Rocas, Brazil. Mar Ecol Prog Ser 609:197–207. https://doi.org/10.3354/meps12821

Higgs ND, Newton J, Attrill MJ (2016) Caribbean Spiny Lobster Fishery Is Underpinned by Trophic Subsidies from Chemosynthetic Primary Production. Curr Biol 26:3393–3398. https://doi.org/10.1016/j.cub.2016.10.034

Jales MC (2015) Influência das condições oceanográficas sobre a estrutura da comunidade fitoplanctônica no Atol das Rocas, Atlântico Sul Equatorial, Brasil. Doctoral Thesis, Federal University of Pernambuco

Krajewski JP, Bonaldo RM, Sazima C, Sazima I (2006) Foraging activity and behaviour of two goatfish species (Perciformes: Mullidae) at Fernando de Noronha Archipelago, tropical West Atlantic. Environ Biol Fishes 77:1–8. https://doi.org/10.1007/s10641-006-9046-z

Leletkin VA (2000) The Energy Budget of Coral Polyps. Russ J Mar Biol 26:389–398. https://doi.org/10.1023/A:1009497303413

Lira SM de A, Teixeira I de Á, Lima CDM de, et al (2014) Spatial and nycthemeral distribution of the zooneuston off Fernando de Noronha, Brazil. Braz J Oceanogr 62:35–45. https://doi.org/10.1590/s1679-87592014058206201

Longo GO, Morais RA, Martins CDL, et al (2015) Between-Habitat Variation of Benthic Cover, Reef Fish Assemblage and Feeding Pressure on the Benthos at the Only Atoll in South Atlantic: Rocas Atoll, NE Brazil. PLOS ONE 10:e0127176. https://doi.org/10.1371/journal.pone.0127176

Matott MP, Motta PJ, Hueter RE (2005) Modulation in Feeding Kinematics and Motor Pattern of the Nurse Shark Ginglymostoma cirratum. Environ Biol Fishes 74:163–174. https://doi.org/10.1007/s10641-005-7435-3

366 Mendes TC, Quimbayo JP, Bouth HF, et al (2019) The omnivorous triggerfish Melichthys niger is a
367 functional herbivore on an isolated Atlantic oceanic island. J Fish Biol 95:812–819.
368 https://doi.org/10.1111/jfb.14075
369
370 Morato T, Lemey E, Menezes G, et al (2016) Food-Web and Ecosystem Structure of the Open-
371 Ocean and Deep-Sea Environments of the Azores, NE Atlantic. Front Mar Sci 3:.
372 https://doi.org/10.3389/fmars.2016.00245
373
374 Netto SA, Attrill MJ, Warwick RM (2003) The relationship between benthic fauna, carbonate
375 sediments and reef morphology in reef-flat tidal pools of Rocas Atoll (north-east Brazil). J Mar
376 Biol Assoc U K 83:425–432. https://doi.org/10.1017/S0025315403007288h
377
378 Neumann-Leitão S, Sant'anna EME, Gusmão LMDO, et al (2008) Diversity and distribution of the
379 mesozooplankton in the tropical Southwestern Atlantic. J Plankton Res 30:795–805.
380 https://doi.org/10.1093/plankt/fbn040
381
382 Opitz, Silvia. Trophic interactions in Caribbean coral reefs. Vol. 1085. WorldFish, 1996.
383
384 Pereira PHC, Barros B, Zemoi R, Ferreira BP (2015) Ontogenetic diet changes and food
385 partitioning of Haemulon spp. coral reef fishes, with a review of the genus diet. Rev Fish Biol
386 Fish 25:245–260. https://doi.org/10.1007/s11160-014-9378-2
387
388 Pinheiro BR, Pereira NS, Agostinho PGF, et al (2017) Population dynamics of Siderastrea stellata
389 Verrill, 1868 from Rocas Atoll, RN: implications for predicted climate change impacts at the
390 only South Atlantic atoll. An Acad Bras Ciênc 89:873–884. https://doi.org/10.1590/0001-
391 3765201720160387
392
393 Scott E, Serpetti N, Steenbeek J, Heymans JJ (2016) A Stepwise Fitting Procedure for automated
394 fitting of Ecopath with Ecosim models. SoftwareX 5:25–30.
395 https://doi.org/10.1016/j.softx.2016.02.002
396
397 Silvano RAM (2001) Feeding Habits and Interspecific Feeding Associations of Caranx Latus
398 (Carangidae) in a Subtropical Reef. Environ Biol Fishes 60:465–470.
399 https://doi.org/10.1023/A:1011064923544
400

Silvano RAM, Güth AZ (2006) Diet and feeding behavior of Kyphosus spp. (Kyphosidae) in a Brazilian subtropical reef. Braz Arch Biol Technol 49:623–629. https://doi.org/10.1590/S1516-89132006000500012

Sley A, Jarboui O, Ghorbel M, Bouain A (2009) Food and feeding habits of Caranx crysos from the Gulf of Gabès (Tunisia). J Mar Biol Assoc U K 89:1375–1380. https://doi.org/10.1017/S0025315409000265

Souza AT, Ilarri MI, Rosa IL (2011) Habitat use, feeding and territorial behavior of a Brazilian endemic damselfish Stegastes rocasensis (Actinopterygii: Pomacentridae). Environ Biol Fishes 91:133–144. https://doi.org/10.1007/s10641-010-9765-z

Tan BC, Anticamara J, Villanueva C-M (2018) Modeling of degraded reefs in Leyte Gulf, Philippines in the face of climate change and human-induced disturbances. Clim Disaster Dev J 3:1–12. https://doi.org/10.18783/cddj.v003.i01.a01

Turingan RG, Wainwright PC, Hensley DA (1995) Interpopulation variation in prey use and feeding biomechanics in Caribbean triggerfishes. Oecologia 102:296–304. https://doi.org/10.1007/BF00329796

438 **References Section 2**

Butcher JC. 2000. Numerical methods for ordinary differential equations in the 20th century. Journal of Computational and Applied Mathematics 125:1–29. http://www.sciencedirect.com/science/article/pii/S0377042700004556. Last accessed 17/04/2020

Christensen V, Walters CJ. 2004. Ecopath with Ecosim: methods, capabilities and limitations. Ecol Model 172:109–39.

Froese R, Pauly D. 2019. FishBase. World Wide Web electronic publication. www.fishbase.org

Palomares MLD, Pauly D. 1998. Predicting food consumption of fish populations as functions of mortality, food type, morphometrics, temperature and salinity. Mar Freshwat Res 49:447–53.

Pauly D. 1980. On the interrelationships between natural mortality, growth parameters, and mean environmental temperature in 175 fish stocks. ICES J Mar Sci 39:175–92.

Scott E, Serpetti N, Steenbeek J, Heymans JJ. 2016. A Stepwise Fitting Procedure for automated fitting of Ecopath with Ecosim models. SoftwareX 5:25–30. http://www.sciencedirect.com/science/article/pii/S2352711016000054. Last accessed 26/11/2019

Walters C, Christensen V, Pauly D. 1997. Structuring dynamic models of exploited ecosystems from trophic mass-balance assessments. Reviews in Fish Biology and Fisheries 7:139–72. https://doi.org/10.1023/A:1018479526149. Last accessed 16/04/2020?

Chapter 3

Fish body size and temperature relationship: new insights from the Western Atlantic Ocean

Authors: Leonardo Capitani[1,2], Asta Audzijonyte[3,4], Ronaldo Angelini[5], Guilherme Ortigara Longo[2]

Address

[1] Post-Graduate Program in Ecology, Bioscience Center, Universidade Federal do Rio Grande do Norte, Natal, 59072-970, Brazil

[2] Marine Ecology Laboratory, Department of Oceanography and Limnology, Universidade Federal do Rio Grande do Norte, Natal, RN, 59014-002, Brazil

[3] Institute for Marine and Antarctic Studies, University of Tasmania, Hobart, Tasmania, Australia.

[4] Centre for Marine Socioecology, University of Tasmania, Hobart, Tasmania, Australia

[5] Department of Civil Engeneering, Universidade Federal do Rio Grande do Norte, Natal, 59078-970, Brazil

Introduction

Temperature strongly regulates physiology and fitness of marine ectotherms (Payne et al. 2016, Dahlke et al. 2020). Fish body size, for instance, is expected to decrease under increased water temperature (Daufresne et al. 2009, Pauly and Cheung 2018), a phenomenon often described as a temperature-size rule (Atkinson 1994), but that remains controversial (Fisher et al. 2010, Siepielski et al. 2019, Audzijonyte et al. 2020). Many studies have measured the temperature dependence of fish body size in controlled laboratory settings (Angilletta et al. 2004, Moyano et al. 2020, Currie and Evans 2020). However, little is known about how temperature influences fish body size in the environment, particularly in the Atlantic Ocean (Rijn et al. 2017, Goldberg et al. 2019), so the ecological significance of the temperature-size rule for marine ectotherms organisms is unclear (Lefevre et al. 2021).

Body size is a fundamental trait to life because it influences, among other things, individual fecundity and the likelihood of predation (Audzijonyte et al. 2013, Clarke 2017)(Clarke, 2017). For example, water temperature affected the fish biomass production in temperate and boreal lakes mainly through shifts in size− and age−distributions toward a higher proportion of young and small individuals (Dorst et al., 2019). Regions with stable temperatures (for example, the Northeast Pacific and Gulf of Mexico) show little change in species dominance structure, while areas with warming (for example, the North Atlantic) experience strong shifts towards warm-water species dominance (Burrows et al. 2019). In addition, increase in water temperature may cause rapid behavioral responses such as presented by omnivorous fishes that expand into ecosystems where they were previously rare or absent, resulting in topological rewiring of the food webs (Bartley et al., 2019; Inagaki et al. 2020). These changes may restructure food webs, with consequences for the stability and resilience of local ecosystems to other

external stressors, such as fishing and coastal pollution (Kirby et al., 2009; Sokolova & Lannig, 2008; Tunney et al., 2012).

There is no general consensus on whether the relationship between temperature and fish length is linear or non-linear (Neuheimer et al. 2011, Ramler et al. 2014, Oke et al. 2020). This lack of consensus can be explained by the fact that sea water temperature can influence biotic factors that are related to fish length (e.g., nutrient dynamics, food availability, species population dynamics, predation and competition) (Thorson et al. 2017, Reynolds et al. 2018, Dunstan et al. 2018). Among the various models proposed for the body size-temperature relationship, power-law models are among the most flexible (Marquet et al. 2005, Lindmark et al. 2018). The simplest power-law model is described by a power function of the form $Y = a \cdot X^{\beta}$ where a is a constant (Y value at X = 1) and β is the dimensionless scaling exponent (Huxley and Teissier 1936, Gayon 2000). Relationships that have β equal to zero do not change with the variable of interest and are therefore described as invariant with respect to temperature. When, $\beta = 1$ indicates that body size increases proportionally (linearly) to temperature, while $0 < \beta < 1$ or $\beta > 1$ indicates shallower or steeper increase of body size in relation to temperature, respectively. When $\beta < 0$ the relationship is known as an inverse power law, as the more temperature increases, the more body size shrinks.

To understand variation in fish body size across spatial temperature gradients, we need to recognize that the amount of fish biomass and production into the oceans is mediated by underlying individual attributes (e.g., fish body size) and how these respond to variation in temperature (Brandl et al. 2020, Morais and Bellwood 2020). The aims of this study are (1) to describe empirical relationships between seawater temperature and fish body size across marine fish from temperate to tropical western Atlantic's reef ecosystems; (2) to test whether relationships between seawater temperature and fish body size depend on fish species.

Previous research has shown an overall negative effect of temperature on fish body size, both among species (Rijn et al. 2017, Goldberg et al. 2019, Audzijonyte et al. 2020) and within species (Huss et al. 2019, Oke et al. 2020). Various explanations have been developed for a warm-induced limitation to fish body size, such as accelerated maturity in relation to growth in the warmth (Angilletta et al. 2004) or an allometric limitation of gill surface area causing an oxygen dependence of maximum body size (Pauly and Cheung 2018).

Here, we expect a nonlinear (power-law) relationship between fish body size and the annual mean sea surface temperature (SST) (i.e., $\beta \neq 1$ **).** Specifically we hypothesize that large bodied species are more likely to decrease in mean body size with an increase in SST, (i.e.,$\beta > 0$) while small bodied species are more likely to increase in mean body size with an increase in SST (i.e.,$\beta < 0$) (Pauly and Cheung 2018, Verberk et al. 2021).

Materials and methods

Reef fish data

Our analysis is based on 1,133 underwater video surveys made in between 2011 and 2014, from 69 sites nested in 17 locations across 61° of latitude (from 34°N to 27°S) of the Western Atlantic Ocean (Figure 1a). On average ~4 sites/location and ~17 videos per site were surveyed. In each video, every fish feeding on the benthos was identified at species-taxonomic level and had its total length estimated. Fish sizes were recorded in size (length) bin categories, with bin widths of 1 cm. Full Details of field procedures are provided in Longo et al. (2019).

Seawater temperature data

We grouped all fish survey sites into 0.01° grid cells (1.23 km^2). For each of these cells, we then extracted Sea Surface Temperature (SST) values using daily temperature records from Multi-scale

Ultra-high Resolution (MUR) Sea Surface Temperature database by the NASA Making Earth System Data Records program (https://podaac.jpl.nasa.gov/dataset/MUR-JPL-L4-GLOB-v4.1). For the statistical analysis we compute the average SST of the 5 years prior to the survey for each site.

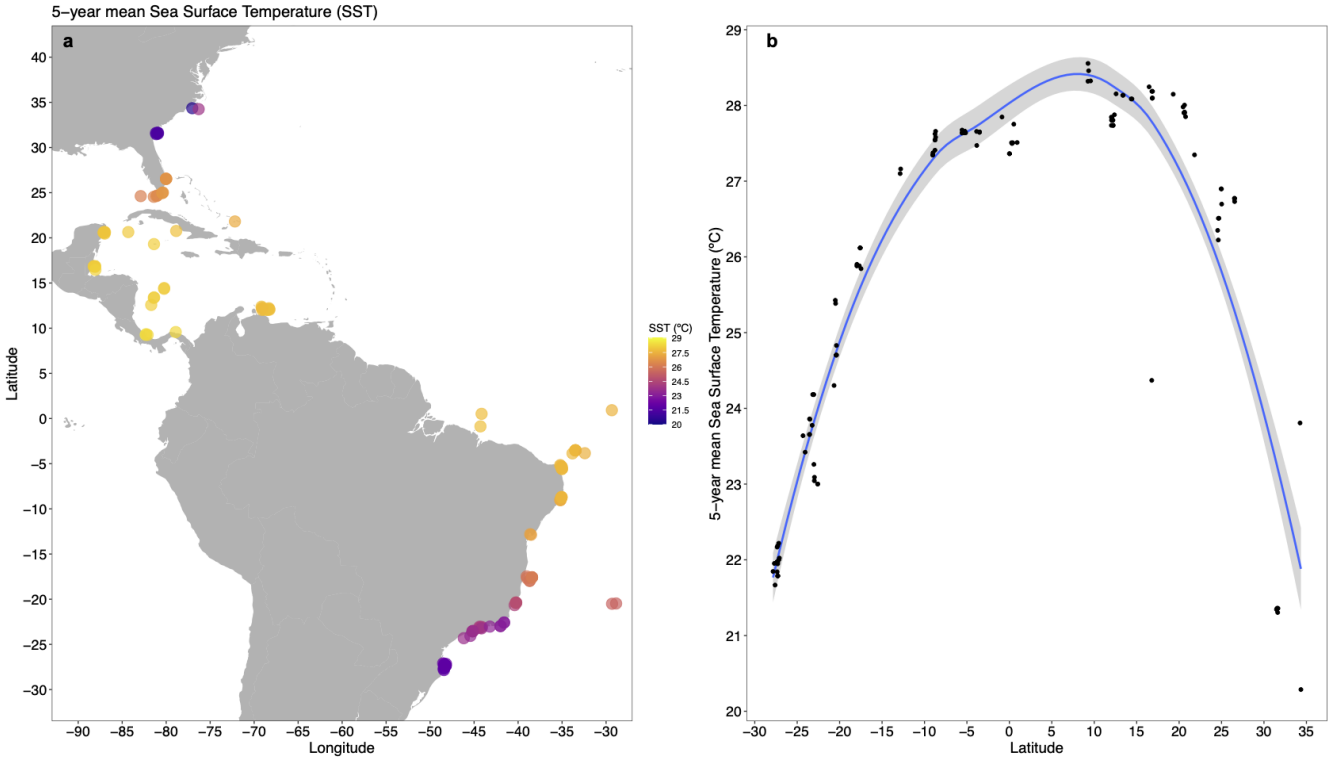

Figure 1 a: Spatial distribution of the 5-year mean sea surface temperature at the sites used in this study. **b:** Latitudinal trend of sea water temperature (ºC) in the 69 sites covered by the study. The blue line represents the locally estimated scatterplot smoothing regression (LOESS). Shaded area represents 95% confidence intervals.

Data filtering

To ensure data quality and statistical power to infer fish body size responses accounting for spatial variation, the dataset used in the analyses was restricted to taxa identified to species level and only species containing at least twenty individuals per location occurring in at least five locations (for example a species with twenty individuals observed in a three locations was excluded). The selection criteria resulted in nineteen (19) species belonging to twelve different genera. (Table S1, Supplementary Materials).

Model description

Since there is evidence that the body size-temperature relationship is species-specific and spatially dependent (Morais et al. 2017, Rijn et al. 2017, Audzijonyte et al. 2020), we tested whether these two groups (i.e. species and site) were important group factors in our database. Therefore, we calculated the intra-class correlation coefficient (ICC), which is a metric that indicates the proportion of the total variance explained by the grouping structure in the raw data (Hox et al. 2017). To calculate ICC, we defined an "empty" version of the full regression model in which the observations within each species and each site nested in location groups get their own regression line. In this way, each species or site's regression line has a unique intercept. The "empty model" was defined as:

$$Y_i \sim 1 + (1 + species) + (1 + location/site)\,(1)$$

where Y_i is the mean fish body length of the species (i) in each sampled site (s) nested in location.

When the ICC is below 0.05 (although there is no set threshold; judgment is definitely involved as well), one may be able to run a model without random effects and still get an accurate result (Sommet and Morselli 2017). In other words, ICC ~ 0 indicates perfect independence of residuals: the observations do not depend on group membership. We performed the ICC analysis by using the *icc* function from the *performance* package version 0.7.1, in R software version 4.0.5 (R Core Team 2021, Lüdecke et al. 2021).

From the preliminary analysis done, it follows that species is an important factor to consider in the relationship between fish body size and seawater temperature ($ICC_{species}$ = 0.89). On the contrary, site nested in location has no relevance in explaining part of the variance observed in the response variable (i.e. mean fish body size) ($ICC_{location}$ = 0.02; $ICC_{location/site}$ = 0.01). Therefore, we have chosen to

exclude the location and site factors from the following analyzes and include only the species as a group factor.

As traditionally performed, we used log-transformed values in the full model formulation because power-law relationships are typically described by a power function ($Y = a \cdot X^{\beta}$) which is linearized when log-transformed. We use "log" to refer to the natural logarithm (log base *e*, not base 10) because, coefficients on the natural-log scale are directly interpretable as approximate proportional differences. For each fish body length observation, we estimated the overall relationship with sea water temperature, and also allowed the slope and intercept of the relationship to vary for each species in the dataset.

We fitted generalized linear mixed-effects model (GLMM) of mean fish body size as a function of the mean five years daily sea surface temperature and with species as grouping variable (Equation 2).We set species as a group effect on the intercept and slope to reflect differences among species in fish body size. The overall model structure implemented was:

$$\ln(Y_i) = \ln(\beta_0 + \beta_{0,i}) + (\beta_1 + \beta_{1,i}) \cdot \ln(X) + \varepsilon \quad (2)$$

where $Y_i$is the observed individual fish body length of the species i in centimeters, X is the mean five years daily sea surface temperature in each sampled site expressed in degrees celsius. β_0 and β_1 are the overall intercept and linear slope (i.e., power law's scaling exponent). $\beta_{0,i}$ and $\beta_{1,i}$ are the departures for each species-taxon group from $\beta_0$and β_1 (respectively). We extracted the linear slopes β_1 and $\beta_{1,i}$ from the model, which summarize the spatial trend for mean annual temperature change. A positive estimate for β_1 would indicate an overall positive association between mean sea surface temperature and fish body length.

We summarize the parameters uncertainty with the 95 % highest density interval (HDI), which contains the parameter values of highest probability and that span the 95 % most probable values. Given estimates of the slope of fish body size against SST (β_1) for all species, we then assessed whether these slopes were linearly associated with species maximum body size. For the maximum observed body size we used the median value of the five largest observed body size records, which alleviated potential observation errors in the datasets. Bayesian methods were used to estimate the regression coefficients and their associated uncertainty. We defined random effect of "(maximum body size | species)" to allow for a separate slope and intercept to be estimated for each species. Default uninformative priors were adopted for the *y*-intercept and slope (Gaussian[0,1] in both cases), and a t-Student prior of [3, 0, 2.5] was also assumed for the standard deviation describing the variation in the β_1 estimates about the fitted regression line.

Model fitting

We fitted the models using the *brm* function in the brms package (version 2.15.0) within R (version 4.0.5, R Core Team 2020). The brms package provides an interface to fit generalized (non-)linear multivariate models using Stan performing full Bayesian inference (Carpenter et al. 2017, Bürkner 2017). Markov chain Monte Carlo sampling (MCMC) was run with 3 chains of 3000 iterations each, of which the first 750 were discarded as the burn-in. The last 2250 were used to generate posterior probability density ranges. The convergence of the MCMC chains was assessed by visually inspecting the chains and was tested using the Gelman-Rubin statistic (Gelman and Rubin 1992).

Results

Our results showed that the overall relationship between fish body size and sea water temperature was statistically indistinguishable from zero (Figure 3 and Figure 4). The overall SST effect on fish body size is: β_1 = -0.40 (-1.42, 0.60; 95% HDI, R^2 = 0.52) (Figure 3 black line).

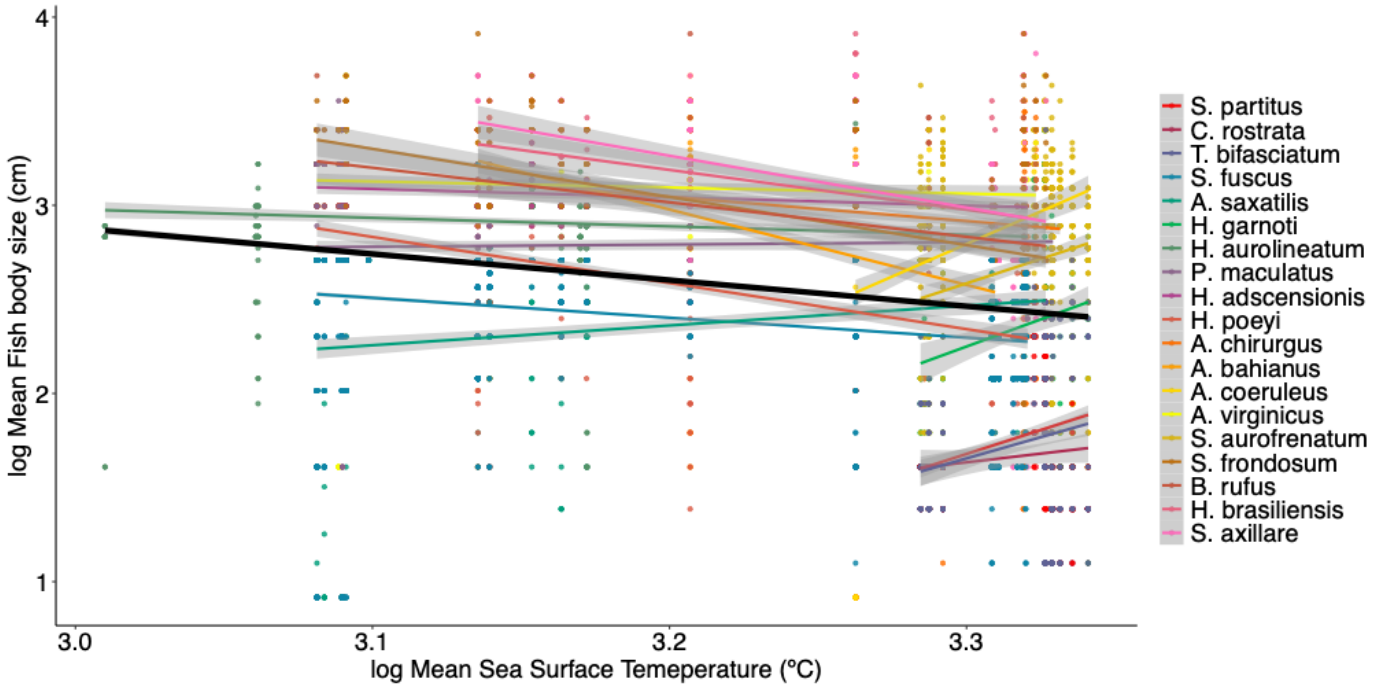

Figure 3 Fish body size (cm) ~ Sea Surface Temperature (SST) interspecific linear relationships. Lines represent the posterior fits from Bayesian generalized linear mixed model. Solid black line shows the overall relationship. Coloured lines show interspecific linear relationships for each fish species. Credible intervals are omitted for clarity. Inset shows β-scaling exponent value and its 95% credible interval. See Figure 4 for species-specific model regression slopes estimates.

Six species *(Sparisoma frondosum, Sparisoma axillare, Halichoeres poeyi, Halichoeres brasiliensis, Bodianus rufus, Acanthurus bahianus)* showed negative scaling exponent (95% of the HDI of the regression slopes was below zero) (Figure 4). Three species (*Sparisoma aurofrenatum, Acanthurus coeruleus, Halichoeres garnoti*) showed positive scaling exponent (95% of the HDI of the regression slopes was above zero) (Figure 4). Of the three species that have a positive relationship with sea water temperature, two are large-bodied (TL > 35 cm). While of the six species that have a negative relationship with sea water temperature, four are large-bodied (TL > 35 cm) (Figure 4). The relative

change in species' mean body length was, on average, not related to their maximum body length (Figure 5).

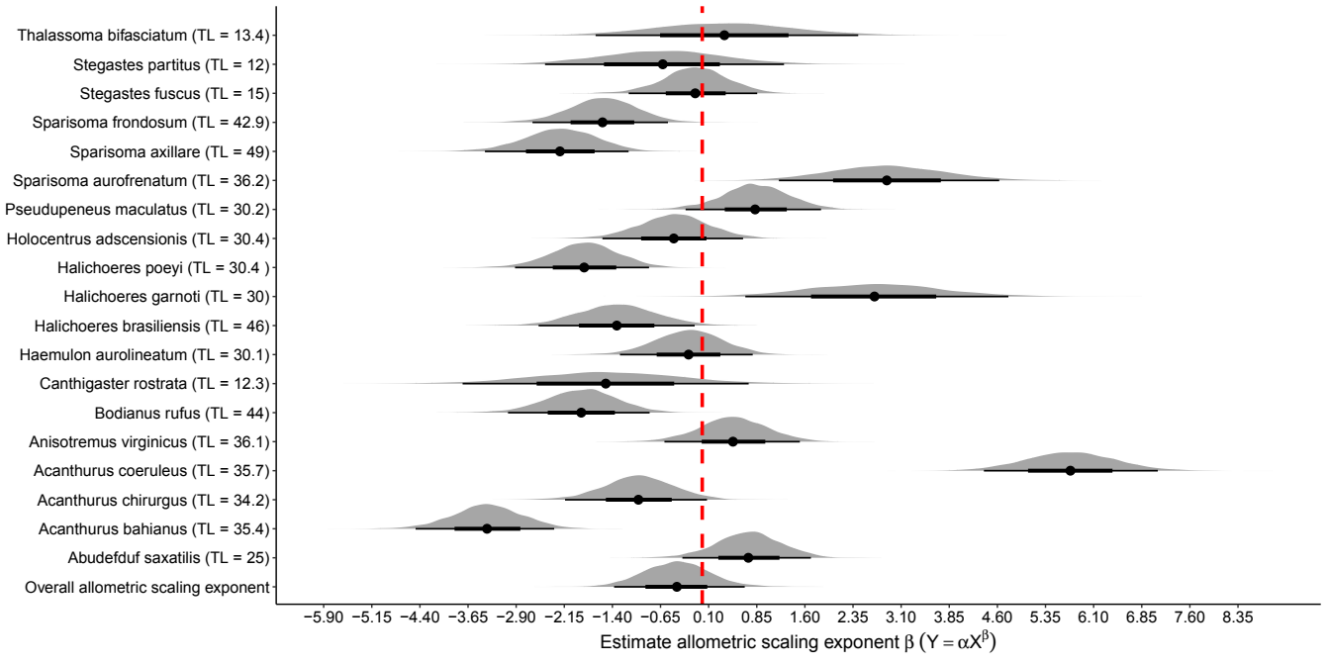

Figure 4 Density ridges of the posterior distributions of the interspecific regression slope coefficients. The dots are the posterior medians, the thick inner lines the 50% intervals, and the thinner outer lines the 95% Bayesian credible intervals. Red dotted line shows the 0.0 scaling exponent value. TL: maximum observed length.

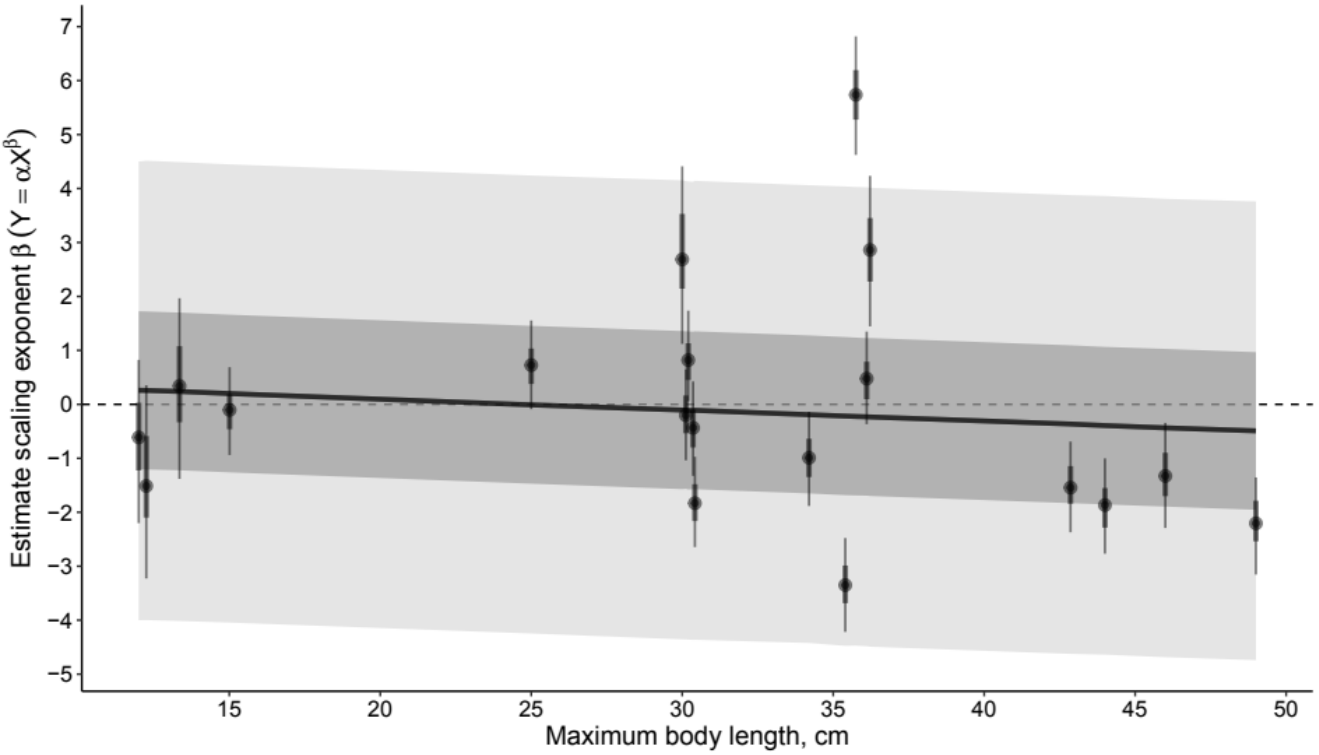

Figure 5. The relative change in species' mean body length related to their observed maximum body length. Dots and vertical bars represent the median, 50% and 95% HDI ranges of individual species responses, respectively. Solid black line is the linear regression weighted according to the individual species' uncertainty level. Grey shading depicts the 50% and 95% credible interval for the regression.

Discussion

To our knowledge, this study provides the first empirical evidence of the existence of a nonlinear relationship between the reef fish body size and the sea water temperature in the Western Atlantic Ocean. There is clear indication that seawater temperature may be affecting the mean body length of reef fish within species, but this effect varies with species in an unanticipated way. We provide comprehensive evidence that 31% of species (n= 6) were smaller in warmer waters, while 15% (n = 3) were bigger in warmer waters throughout the species' natural distribution. We also found no relationship between the species' maximum observed length and the sensitivity to increasing sea water temperature in the spatial distribution range observed for each species. These results extend the

findings of other recent studies that also show impacts of sea water temperature on fish body size (Huss et al. 2019, Audzijonyte et al. 2020, Oke et al. 2020).

There are various hypotheses regarding the maximum size of the fish and its response to the increase in water temperature. Experimental evidence shows that fish grow to smaller sizes in warmer temperatures (Gardner et al. 2011, Ilha et al. 2018). Findings have been interpreted to be related to limited oxygen supply to tissues and indicate that oxygen limitation may contribute to decreasing animal body size in warming aquatic environments (e.g., oxygen− and capacity-limited thermal tolerance" (OCLTT) hypothesis) (Pauly and Cheung 2018, Pörtner 2021). On the other hand, fish body growth increased substantially after warming, but the extent depended on body size: only among small-bodied perch (*Perca fluviatilis*) did growth increase with temperature (Huss et al. 2019). Phylogenetic meta-analyses from 39 longitudinal studies found no evidence that warmer environments were associated with selection for smaller body size (Siepielski et al. 2019). In our study, we did not find a clear relationship between fish body size and seawater temperature. These findings suggest that selection for smaller body size is not a general phenomenon, and hence that adaptive evolutionary responses to changed selection pressures imposed by a warming ocean, as would have been expected under Bergmann's rule or the OCLTT hypothesis, is unlikely to be a general explanation for recent declines in reef fish body size where they have occurred (Teplitsky and Millien 2014, Audzijonyte et al. 2019, Siepielski et al. 2019).

The nonlinear and species-specific relationship observed in our study may derive from various interrelated factors. First, the scarcity of food resources can generate nonlinear responses through juvenile mortality (Brodersen et al. 2011, Oke et al. 2020). At the same time, the presence of a greater number of conspecific competitors or predators can generate negative feedback between growth and fish body size (Hamrin and Persson 1986, Watz et al. 2019). High levels of competition, combined with reduced prey availability, led to severe reductions in growth of rainbow trout (Korman et al. 2021). In

geothermal streams, if nutrient supply increases with temperature, there will be enough resources to sustain larger consumers at higher trophic levels (O'Gorman et al. 2017). Therefore, the species-specific power-law relationships observed in this study could arise from species dense-dependent growth and resource availability processes that take place over the broad spatial gradient observed in our study.

We acknowledge that other external factors such as fishing pressure may impact the body size of wild fish populations (Robinson et al. 2017, Tu et al. 2018, Morais et al. 2020). For example, reef fish species that in this study presented a negative relationship with temperature are important fishing targets for the artisanal fisheries in Brazil, such as the parrotfish within the genus *Sparisoma* (Floeter et al. 2006, Nunes et al. 2012, Bender et al. 2014). These species are protogynous hermaphrodites so size of reproduction and maturation are a critical trait of its reproductive biology (van Rooij et al. 1995, Roos et al. 2016). We observed that these species are smaller in warmer waters, so considering ocean warming projections, the decrease in body size of these species will threaten the long-term sustainability of fisheries not only through decreased biomass, but also by affecting the population dynamics of these species (Magris et al. 2021).

Together, these findings reveal that fish body sizes of tropical reef assemblages differ from temperate reefs. The decrease in length of 31% of the species analyzed in this study calls attention to which mechanisms can co-found the negative effect of temperature (i.e. reduced food availability, competition). Furthermore, in the face of probable ocean warming, it is necessary to constantly monitor the populations of the reef fish of the western Atlantic Ocean to avoid possible ecosystem changes that have already been announced for too long.

References

Angilletta, M. J. et al. 2004. Temperature, Growth Rate, and Body Size in Ectotherms: Fitting Pieces of a Life-History Puzzle. - Integr Comp Biol 44: 498–509.

Atkinson, D. 1994. Temperature and organism size-A biological law for ectotherms? Advances in Ecological Research 25: 1. - Res. in press.

Audzijonyte, A. et al. 2013. Ecological consequences of body size decline in harvested fish species: positive feedback loops in trophic interactions amplify human impact. - Biology letters 9: 20121103.

Audzijonyte, A. et al. 2020. Fish body sizes change with temperature but not all species shrink with warming. - Nature Ecology & Evolution 4: 809–814.

Bender, M. G. et al. 2014. Local Ecological Knowledge and Scientific Data Reveal Overexploitation by Multigear Artisanal Fisheries in the Southwestern Atlantic. - PLOS ONE 9: e110332.

Brandl, S. J. et al. 2020. Extreme environmental conditions reduce coral reef fish biodiversity and productivity. - Nature Communications 11: 3832.

Brodersen, J. et al. 2011. Temperature and Resource Availability May Interactively Affect Over-Wintering Success of Juvenile Fish in a Changing Climate. - PLOS ONE 6: e24022.

Burrows, M. T. et al. 2019. Ocean community warming responses explained by thermal affinities and temperature gradients. - Nature Climate Change 9: 959–963.

Clarke, A. 2017. Principles of Thermal Ecology: Temperature, Energy and Life. - Oxford University Press.

Currie, S. and Evans, D. H. 2020. The Physiology of Fishes. - CRC Press.

Dahlke, F. T. et al. 2020. Thermal bottlenecks in the life cycle define climate vulnerability of fish. - Science 369: 65–70.

Daufresne, M. et al. 2009. Global warming benefits the small in aquatic ecosystems. - PNAS 106: 12788–12793.

Dunstan, P. K. et al. 2018. Global patterns of change and variation in sea surface temperature and chlorophyll a. - Scientific Reports 8: 14624.

Fisher, J. A. D. et al. 2010. Breaking Bergmann's rule: truncation of Northwest Atlantic marine fish body sizes. - Ecology 91: 2499–2505.

Floeter, S. R. et al. 2006. Effects of fishing and protection on Brazilian reef fishes. - Biological Conservation 128: 391–402.

Gayon, J. 2000. History of the Concept of Allometry1. - American Zoologist 40: 748–758.

Goldberg, D. et al. 2019. Decreases in length at maturation of Mediterranean fishes associated with higher sea temperatures. - ICES Journal of Marine Science 76: 946–959.

Hamrin, S. F. and Persson, L. 1986. Asymmetrical Competition between Age Classes as a Factor Causing Population Oscillations in an Obligate Planktivorous Fish Species. - Oikos 47: 223–232.

Hox, J. J. et al. 2017. Multilevel analysis: Techniques and applications. - Routledge.

Huss, M. et al. 2019. Experimental evidence of gradual size-dependent shifts in body size and growth of fish in response to warming. - Global Change Biology 25: 2285–2295.

Huxley, J. S. and Teissier, G. 1936. Terminology of Relative Growth. - Nature 137: 780–781.

Korman, J. et al. 2021. Changes in prey, turbidity, and competition reduce somatic growth and cause the collapse of a fish population. - Ecological Monographs 91: e01427.

Lefevre, S. et al. 2021. The role of mechanistic physiology in investigating impacts of global warming on fishes. - Journal of Experimental Biology in press.

Lindmark, M. et al. 2018. Temperature-dependent body size effects determine population responses to climate warming. - Ecology Letters 21: 181–189.

Lüdecke, D. et al. 2021. performance: Assessment of Regression Models Performance.

Magris, R. A. et al. 2021. A blueprint for securing Brazil's marine biodiversity and supporting the achievement of global conservation goals. - Diversity and Distributions 27: 198–215.

Marquet, P. A. et al. 2005. Scaling and power-laws in ecological systems. - Journal of Experimental Biology 208: 1749–1769.

Morais, R. A. and Bellwood, D. R. 2020. Principles for estimating fish productivity on coral reefs. - Coral Reefs 39: 1221–1231.

Morais, R. A. et al. 2017. Spatial patterns of fish standing biomass across Brazilian reefs. - Journal of Fish Biology 91: 1642–1667.

Morais, R. A. et al. 2020. Human exploitation shapes productivity–biomass relationships on coral reefs. - Global Change Biology 26: 1295–1305.

Moyano, M. et al. 2020. Linking individual physiological indicators to the productivity of fish populations: A case study of Atlantic herring. - Ecological Indicators 113: 106146.

Neuheimer, A. B. et al. 2011. Tolerance limit for fish growth exceeded by warming waters. - Nature Climate Change 1: 110–113.

Nunes, J. de A. C. da C. et al. 2012. Reef fishes captured by recreational spearfishing on reefs of Bahia State, northeast Brazil. - Biota Neotropica 12: 179–185.

O'Gorman, E. J. et al. 2017. Unexpected changes in community size structure in a natural warming experiment. - Nature Climate Change 7: 659–663.

Oke, K. B. et al. 2020. Recent declines in salmon body size impact ecosystems and fisheries. - Nature Communications 11: 4155.

Pauly, D. and Cheung, W. W. L. 2018. Sound physiological knowledge and principles in modeling shrinking of fishes under climate change. - Global Change Biology 24: e15–e26.

Payne, N. L. et al. 2016. Temperature dependence of fish performance in the wild: links with species biogeography and physiological thermal tolerance. - Functional Ecology 30: 903–912.

R Core Team 2021. R: A Language and Environment for Statistical Computing. - R Foundation for Statistical Computing.

Ramler, D. et al. 2014. Nonlinear effects of temperature on body form and developmental canalization in the threespine stickleback. - Journal of Evolutionary Biology 27: 497–507.

Reynolds, P. L. et al. 2018. Latitude, temperature, and habitat complexity predict predation pressure in eelgrass beds across the Northern Hemisphere. - Ecology 99: 29–35.

Rijn, I. van et al. 2017. Large but uneven reduction in fish size across species in relation to changing sea temperatures. - Global Change Biology 23: 3667–3674.

Robinson, J. P. W. et al. 2017. Fishing degrades size structure of coral reef fish communities. - Global Change Biology 23: 1009–1022.

Roos, N. C. et al. 2016. Multiple management strategies to control selectivity on parrotfishes harvesting. - Ocean & Coastal Management 134: 20–29.

Siepielski, A. M. et al. 2019. No evidence that warmer temperatures are associated with selection for smaller body sizes. - Proceedings of the Royal Society B: Biological Sciences 286: 20191332.

Sommet, N. and Morselli, D. 2017. Keep calm and learn multilevel logistic modeling: A simplified three-step procedure using Stata, R, Mplus, and SPSS. - International Review of Social Psychology in press.

Thorson, J. T. et al. 2017. The relative influence of temperature and size-structure on fish distribution shifts: A case-study on Walleye pollock in the Bering Sea. - Fish and Fisheries 18: 1073–1084.

Tu, C.-Y. et al. 2018. Fishing and temperature effects on the size structure of exploited fish stocks. - Scientific Reports 8: 7132.

van Rooij, J. et al. 1995. Plastic growth of the herbivorous reef fish Sparisoma viride: field evidence for a trade-off between growth and reproduction. - Marine Ecology Progress Series 122: 93–105.

Verberk, W. C. E. P. et al. 2021. Shrinking body sizes in response to warming: explanations for the temperature–size rule with special emphasis on the role of oxygen. - Biological Reviews 96: 247–268.

Watz, J. et al. 2019. Temperature-dependent competition between juvenile salmonids in small streams. - Freshwater Biology 64: 1534–1541.

Supplementary Materials

Table 1 Number of observed species' individuals by location. TL= maximum observed length (cm); TN= total number of locations where species appears; NC= North Carolina, USA (34ºN); GE= Georgia, USA (31ºN); CF: Central Florida, USA (26ºN); FK: Florida Keys, USA (24ºN); YM: Yucatan, Mexico (20ºN); CB: Carrie Bow Cay, Belize (16ºN); CI: Caribbean, Curaçao Island (12ºN); ML: Manoel Luís Marine Reserve, Brazil (0º); RA: Rocas Atoll, Brazil (3ºS); RN: Rio Grande do Norte, Brazil (5ºS); PE: Pernambuco, Brazil (8.75ºS); AL: Alagoas, Brazil (9ºS); AB: Abrolhos, Brazil (17ºS); GU: Guarapari, Brazil (20ºS); AR: Arraial do Cabo, Brazil (22ºS); SP: São Paulo, Brazil (23ºS); SC: Santa Catarina (27ºS).

Species	**TL**	**TN**	**Locations**															
			NC	**GE**	**CF**	**FK**	**YM**	**CB**	**CI**	**ML**	**RA**	**RN**	**PE**	**AL**	**AB**	**GU**	**AR**	**SP**	**SC**
Abudefduf saxatilis	25	9	0	0	0	0	0	0	43	0	145	50	41	37	44	0	71	198	294
Acanthurus bahianus	35.4	5	0	0	0	0	0	0	0	0	0	0	0	26	536	111	274	23	0
Acanthurus chirurgus	34.2	9	0	0	49	20	79	0	0	128	329	242	0	0	0	30	29	38	0
Acanthurus coeruleus	35.75	8	0	0	42	66	102	29	76	0	48	53	0	0	233	0	0	0	0
Anisotremus virginicus	36.11	8	0	0	29	0	0	0	0	28	0	31	0	0	74	27	36	88	222
Bodianus rufus	44	6	0	0	23	0	0	0	24	0	0	47	0	0	0	28	0	21	47
Canthigaster rostrata	12.25	5	0	0	41	40	71	39	66	0	0	0	0	0	0	0	0	0	0
Haemulon aurolineatum	30.12	6	45	45	0	0	0	0	0	0	0	61	0	0	80	0	0	401	250
Halichoeres brasiliensis	46	5	0	0	0	0	0	0	0	0	0	24	0	33	40	0	39	22	0
Halichoeres	30	5	0	0	42	64	62	95	79	0	0	0	0	0	0	0	0	0	0

Species	TL	TN	Locations															
			NC	GE	CF	FK	YM	CB	CI	ML	RA	RN	PE	AL	AB	GU	AR	SP	SC
garnoti																			
Halichoeres poeyi	30.42	8	0	0	0	0	0	0	0	0	0	48	21	51	75	26	154	38	158
Holocentrus adscensionis	30.36	5	0	0	0	0	0	0	0	0	118	22	0	0	0	0	65	38	55
Pseudupeneus maculatus	30.2	6	0	0	45	0	57	0	0	0	0	28	0	0	0	35	81	0	263
Sparisoma aurofrenatum	36.22	5	0	0	95	160	230	181	131	0	0	0	0	0	0	0	0	0	0
Sparisoma axillare	49	9	0	0	0	0	0	0	0	32	54	45	54	27	112	38	41	25	0
Sparisoma frondosum	42.86	7	0	0	0	0	0	0	0	65	0	134	0	24	29	0	52	33	39
Stegastes fuscus	15.01	8	0	0	0	0	0	0	0	0	0	300	1258	2095	832	21	864	359	975
Stegastes partitus	12	5	0	0	100	127	60	56	188	0	0	0	0	0	0	0	0	0	0
Thalassoma bifasciatum	13.35	5	0	0	55	61	95	47	109	0	0	0	0	0	0	0	0	0	0

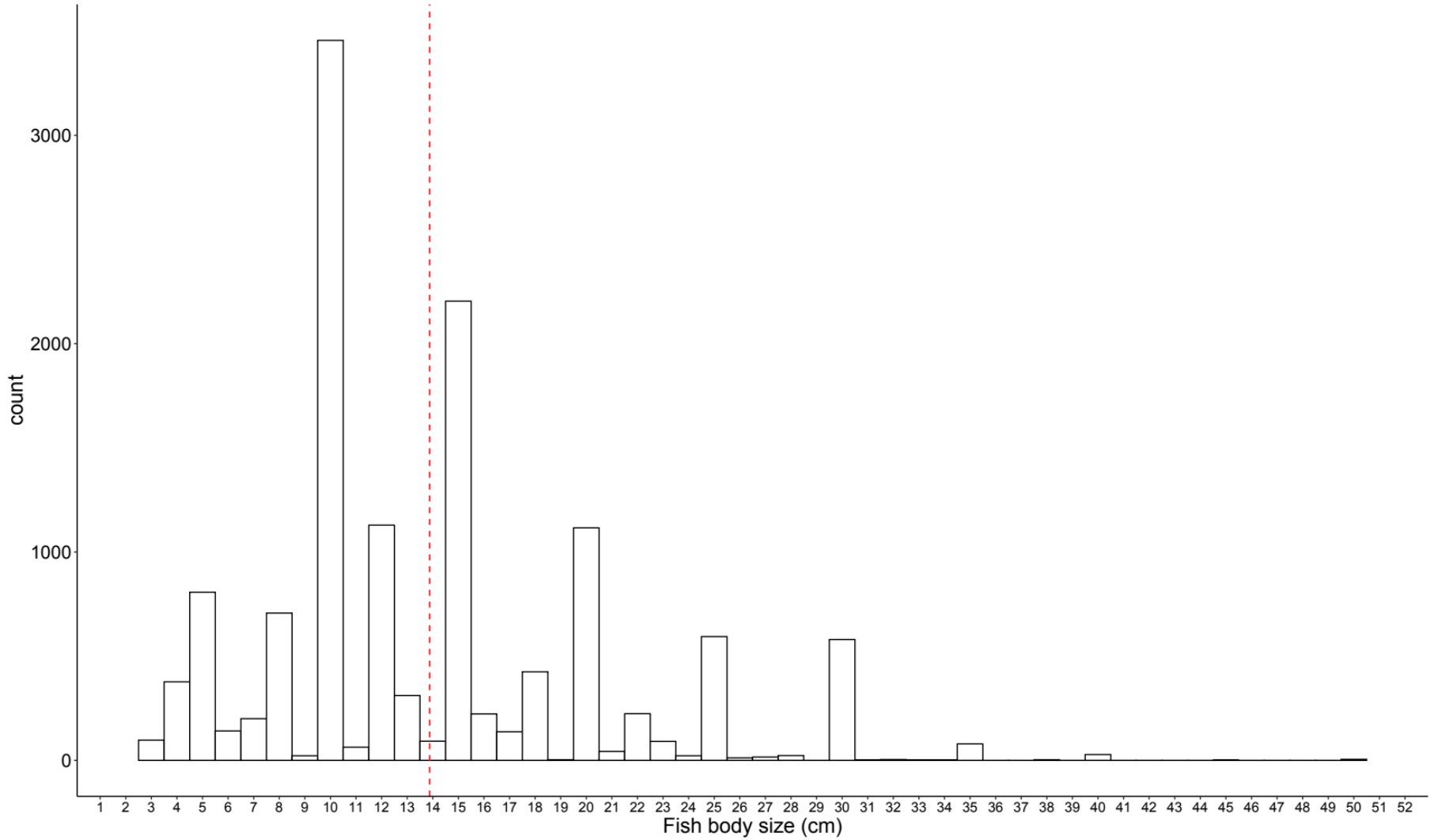

Figure S1 Histogram of the overall mean fish length of the raw data used in this study (n= 16,837 obs.). Band width = 1 cm.

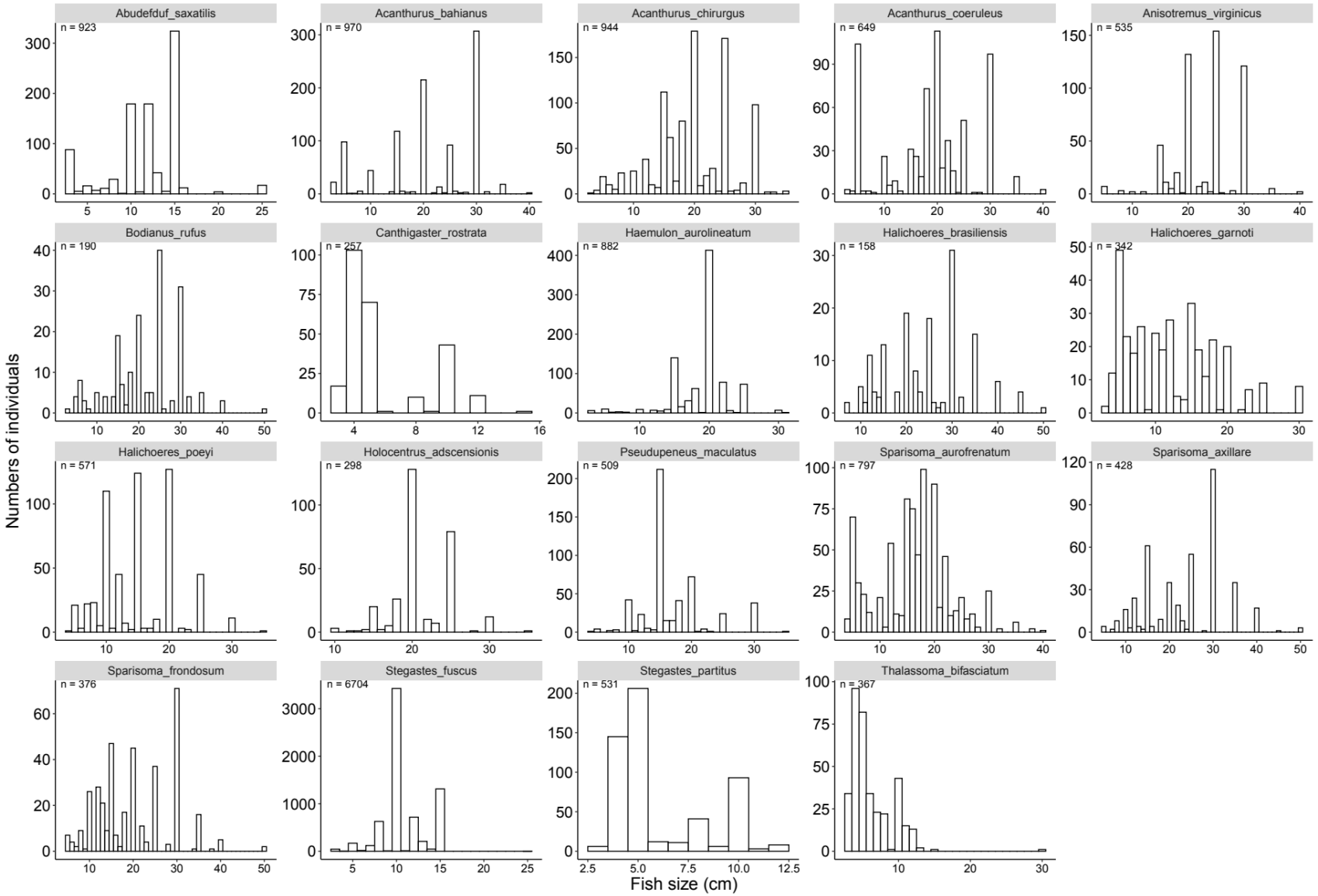

Figure S2 Histogram of the species' mean fish length of the raw data used in this study (n = number of individual observed). Band width = 1 cm.

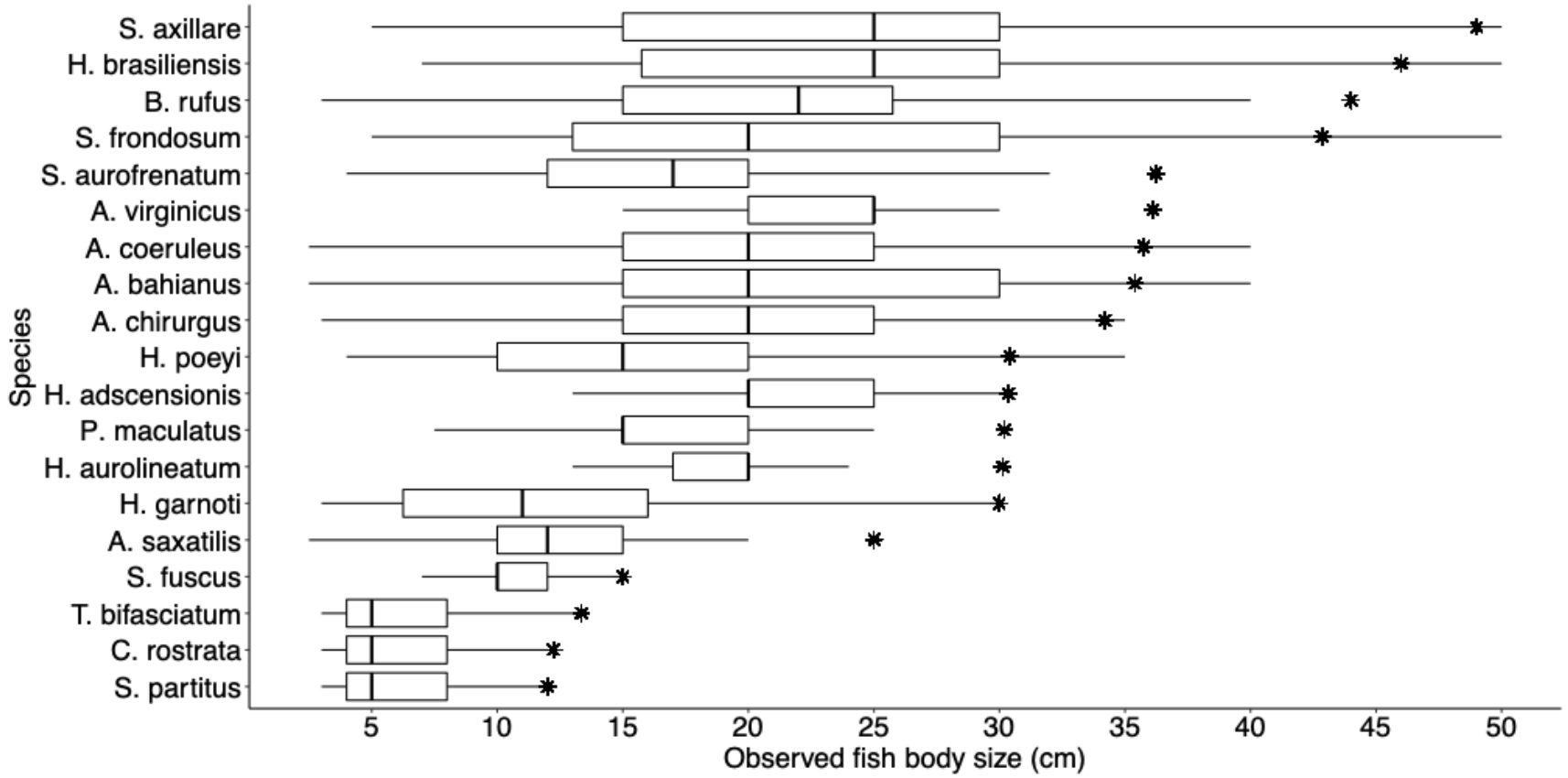

Figure S3 Observed species' fish body size used in the statistical analysis. The asterisks indicate the maximum observed lengths estimated by median value of the five largest observed body size records.

Table S2 List of localities of underwater visual census, with information about the period, coordinates (longitude and latitude), number, and depth at which they were taken.

Locality	Period	Longitude	Latitude	N (UVC)	Depth (m)
Abrolhos					
Chapeirao	2014	-38.6625	-17.96277778	44	5-20
Mato Verde	2014	-38.69527778	-17.96472222	25	3-8
Portinho Norte	2014	-38.69777778	-17.96138889	50	1.5-7
Siriba	2014	-38.71583333	-17.97055556	45	2-8
Sum of samples				**164**	
Arraial do Cabo					
Anequim	2011	-41.984482	-22.980484	90	2-13
Boqueirão	2007	-42.013053	-22.997858	64	4-22
Cardeiros	2011	-42.00165556	-22.96514167	20	4-9
Maramut	2005	-41.998779	-22.991111	63	2-9
Paredão	2008	-42.006865	-23.010107	30	3-35
Pedra Vermelha	2006	-41.992642	-22.986281	61	5-13

Porcos Oeste	2011	-41.993723	-22.96573	87	2-20
Porcos Sul	2005	-41.99416	-22.968393	67	1-19
Pta Água	2006	-42.004126	-22.969878	64	1.5-10
Pta Leste	2006	-41.979754	-22.978203	63	4-28
Saco Ingleses	2007	-42.008008	-23.006383	46	2-26
Sum of samples				**655**	
Belize					
CBC1	2013	-88.267778	16.836111	4	10
CBC2 SouthWater	2013	-88.229167	16.850278	5	14
CBC3	2013	-88.232222	16.846944	5	8.2-13.9
CBC4	2013	-88.211944	16.8825	6	9
CBC5	2013	-88.221944	16.8325	5	9
Site Coleta	2013	-88.241944	16.8225	10	4.5
Sum of samples				**35**	
Curaçao					
Marie Pumpoin	2013	-68.8	12.033333	5	8.5-11.5
Playa Largo	2013	-68.816667	12.033333	4	9-12.5

Port Marie	2013	-68.983333	12.133333	5	11-13.5
Snake Bay	2013	-68.95	12.1	5	9-13
Water Factory	2013	-69.15	12.366667	5	8-13
Westpunt Playa Kalki	2013	-69.2	12.366667	4	10-15
Sum of samples				**28**	
Florida Keys					
Conch	2013	-80.458333	24.953056	9	5-18
Molasses	2013	-80.370833	25.013889	15	5-15
Picles	2013	-80.414444	24.9875	10	5-17
Sum of samples				**34**	
Gray's Reef National Marine Santuary					
BP06N	2013	-80	26.883333	5	18
FS15	2013	-80.016667	26.9	5	19
FS17	2013	-80	26.866667	5	20
Monitoring Site	2013			5	18

Sum of samples				**20**	
Guarapari					
Escalvada	2001-2012	-40.407589	-20.699631	242	1-23
Ilhas Rasas	2012	-40.278388	-20.363218	11	6.3-15
Itatiaia	2001	-40.378777	-20.612348	39	2-12
Três ilhas	2001	-40.378777	-20.612348	71	1-12
Sum of samples				**363**	
Ilhabela					
Alcatrazes Centro Portinho	2013	-45.698116	-24.100227	10	5-10
Alcatrazes Noroeste Portinho	2013	-45.693289	-24.095842	10	5-7
Alcatrazes Saco do Funil	2013	-45.688487	-24.097748	10	3-5
Alcatrazes Sudoeste Portinho	2013	-45.702491	-24.105182	10	5-10
Ilha das Cabras	2013	-45.393889	-23.830333	20	4-10
Ilha dos búzios Saco do Urubu	2013	-45.158123	-23.805783	21	6-16
Ponta de Enchova	2013	-45.336333	-23.920083	24	6-13
Saco do Diogo	2013	-45.283621	-23.935384	20	3-11
Saco do Sombrio	2013	-45.243995	-23.893302	21	4-12

Sum of samples				**146**	
Laje de Santos					
Âncoras	2008	-46.176212	-24.316838	21	0-15
Ponta Leste	2006-2008	-46.176212	-24.316838	2	0-15
Portinho	2006-2008	-46.176212	-24.316838	75	0-15
Sum of samples				**98**	
Parcel do Manuel Luis					
Ana Cristina	2013	-44.264283	-0.869867	62	10-28
Basil	2013	-44.279033	-0.8703	21	21-27
Sum of samples				**83**	
Mexico					
Barracudas	2013	-87.033333	20.633333	8	5-8
Cozumel P1	2013	-86.966667	20.466667	5	12-14
Cozumel P2 Paraíso	2013	-87.016667	20.616667	5	9.5
Jardines	2013	-87.1	20.566667	12	6-9
Moche	2013	-86.983333	20.466667	13	5-8

Sabalos	2013	-87.116667	20.583333	18	5-10
Sum of samples				**61**	
North Carolina					
210 Rock N	2013	-77.251667	34.627778	3	30
Key Post	2013	-76.5275	34.424444	2	12-24
Station Rock	2013	-77.31667	34.657778	6	12-24
SW Knuckle Buoy	2013	-76.5275	34.54444	6	12-24
West Rock	2013	-77.41667	34.37778	4	12-24
Sum of samples				**21**	
Rio Grande do Norte					
Barreirinha	2011-2013	-35.039283	-5.956183	25	11.7-15
Batente das Agulhas	2013	-35.0725	-5.56435	18	13-20
Batentinho	2013	-35.071417	-5.591367	10	17-19
Cabeço do Leandro	2013	-35.037183	-5.950039	17	15-16
Laje dos Meros	2011	-35.04745	-5.9268	3	16-17
Maracajaú	2011	-35.258986	-5.394114	30	2-3

Mestre Vicente	2013	-35.034417	-6.000694	14	18-20
Parrachos de Rio do Fogo	2013	-35.363432	-5.262117	17	0.5-1.5
Pedra do Silva	2013	-35.090067	-5.564467	24	15-19
Pirangi	2011	-35.109492	-5.980833	30	2-3
Sum of samples				**188**	
Rocas Atoll					
Âncoras	2012	-46.176212	-24.316838	17	0.5-3.5
Barretinha	2012	-33.81805	-3.859675	5	1.5-3
Cemitério	2012	-33.81776944	-3.866636111	25	0.5-4
Falsa Barreta	2012	-33.81884444	-3.860347222	5	2-4
Laguna	2012	-33.79378611	-3.862211111	23	1-3
Piscina das Rocas	2012	-33.79191111	-3.86895	20	0.5-2
Podes Crer	2012	-33.81225833	-3.866	8	1-2.5

			3.872955556		
			-		
Poita do Zeca	2012	-33.82061944	3.857916667	21	8-11
Salão	2012	-33.80944167	-3.874725	6	5-10
			-		
Tartarugas	2012	33.80944167	3.872986111	20	1-.35
			-		
Zulu	2012	-33.87251667	3.798291667	6	1-2
Sum of samples				**156**	
Santa Catarina					
Arvoredo Baía da Tartaruga	2009-2011	-48.363806	-27.290608	47	4-9
Arvoredo Capim	2008	-48.363806	-27.284357	20	5-12
Arvoredo Engenho	2009-2011	-48.367013	-27.290608	32	4-13.5
Arvoredo Rancho Norte	2008	48.372456	-27.278331	20	3-8
Arvoredo Saco D'água	2008-2013	-48.368482	-27.277044	54	4-13.5
Arvoredo Saco do Vidal	2010	-48.361041	-27.298217	18	4.5-11
Campeche Norte	2008-2013	-48.467386	-27.690447	53	3-12.5

Campeche Sul	2012	-48.46837	-27.698025	21	3-8
Deserta Norte	2012-2015	-48.331675	-27.264465	64	5-25
Deserta Oeste	2011-2015	-48.331675	-27.264465	62	4-12
Gales Lili	2012	-48.399104	-27.17457	23	5-11
Gales Ptbras	2012-2013	-48.399104	-27.17457	41	4-11
Moleques 1	2012	-48.431996	-27.845503	34	3-12
Porto Belo Ponta Araçá 1 Costão Direito	2015	-48.51361	-27.11806	15	5-8
Porto Belo Ponta Araçá 2 Costão Esquerdo	2015	-48.52111	-27.11778	16	3-7
Porto Belo Ponta Araça 3 Caixa D'aço	2015	-48.52417	-27.12222	15	3-6
Xavier Oeste	2014	-48.387576	-27.603507	8	3-13.5
Xavier Ponta Sul	2013	-48.387576	-27.603507	14	4.5-10
Sum of samples				**557**	
Total of samples				**2609**	

Conclusão geral

Nesta tese contribuímos em três principais aspectos relacionados ao estudo dos fatores (abióticos e bióticos) que influenciam um dos processos mais importantes nos ecossistemas recifais do Oceano Atlântico ocidental: o consumo alimentar (predação) e a consequente conversão de recursos em nova biomassa disponível.

Através de uma abordagem experimental de campo no Atol das Rocas e modelagem matemática, a primeira contribuição consiste em sustentar a hipótese de que a taxa de consumo per capita de algas (e.g. resposta funcional) do peixe herbívoro *Acanthurus chirurgus* depende tanto da densidade do recurso disponível como também do número de *A. chirurgus* presentes no ecossistema recifal. Este resultado implica que dada uma determinada densidade de alga, a taxa per capita de consumo diminua conforme aumentar a densidade de *A. chirurgus* no ambiente de forrageio, sugerindo que o provável mecanismo biológico por trás do padrão observado é a interferência intra-específica por meio de maior número de interações agonísticas. A partir das evidências apresentadas no primeiro capítulo da tese, deduzimos a importância de considerar as interações intra-específicas para descrever a dinâmica algas-peixes herbívoros nos ecossistemas recifais do Oceano Atlântico Ocidental. Em vista do fato de que peixes herbívoros têm um papel importante no funcionamento de ecossistemas recifais, nossos resultados indicam promissoras áreas de estudo: 1) estequiometria dos produtores primários e reciclagem de nutrientes pelos peixes herbívoros; 2) dinâmica populacional de algas com denso-dependência associada aos peixes herbívoros e 3) interações inter-específicas indiretas nos peixes herbívoros pela presença de predadores e outras espécies de peixes herbívoros.

A segunda contribuição está ligada à primeira através da resposta da taxa per capita de predação à temperatura da água do mar. Por meio de vários estudos empíricos de campo em nível global, sabe-se

atualmente que a quantidade de recurso consumido pelo predadores e herbívoros depende não linearmente de fatores abióticos (temperatura) e bióticos (número, abundância e tipo de espécies presentes no ecossistema) (Bartley et al. 2019, Whalen et al. 2020). No segundo capítulo, modelamos a teia trófica do Atol das Rocas e analisamos as mudanças na biomassa disponível em todos os níveis tróficos como uma resposta ao aumento da temperatura do Oceano Atlântico ao longo do século 21. Os resultados das simulações suportam a hipótese que em um Oceano Atlântico mais quente, as interações tróficas dos organismos recifais, ou seja, a intensidade e frequência com a qual ingerem recursos, devem ser reduzidas, diminuindo a eficiência de transferência de biomassa para os consumidores (Inagaki et al. 2020, Pontavice et al. 2020). No caso do Atol das Rocas, até o final do século, a biomassa total diminuirá em 1%, 8% e 44% em diferentes cenários de aquecimento do oceano. À medida que a biomassa total do ecossistema diminuirá, a estrutura trófica do ecossistema mudará, deixando a dominancia da comunidade para peixes invertívoros, zooplâncton e algas enquanto os corais sofrerão severa queda. A eficiência média de transferência trófica deverá diminuir em ~ 2% entre 2012 e 2100 sob o RCP 8.5, enquanto o tempo de residência da biomassa (tempo médio que uma unidade de biomassa permanece no ecossistema) diminuirá em ~ 10%. Tal degradação da teia alimentar pode alterar o fluxo de biomassa dominante, prejudicando a reposição de biomassa, resultando em um ecossistema menos produtivo com dependência crescente de subsídios pelágicos. Os resultados preditos neste capítulo devem servir como referência e alerta para sociedade em geral. Se de um lado faz-se importante o monitoramento constante dos ecossistemas recifais pristinos como o Atol das Rocas para conferir o estado de conservação deles, do outro lado estes ecossistemas, atualmente sob ameaças sutis, têm emitido sinais de alterações que servem como alertas e não podem ser subestimadas sob pena de uma irreversível perda de espécies únicas e serviços ecossistêmicos associados.

A terceira contribuição está relacionada à segunda contribuição pelo fator abiótico temperatura. Este fator deve ser considerado fundamental para descrever as relações bióticas em ecossistemas marinhos, uma vez que influencia o crescimento, reprodução e nutrição dos principais organismos vertebrados (Pörtner and Knust 2007, Gardner et al. 2011, Huss et al. 2019, Little et al. 2020). No terceiro capítulo destacamos que existe uma relação não linear entre o comprimento médio de peixes recifais e a temperatura da água do Oceano Atlântico ocidental. Fornecemos evidências de que 31% das espécies (n = 6) são menores em águas mais quentes, enquanto 15% (n = 3) são maiores em águas mais quentes ao longo do gradiente de distribuição espacial de cada espécie. Também não encontramos nenhuma relação entre o comprimento máximo observado da espécie e a sensibilidade ao aumento da temperatura da água do mar. As implicações ecológicas e de aptidão desses resultados são difíceis de prever, mas podem prejudicar as interações predador-presa e remodelar as teias alimentares no esperado Oceano Atlântico mais quente. Nossos resultados implicam que previsões precisas sobre o tamanho e consequente biomassa disponível dos peixes em um futuro oceano mais quente requerem o reconhecimento de que as respostas ao crescimento podem variar em função das características fisiológicas e comportamentais de uma espécie. Para o aprimoramento da pesquisa, fatores bióticos, como disponibilidade de alimentos e competição interespecífica por recursos, deverão ser incluídos como importantes variáveis preditoras do comprimento médio das espécies de peixe analisadas (Cline et al. 2019, Oke et al. 2020, Korman et al. 2021).

A estabilidade das comunidades ecológicas depende fortemente das características quantitativas das interações populacionais (respostas funcionais do tipo recurso vs. predador dependente) e da distribuição dos tamanhos corporais entre as espécies (Sentis et al. 2017, Uszko et al. 2017, Letten and Stouffer 2019). Até agora, esses dois aspectos têm sido quase exclusivamente tratados separadamente, deixando uma lacuna substancial em nossa compreensão geral do funcionamento dos ecossistemas

marinhos. Nesta tese evidenciamos que as respostas funcionais de peixes herbívoros são denso-dependentes sugerindo que o numero de herbívoros e a quantidade dos recursos agem em conjunto para definir as forças de interação entre produtores primários e herbívoros. Mostramos também que a extensão em que o cumprimento das especies de peixes recifais é afetado pela temperatura depende da identidade taxonômica. Os capitulo 1 e 3, encaixam-se no exercício de modelagem ecossistemica do capitulo 2, justificando a necessidade de considerar a identidade taxonômica junto com o tamanho corporal e a temperatura do ambiente para aumentar a capacidade preditiva dos *global climate food-web models*. Portanto, com os resultados obtidos nesta tese, queremos propor a comunidade cientifica o uso e inclusão de respostas funcionais especies-especificas que possam predizer mudanças quantitativa da predação em função do tamanho da presa e do predador nos ecosistemas marinhos diante das mudanças climáticas.

Por fim, com esta tese, tentamos dar uma contribuição robusta sobre como fatores abióticos (temperatura) e fatores bióticos (competição intra-específica, relação predador-presa) intervêm na modificação e estruturação dos ecossistemas recifais do Oceano Atlântico Ocidental. Concluímos com a esperança de que esta tese seja considerada uma contribuição científica qualitativa e quantitativa relevante para o avanço de pesquisas teórica e aplicada sobre ecossistemas recifais diante das mudanças climáticas.

References

Bartley, T. J. et al. 2019. Food web rewiring in a changing world. - Nature Ecology & Evolution 3: 345–354.

Cline, T. J. et al. 2019. Effects of warming climate and competition in the ocean for life-histories of Pacific salmon. - Nature Ecology & Evolution 3: 935–942.

Gardner, J. L. et al. 2011. Declining body size: a third universal response to warming? - Trends in Ecology & Evolution 26: 285–291.

Huss, M. et al. 2019. Experimental evidence of gradual size-dependent shifts in body size and growth of fish in response to warming. - Global Change Biology 25: 2285–2295.

Inagaki, K. Y. et al. 2020. Trophic interactions will expand geographically but be less intense as oceans warm. - Global Change Biology in press.

Korman, J. et al. 2021. Changes in prey, turbidity, and competition reduce somatic growth and cause the collapse of a fish population. - Ecological Monographs 91: e01427.

Letten, A. D. and Stouffer, D. B. 2019. The mechanistic basis for higher-order interactions and non-additivity in competitive communities. - Ecology Letters 22: 423–436.

Little, A. G. et al. 2020. What do warming waters mean for fish physiology and fisheries? - Journal of Fish Biology 97: 328–340.

Oke, K. B. et al. 2020. Recent declines in salmon body size impact ecosystems and fisheries. - Nature Communications 11: 4155.

Pontavice, H. du et al. 2020. Climate change undermines the global functioning of marine food webs. - Global Change Biology 26: 1306–1318.

Pörtner, H. O. and Knust, R. 2007. Climate Change Affects Marine Fishes Through the Oxygen Limitation of Thermal Tolerance. - Science 315: 95–97.

Sentis, A. et al. 2017. Temperature-size responses alter food chain persistence across environmental gradients. - Ecology Letters 20: 852–862.

Uszko, W. et al. 2017. Effects of warming on predator–prey interactions – a resource-based approach and a theoretical synthesis. - Ecology Letters 20: 513–523.

Whalen, M. A. et al. 2020. Climate drives the geography of marine consumption by changing predator communities. - PNAS in press.